

***Deracemization of less reactive
conglomerates through enabling
technologies***

Giulio Valenti

A thesis submitted for the degree of

Doctor of Philosophy

in the Faculty of Science of the University of Strathclyde

Supervisors: Prof. Richard M. Kellogg and Prof. Joop H. ter Horst

Strathclyde Institute of Pharmacy and Biomedical Sciences

Abstract

Crystallization enhanced deracemization (CED) techniques represent robust and scalable processes that can be embedded into the synthetic routes for the production of active pharmaceutical ingredients (APIs). Just like all the other strategies to obtain one single enantiomer, CED techniques are not universally applicable, since only roughly 10% of the enantiomers known in the literature are conglomerates in the solid state. In a conglomerate the enantiomeric molecules crystallize as separate phases. This is a requirement for crystallization induced deracemization. However, it is possible to find conglomerate derivatives along the synthetic route, for instance through reversible covalent functionalization or through salts and co-crystals formation. In addition, solution racemization of such molecules, necessary for deracemization, requires reaction conditions that often turn out to be inconvenient when combined with a crystallization process.

The aim of this thesis is to find new pharmaceutically interesting conglomerates together with the development of new racemization methods that can be embedded in CED techniques. This thesis is constituted of three parts where three different pharmaceutically interesting conglomerates are used as targets to achieve one single enantiomer out of the racemic mixture. One part focuses on the characterization of 2-chlorophenylglycinamide, a conglomerate intermediate in the synthesis of Clopidogrel (Chapter 2), the discovery of racemization in the melt without the use of external bases and thus the potential of melt crystallization as a deracemization technique. This easily racemizable compound was then used in preliminary experiments where solution racemization and crystallization were conducted simultaneously in two different units allowing the selective recirculation of the mother liquor.

The second part focuses on the identification of a new conglomerate along the synthetic route to the API Praziquantel (Chapter 3) by using a set of analytical methods on a library of derivatives, reversibly functionalized through covalent bonds. The racemization of the novel conglomerate was studied in flow, in the recycle of the mother liquor and eventually successfully applied to two CED techniques, namely crystallization induced asymmetric transformation (CIAT) and temperature cycling induced deracemization (TCID).

The third part focuses on the application of the base- and bio-catalyzed racemization of two Flurbiprofen salts (Chapter 4) known to be conglomerate from patent literature after a thorough characterization of the solid state of such salts.

The developed flow system demonstrated a first proof of principle and gave insights into the parameters that need to be considered for this kind of deracemization approach.

Table of contents

Chapter 1 : Introduction	8
1.1. An introduction of crystallization-enhanced deracemization	9
1.2. Phase diagrams in conglomerate-based technology	12
1.2.1. Importance of phase diagrams in CED techniques	13
1.2.2. Binary Phase Diagrams.....	14
1.2.3. Ternary Phase Diagrams	15
1.2.4. Practical Considerations.....	17
1.3. Aim of the thesis	17
1.4. Impact and outputs.....	20
1.5. References.....	21
Chapter 2 : Testing New Crystallization-Enhanced Deracemization Techniques Using 2-Chlorophenylglycinamide	23
2.1. Introduction	24
2.2. Methods.....	27
2.2.1. Synthesis of 2-chlorophenylglycinamide	27
2.2.2. Deracemization of 2-chlorophenylglycinamide by attrition enhanced deracemization starting from racemic mixture	28
2.2.3. Deracemization of 2-chlorophenylglycinamide by using a decoupled system starting from scalemic mixture	28
2.2.4. Racemization of 2-chlorophenylglycinamide in the melt	29
2.3. Results.....	30
2.3.1. Racemization of 2-chlorophenylglycinamide in the melt.	30
2.3.2. Deracemization by means of a decoupled system	38
2.4. Discussion.....	44

2.5. Conclusion	45
2.6. References.....	45
Chapter 3 : Deracemization of a conglomerate derivative of Praziquantel: A route to enantiomerically pure (<i>R</i>)-Praziquantel.	47
3.1. Introduction	48
3.2. Methods	50
3.2.1. Conglomerate search	50
3.2.2. Racemization	51
3.2.3. Deracemization	53
3.2.4. Conglomerate hydrolysis	56
3.3. Results	57
3.3.1. Conglomerate search	57
3.3.2. Racemization	74
3.3.3. Deracemization	82
3.4. Discussion.....	87
3.4.1. Conglomerate search	89
3.4.2. Racemization	89
3.4.3. Deracemization	89
3.5. Conclusion	90
3.6. Appendix	91
3.6.2. References.....	97
Chapter 4 : Investigation of strategies for deracemization of Flurbiprofen	100
4.1. Introduction	101
4.1.1. Flurbiprofen as Active Pharmaceutical Ingredient.....	101
4.1.2. Available strategies for the production of (<i>S</i>)-Flurbiprofen.....	101
4.1.3. Conglomerate salts of Flurbiprofen	104

4.1.4. Racemization of Flurbiprofen.....	105
4.1.5. Crystallization enhanced deracemization	108
4.1.6. Preferential crystallization	112
4.2. Methods	113
4.2.1. Racemization of Flurbiprofen.....	114
4.2.2. X-Ray Powder Diffraction (XRPD).....	114
4.2.3. Single Crystal X-ray Diffraction (SC-XRD)	114
4.2.4. Preferential crystallization (PC).....	115
4.2.5. Solubility measurements.....	115
4.3. Results	116
4.3.1. Benzylammonium Flurbiprofen salt.....	116
4.3.2. Dibenzylammonium Flurbiprofen salt	139
4.4. Discussion.....	148
4.4.1. Single Crystal X-Ray Diffraction (SC-XRD).....	148
4.4.2. X-Ray Powder Diffraction (XRPD).....	148
4.4.3. Base-catalyzed racemization.....	149
4.4.4. Biocatalyzed racemization	149
4.4.5. Photoisomerization of Flurbiprofen.....	149
4.4.6. Preferential crystallization (PC).....	150
4.5. Conclusion	150
4.6. References.....	151
Chapter 5 : Conclusions and future works.....	153
5.1. Conclusions	154
5.2. Future work.....	155
5.2.1. Preferential crystallization of Flurbiprofen benzylammonium salt	155
5.2.2. Biocatalytic racemization of Flurbiprofen benzylammonium salt	155

5.3. General conclusion..... 156

Chapter 1: Introduction

1.1. An introduction of crystallization-enhanced deracemization

The demonstration by Noorduyn et al that the solid state of racemates of certain intrinsically chiral compounds can be converted virtually quantitatively to either enantiomer without the intervention of external chiral sources stimulated industrial and academic interest.^[1] The solid state must be ground to achieve deracemization. The direction of deracemization can be controlled by a small enantiomeric excess (*E*) of the desired enantiomer, a bias in the crystal size distribution (CSD) and by chiral additives.^[2] The enantiomeric excess of the desired enantiomer in the solid state in such a Viedma Ripening shows close to exponential growth.

There are strict requirements in order for crystallization-enhanced deracemization to proceed. First, the compound should either be achiral in solution or, in case of intrinsically chiral compounds, be able to racemize in solution (or epimerize in solution in case of multiple stereocenters). Second, the compound should show conglomerate behavior; that is to say that the crystalline form consists of equal portions of enantiomorphous crystals.

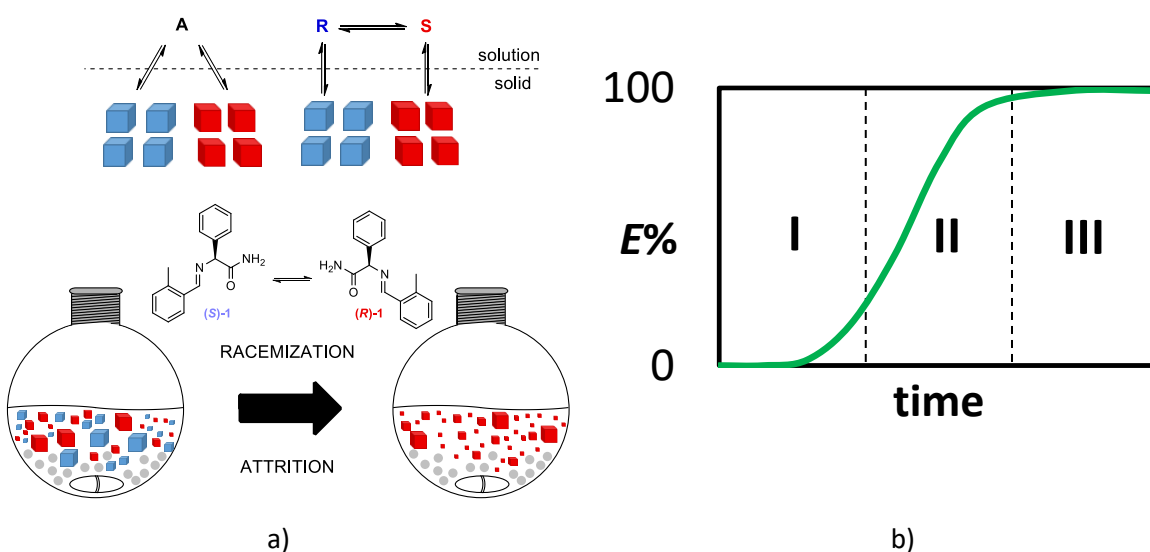
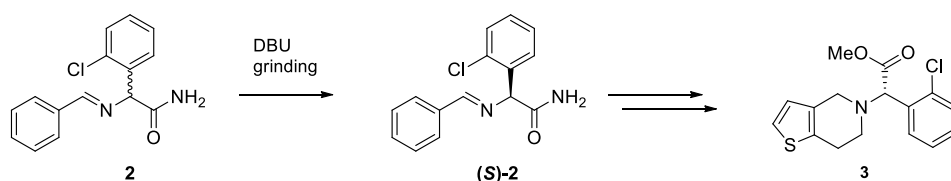


Figure 1: a) the top part of the figure schematically shows the equilibria between liquid and solid phase. The target compound can be achiral (A) in solution or it can present one or multiple stereocenter, but in both cases it might crystallize in crystals of opposite handedness. The bottom part shows the first deracemization of an intrinsically chiral compound performed by Noorduyn.^[1] b) A typical crystallization-enhanced deracemization curve starting from completely racemic mixture divided in 3 regions. In the first symmetry breaking (the initial bias) needs to take place and deracemization rate remains slow. In the second region the deracemization occurs in an autocatalytic fashion. In the third region a plateau is reached in proximity of the optical purity.

An example of the application of this technology to a commercially important compound is the deracemization of an imine of 2-(2-chlorophenyl)glycine amide (compound **2**). The imine illustrated (Scheme 1-1) is a conglomerate. Deracemization occurs in the presence of the strong base DBU (1,8-diazabicyclo[5.4.0]undec-7-ene) as racemization catalyst. The enantiomerically pure imine **2** subsequently can be converted to the blockbuster drug Clopidogrel.^[3]



Scheme 1-1: deracemization of 2-chlorophenylglycine f.

The basis of this attrition-enhanced deracemization procedure was laid by Viedma, who demonstrated that a crystal suspension of intrinsically achiral NaClO_3 or NaBrO_3 in contact with a liquid phase could be deracemized by attrition of the crystal phase. The necessary chirality was embedded in the fact that these salts crystallize in a chiral space group to form a conglomerate. These are two separate solid phases. Interconversion, i.e. deracemization, between these two enantiomorphous states proceeds via the achiral solution.^[4]

This deracemization procedure is often referred to as Viedma Ripening.^[2c] Several mechanisms by which any enantiomeric imbalance is propagated have been proposed (Figure 2a).^[2c, 4a, 5] In principle it does not require knowledge on solubility, it is conducted at isothermal conditions and the scale up was demonstrated to be feasible.^[6] Other techniques for deracemization, relying on this selective crystallization combined with racemization, have been developed.

One of the most popular is the Temperature Cycling Induced Deracemization (TCID, Figure 2b) developed for the first time by Suwannasang et al.^[7]: induced crystal growth events occur by means of controlled cooling in presence of an initial bias in the solid in favor of the desired enantiomer. This depletes the solution of this preferred enantiomer more than its unwanted counterpart, leading to an enrichment of the mother liquor in the counter enantiomer. Under racemization conditions in solution, the unwanted enantiomer is therefore converted into the desired one, allowing progressive conversion to the desired enantiomer in the solid phase. The eventual remaining unwanted enantiomer can be dissolved by a controlled increase in temperature according to the solubility of the racemate which tends to be twice as

soluble as the pure enantiomer.^[8] The desired enantiomer remains thus in excess in the solid phase. This sequence is repeated until enantiopure product is achieved. As for Viedma ripening the starting point is a suspension, therefore accurate solubility measurements are not necessary to carry out a deracemization. However, in order to come to a good process design, knowledge about solubility is highly desirable.

Another technique, Crystallization Induced Asymmetric Transformation (CIAT, also referred to Second Order Asymmetric Transformation or SOAT, Figure 2c)^[9], consists in a single cooling ramp applied to a saturated solution seeded with the desired enantiomer. It is limited to system where the racemization rate is fast enough to prevent *primary nucleation* (which is the formation of crystals from a homogenous supersaturated solution) of the counter enantiomer, otherwise a recrystallization is necessary to obtain high optical purity. Accurate solubility measurements are needed in order to make sure that all the unwanted enantiomer is dissolved while the desired amount of seeds survives in suspension before the start of the cooling ramp.

Not necessarily all crystallization enhanced deracemization techniques have to be conducted in presence of solvent. Kondepudi in 1999, following the studies of Pincock and Wilson,^[10] developed a deracemization of 1,1'-binaphthyl by melting the solid and cooling while stirring with a magnetic bar (Figure 2d).^[11] Such compound racemizes in the melt and crystallizes from the melt as a conglomerate in presence of constant stirring. The constant stirring allows grinding of the few crystals obtained by primary nucleation. The grinding produces a large surface area available for crystal growth by means of *secondary nucleation*, which is the formation of crystals from at least one parent crystal (in this case, the ones generated by primary nucleation). Even if this work was published before the discovery of the first attrition induced deracemization by Viedma, this technique relies on the same principle of crystal growth combined with racemization in the liquid phase used in all the other crystallization enhanced deracemization techniques. Cooling from the melt, owing to its simplicity, can become an attractive method for the production of pharmaceutically interesting compounds provided that no decomposition occurs during the process. Also for this latter conglomerate based technology there are prerequisites: 1) the melt must be able to return to a crystalline state upon cooling in order to exploit the chiral discrimination in the solid state that characterizes conglomerate systems. 2) The target compound must not decompose in the selected temperature frame. 3) Racemization must occur selectively in the melt and not in the solid state in order to not lose the optical purity and finally, enantiopure crystals must be introduced into the metastable zone (MSZ). The latter is the temperature frame between melting and crystallization from the melt, which is usually found below the melting point.

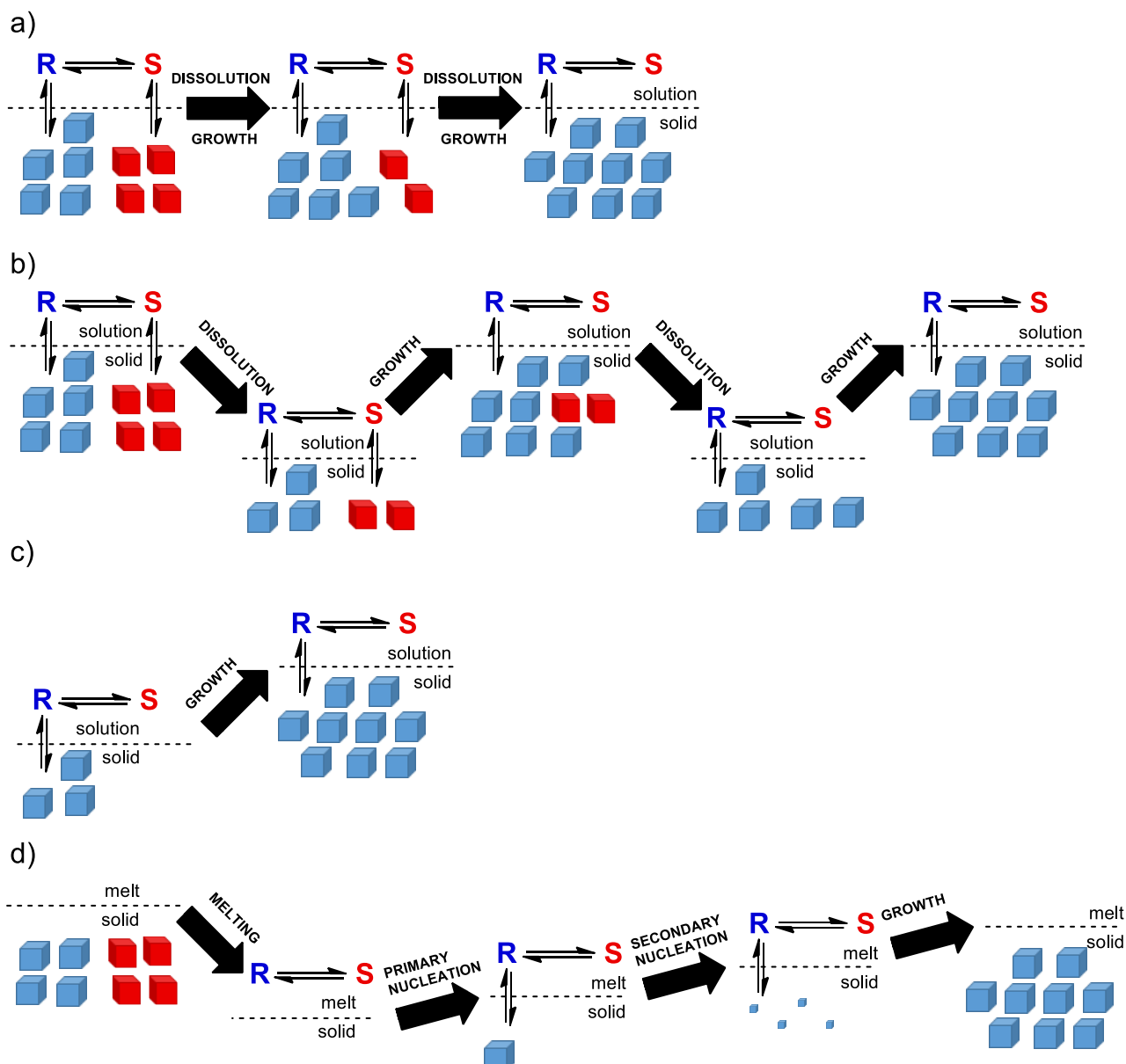


Figure 2: a) representation of attrition enhanced deracemization (Viedma ripening), the only example where dissolution and crystallization occur simultaneously owing to attrition at isothermal condition b) representation of TCID c) representation of CIAT d) representation of the deracemization from the melt. Cases b), c), and d) are represented as ideal cases where primary nucleation of the unwanted enantiomer (red) is suppressed.

1.2. Phase diagrams in conglomerate-based technology

In the context of crystallization-enhanced deracemization (CED), phase diagrams are essential tools for understanding and optimizing the interplay between solubility, crystallization behavior, and racemization. These diagrams represent systems with varying numbers of components (e.g., binary phase diagrams

involve two components, ternary phase diagrams involve three, and so on) and help identify systems where selective crystallization of one enantiomer is feasible, which is a prerequisite for CED.

Before discussing phase diagrams, it is important to define the three main types of solid-state behavior observed in chiral systems:

- A **conglomerate** is a physical mixture of enantiomerically pure crystals. Each enantiomer crystallizes independently, and the racemic mixture consists of a 1:1 mixture of these separate crystals.
- A **racemic compound** is a single crystalline phase in which both enantiomers are present in a 1:1 ratio within the same crystal lattice.
- A **solid solution** is a single crystalline phase in which the two enantiomers are randomly distributed over the same crystallographic sites.

Statistical analyses of known chiral compounds suggest that approximately 90–95% crystallize as racemic compounds, 5–10% as conglomerates, and a small minority as solid solutions.^[12] Since CED techniques require the presence of a conglomerate, this low occurrence rate significantly limits their direct applicability, unless suitable conglomerate derivatives can be identified.

1.2.1. Importance of phase diagrams in CED techniques

Crystallization-Enhanced Deracemization (CED) techniques rely on the interplay between crystallization and racemization to convert a racemic mixture into a single enantiomer. For this to be feasible, the system must allow selective crystallization of one enantiomer while the other remains in solution and undergoes racemization. Phase diagrams are an important tool for identifying such systems and for designing crystallization protocols that exploit the differences in solubility and stability between enantiomers and their mixtures.

In particular, phase diagrams (in most cases binary and ternary) help determine whether a compound crystallizes as a conglomerate, a prerequisite for CED, and define the conditions under which the desired enantiomer can be selectively crystallized. They also provide insight into the temperature and composition ranges where supersaturation can be safely applied without triggering unwanted nucleation of the counter enantiomer. This is especially important in CED processes that involve temperature changes with continuous racemization in solution.

By mapping out the stable and metastable equilibria of the system, phase diagrams guide the development of robust and scalable CED processes, ensuring that crystallization and racemization are effectively coupled.

1.2.2. Binary Phase Diagrams

Binary phase diagrams are fundamental tools for understanding the melting and crystallization behavior of chiral systems. These diagrams typically plot temperature against composition, often expressed as the molar fraction of one enantiomer (e.g., *R*). The topology of the diagram depends on the nature of the solid-state relationship between the enantiomers, which can be classified into three main categories: conglomerates, racemic compounds, and solid solutions (Figure 3).

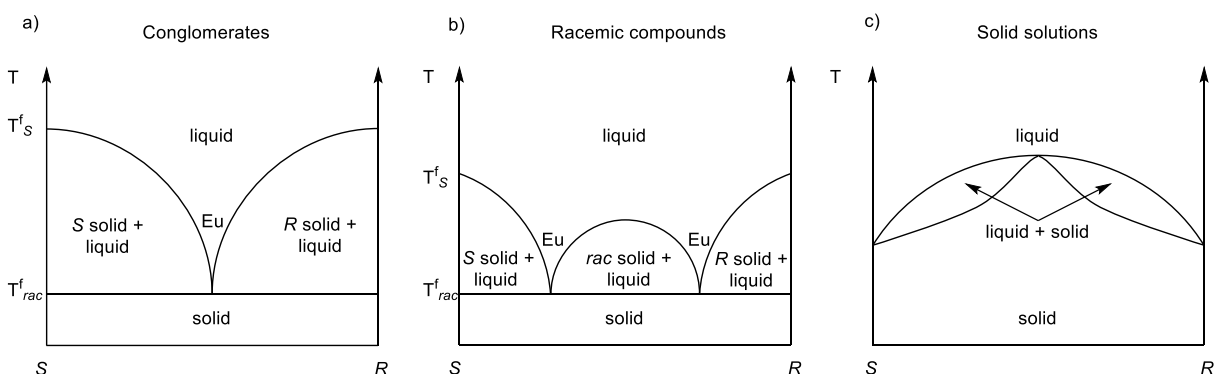


Figure 3: Schematic binary phase diagrams for chiral systems illustrating three types of solid-state behavior: a) conglomerate, b) racemic compound, and c) solid solution. In each diagram, the liquidus and solidus lines are shown. The liquidus line marks the boundary above which the system is fully molten, while the solidus line defines the boundary below which the system is fully solid. In the intermediate region between these lines, solid and liquid phases coexist. In the case of solid solutions (c), the diagram lacks a eutectic point (Eu) and shows continuous solidus and liquidus curves. Whenever the enantiomeric composition of a phase (e.g., liquid or solid) is not explicitly defined within a region of the phase diagram, the enantiomeric composition can vary continuously within that region. *rac* = racemic composition. T_f^{rac} = melting point of the racemic mixture. T_f^S = melting point of the pure (*S*)-enantiomer. Eu = eutectic point.

In a conglomerate system, the two enantiomers crystallize independently as separate pure phases. The binary phase diagram for such a system is symmetric around the racemic composition (50 mol% *R*), and features a eutectic point at this central composition. The eutectic point represents the lowest temperature at which the racemic mixture is fully molten. Above the liquidus line, the system exists as a homogeneous liquid. Between the liquidus and solidus lines, one enantiomer coexists with the melt (*R* +

liquid on the left side, S + liquid on the right). Below the solidus line, both enantiomers crystallize simultaneously, forming a physical mixture of R and S crystals, the hallmark of a conglomerate.

In contrast, a racemic compound is a single crystalline phase in which both enantiomers are present in a 1:1 ratio within the same lattice. The binary phase diagram for such a system typically exhibits two eutectic points, one on each side of the racemic composition. The melting point of the racemic compound appears as a distinct maximum at 50 mol% R . The regions between the liquidus and solidus lines correspond to biphasic domains where either R or S coexists with the melt, depending on the composition. Below the solidus, the system consists of either pure enantiomer or the racemic compound, depending on the overall composition.

In a solid solution, the enantiomers are fully miscible in the solid state, forming a single crystalline phase in which R and S are randomly distributed over equivalent lattice sites. The binary phase diagram in this case lacks a eutectic point. Instead, it features continuous liquidus and solidus curves that span the entire composition range. Above the liquidus, the system is fully molten. Between the liquidus and solidus, a solid solution coexists with the melt. Below the solidus, the system is entirely solid, with the enantiomers mixed at the molecular level within the same crystal lattice. In some cases, a miscibility gap may appear in the solid phase, leading to the coexistence of two distinct solid solutions with different enantiomeric compositions.

Understanding these diagrams is essential for designing crystallization-based processes, as they define the temperature and composition ranges where selective crystallization or deracemization can occur.

1.2.3. Ternary Phase Diagrams

Ternary phase diagrams extend the binary system by incorporating a solvent, resulting in a three-component system typically represented as R – S –Solvent. These diagrams are particularly relevant for solution-based crystallization processes, including those used in crystallization-enhanced deracemization. They are commonly depicted as equilateral triangles, where each vertex corresponds to a pure component and any point within the triangle represents a specific composition of the three.

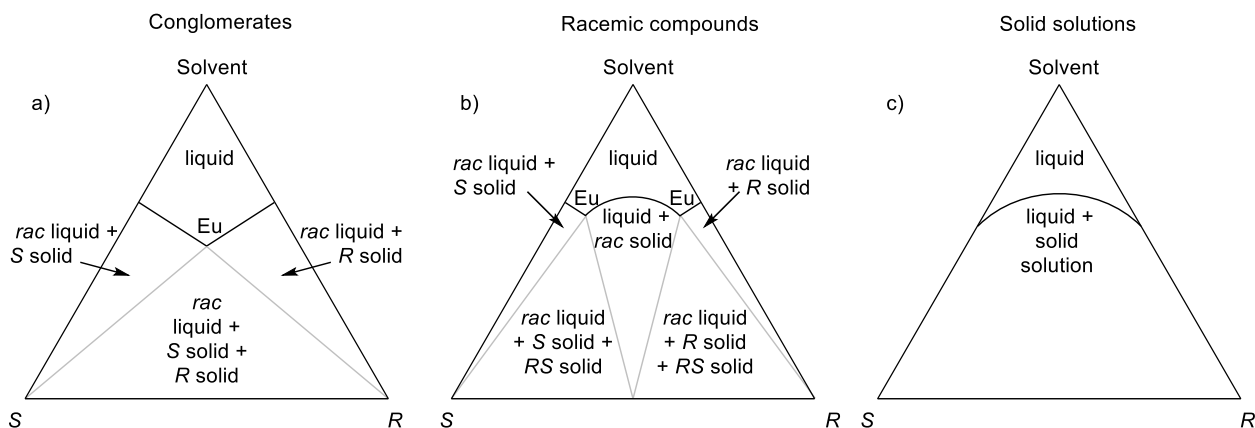


Figure 4: Schematic ternary phase diagrams for chiral systems illustrating the three types of solid-state behavior: (a) conglomerate, (b) racemic compound, and (c) solid solution. Each diagram represents a three-component system (R - S -solvent), where the vertices correspond to pure components and any point within the triangle represents a specific composition. The solubility curves define the boundaries between single-phase solution regions and biphasic or triphasic domains. In the conglomerate system (a), a central eutectic point appears along the R - S axis, and tie-lines connect the solid enantiomers to their corresponding saturated solutions. In the racemic compound system (b), the eutectic points shift toward the enantiomer-rich sides, and triphasic regions may appear where the racemic compound coexists with one enantiomer and the solution. In the solid solution system (c), the solid phase can incorporate varying ratios of R and S , and the diagram lacks a eutectic point. Whenever the enantiomeric composition of a phase (e.g., liquid or solid) is not explicitly defined within a region of the diagram, the enantiomeric composition can vary continuously within that region. *rac* = racemic composition. Eu = eutectic point.

In a **conglomerate system**, the ternary diagram features a central eutectic point along the base (R - S axis), corresponding to the racemic composition. This point represents the lowest temperature at which the racemic mixture is fully dissolved in the solvent. The solubility curves for the pure enantiomers define the boundary between the single-phase solution region and the biphasic regions. Outside the solubility curve, the system enters a two-phase domain where either R or S coexists with its saturated solution. A triphasic region also exists, where both enantiomers coexist with a racemic saturated solution. This region is bounded by tie-lines that connect the solid phases to the corresponding solution compositions.

In the case of a **racemic compound**, the topology of the ternary diagram changes significantly. The eutectic points are no longer centered but shift toward the enantiomer-rich sides, depending on the relative solubilities of the racemic compound and the pure enantiomers. The solubility curve of the racemic compound defines the boundary of the biphasic region where the compound coexists with its saturated solution. In some systems, a triphasic region may also appear, where the racemic compound

coexists with one enantiomer and the solution. The tie-lines in this case connect the racemic compound and the enantiomer to the corresponding solution composition.

For **solid solution systems**, the ternary diagram lacks a eutectic point. Instead, the solid phase is a continuous solid solution that can incorporate varying ratios of R and S. The solubility curve defines the boundary between the single-phase solution and the biphasic region where the solid solution coexists with the saturated solution. If the solid solution is stable across the entire composition range, the diagram is relatively simple. However, if a miscibility gap exists, the diagram may include a region where two distinct solid solutions coexist with the solution phase. This adds complexity to the crystallization behavior and must be carefully considered when designing resolution or deracemization strategies.

Ternary phase diagrams thus provide a comprehensive view of the equilibrium relationships between solid and liquid phases in chiral systems. They are indispensable for identifying suitable operating conditions for selective crystallization, understanding solubility limits, and avoiding unwanted nucleation events.

1.2.4. Practical Considerations

Phase diagrams are typically constructed by measuring solubility and melting behavior across a range of compositions and temperatures. For conglomerate systems, the absence of racemic compounds and solid solutions simplifies interpretation. However, metastable equilibria and kinetic factors must also be considered, especially when designing processes that rely on supersaturation and controlled nucleation.

1.3. Aim of the thesis

The potential of the attrition-enhanced deracemizations described above, and related techniques, served as the basis for a HORIZON 2020 project Continuous Resolution and Deracemization of Chiral Compound by Crystallization (CORE). The CORE Network set the goal to produce remarkable advances in the field of resolution and deracemization. One branch of the network focused on switching from a batchwise to a continuous mode, in order to enhance the productivity. A second branch focused on extending the application of racemization techniques applying principles and technologies so far not exploited in the field of deracemization. Both branches were supported and strengthened by the application of process analytical technologies and modeling platforms. The author has carried out his PhD research under the auspices of this program. The main focus of this PhD thesis is on crystallization enhanced deracemization techniques with a minor focus on preferential crystallization.

Previously, much research^[1, 3] has been addressed to these techniques within Syncom, the contract research organization that hosted most of the research described in this thesis.

At an early stage "Clopidogrel imine" (**1**) was identified in this CORE program as a suitable target using "Viedma Ripening" for continuous deracemization. The author has carried out the deracemization of this compound by using a decoupled flow system. The results of preliminary experiments are described in Chapter 2 of this thesis. The objectives of this work were to test use an easily racemizable compound which did not show any particular issue related to polymorphism to test alternative methods that could be applied to more difficult to racemize compounds. Other crystallization methods, like melt crystallization, were used to attempt deracemization without the use of an external base.

The most interesting organic chiral target compounds for deracemization have racemic crystal structures, i.e. the enantiomers are paired in a single crystal. Conglomerates, wherein the enantiomers crystallize as separate phases, form a minority, estimated to be around 10%.^[12] It is often possible to find derivatives of the compound of interest, formed reversibly, that are conglomerates. These may be covalent derivatives, salts, co-crystals, solvates, or a combination. The second major challenge for application of deracemization techniques is racemization in solution. Many chiral compounds are not readily racemizable and conditions compatible with the crystallization techniques required are not readily found. The third major challenge is the combination of racemization methods not compatible with a traditional one-pot batch equipment. The harsh conditions required for racemization of low reactive compounds (e.g. high temperature and pressure) increase the solubility leading to a lower yielding process. An example of how to solve this issue is described in the Chapter 3^[13] for the highly challenging CORE target compound Praziquantel (Figure 5). The objective of this chapter is to obtain enantiopure (*R*)-Praziquantel through crystallization enhanced deracemization of a previously unknown conglomerate precursor.

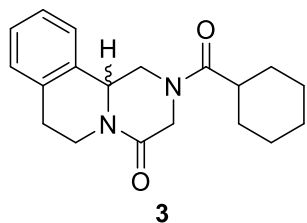


Figure 5: structure of racemic Praziquantel.

Praziquantel is used for treatment of schistosomiasis, a disease that afflicts some 200 million people every year. The (*R*)-enantiomer is more effective although the cheaper racemate is used for treatment.^[14]

Deracemization would therefore be attractive. However, Praziquantel is not a conglomerate and racemization of this compound is extremely challenging. A clean method to carry out racemization at higher temperatures has been accomplished and this has been coupled to a low temperature crystallization technique, temperature cycling, to achieve successful deracemization of the racemate to the desired (*R*)-enantiomer.

Much effort, so far unsuccessful, has been made to deracemize Flurbiprofen (Figure 6). Flurbiprofen is a Non-Steroidal Anti-Inflammatory Drug (NSAID). It was approved as a commercial preparation for the symptomatic treatment of rheumatoid arthritis and osteoarthritis. Unlike other NSAIDs,^[15] Flurbiprofen does not undergo *in vivo* racemization in humans,^[16] therefore it would be highly desirable to administer only the active (*S*)-enantiomer.

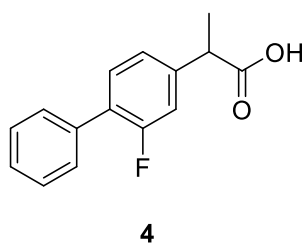
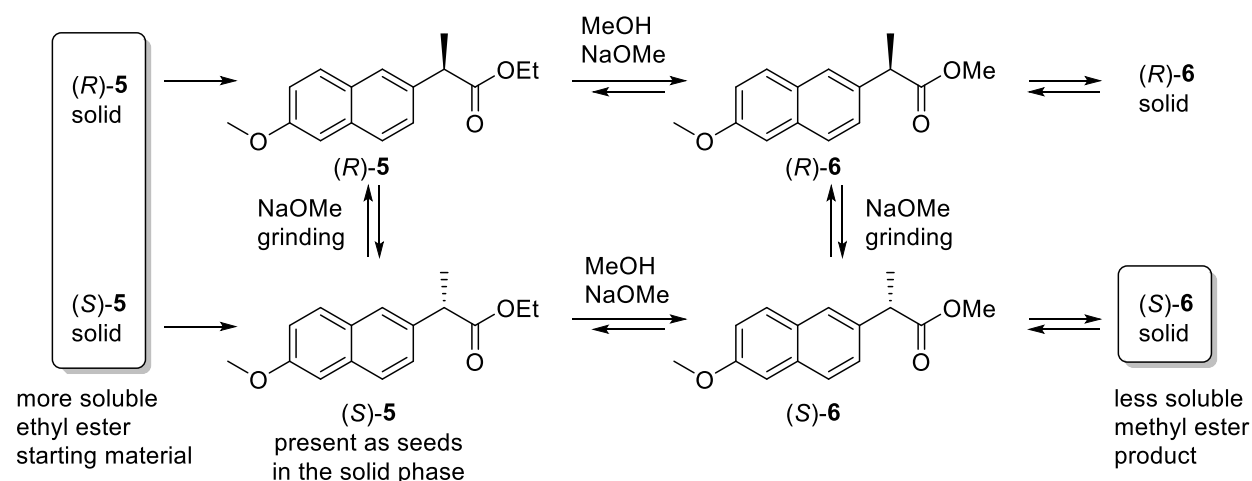


Figure 6: structure of racemic Flurbiprofen.

This β -aryl propionic acid derivative is closely related to Naproxen. The latter as methyl ester (conglomerate) has been deracemized using attrition-enhanced deracemization (Viedma Ripening, Scheme 1-2).^[17]



Scheme 1-2: deracemization of naproxen ester by gradual feeding. The ethyl ester, more soluble conglomerate than the methyl ester, was used as a starting material to speed up the dissolution process of the unwanted enantiomer. In the methanolic solution, sodium methoxyde acted both as a racemization and as a transesterification catalyst. The initially enantiomerically pure

suspension was gradually fed with racemic **5** in order to maintain a high enantiomeric excess in the solid phase and thus, in order to overcome the slowest part of the autocatalytic process.

Benzylamine and dibenzylamine salts of Flurbiprofen are known to be conglomerates.^[18] However, base induced deracemization analogous to the naproxen example requires relatively high temperatures. Racemization and crystallization therefore must be separated. Flow systems have been used as well as specific racemase enzymes in order to find milder racemization conditions. These experiments are described in Chapter 4. The first objective is to identify some racemization method that can possibly be exploited in a crystallization enhanced deracemization technique. The second objective is to characterize the solid state of the conglomerate salts in order to determine the best conditions for enantioselective crystallization exploiting techniques. Another objective is to attempt the deracemization of Flurbiprofen salts by using a decoupled system where the use of a separate racemization unit prevents:

- the need for high amounts of compound to obtain a suspension in the dissolution/crystal growth chamber in the case of base catalysis at high temperature.
- the enzyme to become prematurely inactivated due to grinding or temperature cycles in the case of biocatalysis.

All of this work has been carried out under the auspices of the CORE program. In total 15 PhD students at 6 universities and one company, Syncom, have been involved. There have been regular meetings and summer schools. The author has profited from the free exchange of information with others and from the traineeships. The CORE program has been successful. Publications that have appeared so far are summarized in:^[2a, 13, 19]

1.4. Impact and outputs

This thesis addresses critical limitations in crystallization-enhanced deracemization (CED) techniques, a field with substantial implications for the pharmaceutical, agrochemical, and fine chemical industries. The research presented herein introduces novel methodologies for overcoming challenges associated with racemization and crystallization, extending the applicability of CED to a broader range of compounds and reaction conditions. A key output of this work is the generation of a new library of derivatives, facilitating the identification and utilization of conglomerate systems. Furthermore, the findings of this research have been disseminated through peer-reviewed publication in the *Angewandte Chemie International Edition* (<https://pureportal.strath.ac.uk/en/publications/combining-incompatible-processes-for->

[deracemization-of-praziquantel](#)), demonstrating the impact of combining incompatible processes for deracemization of Praziquantel. The developed technologies and gained insights contribute to more efficient, sustainable, and economically viable methods for producing enantiomerically pure compounds, paving the way for advancements in various sectors reliant on chiral molecules.

1.5. References

- [1] W. L. Noorduin, T. Izumi, A. Millemaggi, M. Leeman, H. Meekes, W. J. P. Van Enkevort, R. M. Kellogg, B. Kaptein, E. Vlieg, D. G. Blackmond, *Journal of the American Chemical Society* **2008**, *130*, 1158-1159.
- [2] a) C. Xiouras, J. H. Ter Horst, T. Van Gerven, G. D. Stefanidis, *Crystal Growth & Design* **2017**, *17*, 4965-4976; b) L.-C. Söğütöglu, R. R. E. Steendam, H. Meekes, E. Vlieg, F. P. J. T. Rutjes, *Chemical Society Reviews* **2015**, *44*, 6723-6732; c) W. L. Noorduin, W. J. P. van Enkevort, H. Meekes, B. Kaptein, R. M. Kellogg, J. C. Tully, J. M. McBride, E. Vlieg, *Angewandte Chemie International Edition* **2010**, *49*, 8435-8438.
- [3] a) M. W. van der Meijden, M. Leeman, E. Gelens, W. L. Noorduin, H. Meekes, W. J. P. van Enkevort, B. Kaptein, E. Vlieg, R. M. Kellogg, *Organic Process Research & Development* **2009**, *13*, 1195-1198; b) P. Wilmink, C. Rougeot, K. Wurst, M. Sanselme, M. van der Meijden, W. Saletta, G. Coquerel, R. M. Kellogg, *Organic Process Research & Development* **2015**, *19*, 302-308.
- [4] a) C. Viedma, G. Coquerel, P. Cintas, *Handbook of Crystal Growth*, Elsevier: Boston, **2015**; b) Y. Saito, H. Hyuga, *Journal of the Physical Society of Japan* **2008**, *77*, 113001; c) M. Uwaha, *Journal of the Physical Society of Japan* **2008**, *77*, 083802-083802.
- [5] a) R. Kellogg, M. Leeman, **2012**; b) R. M. Kellogg, in *Advances in Organic Crystal Chemistry: Comprehensive Reviews 2015* (Eds.: R. Tamura, M. Miyata), Springer Japan, Tokyo, **2015**, pp. 421-443; c) R. M. Kellogg, M. Leeman, in *Comprehensive Chirality* (Eds.: E. M. Carreira, H. Yamamoto), Elsevier, Amsterdam, **2012**, pp. 367-399.
- [6] W. L. Noorduin, P. van der Asdonk, A. A. C. Bode, H. Meekes, W. J. P. van Enkevort, E. Vlieg, B. Kaptein, M. W. van der Meijden, R. M. Kellogg, G. Deroover, *Organic Process Research & Development* **2010**, *14*, 908-911.
- [7] K. Suwannasang, A. E. Flood, C. Rougeot, G. Coquerel, *Crystal Growth & Design* **2013**, *13*, 3498-3504.
- [8] J. Jacques, A. Collet, S. H. Wilen, *Enantiomers, racemates, and resolutions*, Wiley, **1981**.
- [9] G. Levilain, G. Coquerel, *CrystEngComm* **2010**, *12*, 1983-1992.
- [10] a) R. E. Pincock, R. R. Perkins, A. S. Ma, K. R. Wilson, *Science* **1971**, *174*, 1081-1020; b) K. R. Wilson, R. E. Pincock, *Journal of the American Chemical Society* **1975**, *97*, 1474-1478.
- [11] D. K. Kondepudi, J. Laudadio, K. Asakura, *Journal of the American Chemical Society* **1999**, *121*, 1448-1451.
- [12] T. Rekis, *Acta Crystallographica Section B* **2020**, *76*, 307-315.
- [13] G. Valenti, P. Tinnemans, I. Baglai, W. L. Noorduin, B. Kaptein, M. Leeman, J. H. ter Horst, R. M. Kellogg, *Angewandte Chemie International Edition* **2021**, *60*, 5279-5282.
- [14] I. Meister, K. Ingram-Sieber, N. Cowan, M. Todd, M. N. Robertson, C. Meli, M. Patra, G. Gasser, J. Keiser, *Antimicrobial Agents and Chemotherapy* **2014**, *58*, 5466.
- [15] J. V. Andersen, S. H. Hansen, *Journal of Chromatography B: Biomedical Sciences and Applications* **1992**, *577*, 362-365.

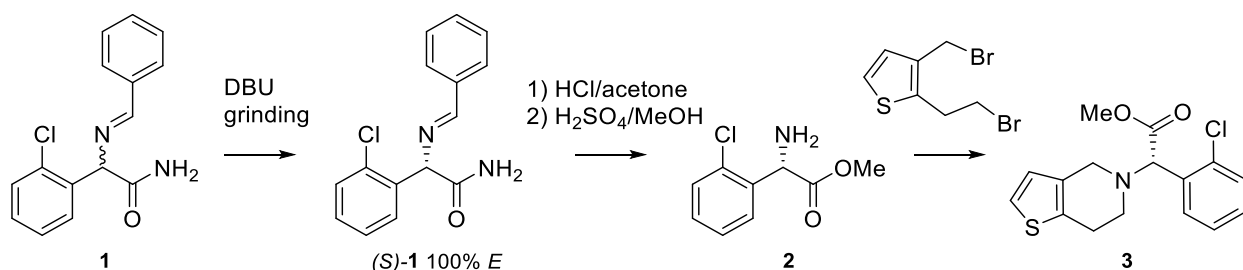
- [16] F. Jamali, B. W. Berry, M. R. Tehrani, A. S. Russell, *Journal of Pharmaceutical Sciences* **1988**, *77*, 666-669.
- [17] W. L. Noorduin, B. Kaptein, H. Meekes, W. J. P. van Enckevort, R. M. Kellogg, E. Vlieg, *Angewandte Chemie International Edition* **2009**, *48*, 4581-4583.
- [18] B. Kaptein, E. Vlieg, W. L. Noorduin, PCT Int. Appl., **2012**, WO2010089343 (A1)
- [19] a) A. H. J. Engwerda, N. Koning, P. Tinnemans, H. Meekes, F. M. Bickelhaupt, F. P. J. T. Rutjes, E. Vlieg, *Crystal Growth & Design* **2017**, *17*, 4454-4457; b) R. M. Kellogg, *Accounts of Chemical Research* **2017**, *50*, 905-914; c) R. R. E. Steendam, J. H. ter Horst, *Crystal Growth & Design* **2017**, *17*, 4428-4436; d) Q. Viel, L. Delbreilh, G. Coquerel, S. Petit, E. Dargent, *The Journal of Physical Chemistry B* **2017**, *121*, 7729-7740; e) G. Belletti, H. Meekes, F. P. J. T. Rutjes, E. Vlieg, *Crystal Growth & Design* **2018**, *18*, 6617-6620; f) B. Bodák, G. M. Maggioni, M. Mazzotti, *Crystal Growth & Design* **2018**, *18*, 7122-7131; g) F. Breveglieri, G. M. Maggioni, M. Mazzotti, *Crystal Growth & Design* **2018**, *18*, 1873-1881; h) T. Fröhlich, C. Reiter, M. E. M. Saeed, C. Hutterer, F. Hahn, M. Leidenberger, O. Friedrich, B. Kappes, M. Marschall, T. Efferth, S. B. Tsogoeva, *ACS Medicinal Chemistry Letters* **2018**, *9*, 534-539; i) R. Oketani, M. Hoquante, C. Brandel, P. Cardinael, G. Coquerel, *Crystal Growth & Design* **2018**, *18*, 6417-6420; j) B. Bodák, G. M. Maggioni, M. Mazzotti, *Crystal Growth & Design* **2019**, *19*, 6552-6559; k) F. Breveglieri, M. Mazzotti, *Crystal Growth & Design* **2019**, *19*, 3551-3558; l) T. Carneiro, S. Bhandari, E. Temmel, H. Lorenz, A. Seidel-Morgenstern, *Crystal Growth & Design* **2019**, *19*, 5189-5203; m) J.-J. Devogelaer, S. J. T. Brugman, H. Meekes, P. Tinnemans, E. Vlieg, R. de Gelder, *CrystEngComm* **2019**, *21*, 6875-6885; n) J.-J. Devogelaer, H. Meekes, E. Vlieg, R. de Gelder, *Acta Crystallographica Section B* **2019**, *75*, 371-383; o) L. C. Harfouche, C. Brandel, Y. Cartigny, J. H. ter Horst, G. Coquerel, S. Petit, *Molecular Pharmaceutics* **2019**, *16*, 4670-4676; p) A. Mbodji, G. Gbabode, M. Sanselme, N. Couvrat, M. Leeman, V. Dupray, R. M. Kellogg, G. Coquerel, *Crystal Growth & Design* **2019**, *19*, 5173-5183; q) R. Oketani, F. Marin, P. Tinnemans, M. Hoquante, A. Laurent, C. Brandel, P. Cardinael, H. Meekes, E. Vlieg, Y. Geerts, G. Coquerel, *Chemistry – A European Journal* **2019**, *25*, 13890-13898; r) R. Oketani, H. Takahashi, M. Hoquante, C. Brandel, P. Cardinael, G. Coquerel, *Journal of Molecular Structure* **2019**, *1184*, 36-40; s) E. Temmel, M. J. Eicke, F. Cascella, A. Seidel-Morgenstern, H. Lorenz, *Crystal Growth & Design* **2019**, *19*, 3148-3157; t) C. Xiouras, G. Belletti, R. Venkatramanan, A. Nordon, H. Meekes, E. Vlieg, G. D. Stefanidis, J. H. Ter Horst, *Crystal Growth & Design* **2019**, *19*, 5858-5868; u) G. Belletti, C. Tortora, I. D. Mellema, P. Tinnemans, H. Meekes, F. P. J. T. Rutjes, S. B. Tsogoeva, E. Vlieg, *Chemistry – A European Journal* **2020**, *26*, 839-844; v) F. Cascella, A. Seidel-Morgenstern, H. Lorenz, *Chemical Engineering & Technology* **2020**, *43*, 329-336; w) F. Cascella, E. Temmel, A. Seidel-Morgenstern, H. Lorenz, *Organic Process Research & Development* **2020**, *24*, 50-58; x) L. C. Harfouche, C. Brandel, Y. Cartigny, S. Petit, G. Coquerel, *Chemical Engineering & Technology* **2020**, *43*, 1093-1098; y) L. C. Harfouche, N. Couvrat, M. Sanselme, C. Brandel, Y. Cartigny, S. Petit, G. Coquerel, *Crystal Growth & Design* **2020**, *20*, 3842-3850; z) A. Mbodji, G. Gbabode, M. Sanselme, Y. Cartigny, N. Couvrat, M. Leeman, V. Dupray, R. M. Kellogg, G. Coquerel, *Crystal Growth & Design* **2020**, *20*, 2562-2569; aa) C. Tortora, C. Mai, F. Cascella, M. Mauksch, A. Seidel-Morgenstern, H. Lorenz, S. B. Tsogoeva, *ChemPhysChem* **2020**, *21*, 1775-1787; ab) J.-J. Devogelaer, H. Meekes, P. Tinnemans, E. Vlieg, R. de Gelder, *Angewandte Chemie International Edition* **2020**, *59*, 21711-21718.

Chapter 2: Testing New Crystallization-Enhanced Deracemization
Techniques Using 2-Chlorophenylglycinamide

(*S*)-2-(2-Chlorophenyl)glycinamide is one of the first pharmaceutically interesting intermediates obtained enantiomerically pure by attrition-enhanced deracemization and subsequently by other crystallization enhanced deracemization (CED) techniques like temperature cycling induced deracemization (TCID). In the published procedures, racemization is always catalyzed by a non-nucleophilic base like DBU. In this work racemization of (*S*)-2-(2-Chlorophenyl)glycinamide is demonstrated in absence of an external base when enantiopure compound is melted. Characterization by means of DSC of crystals of (*S*)-2-(2-Chlorophenyl)glycinamide with different enantiomeric excess suggests the emergence of two different crystal forms. Deracemization through CED without the use of an external base was attempted in two ways. The first consists of melt crystallization, the second one through a homemade decoupled flow system that allows crystals and part of the solution to undergo different operating procedures.

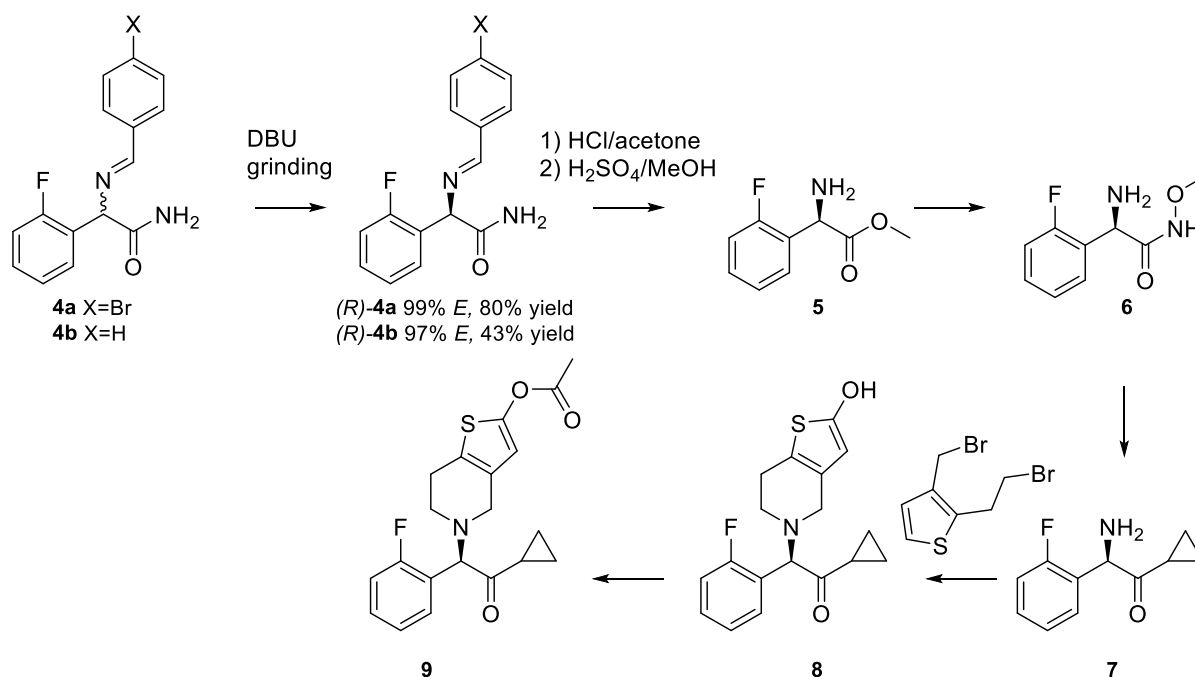
2.1. Introduction

(*S*)-2-(2-Chlorophenyl)glycinamide (**1**) can be used as a key intermediate in the synthesis of the blockbuster drug Clopidogrel (**3**, Scheme 2-1). Clopidogrel (Plavix) is a platelet aggregation inhibitor used for treatment of ischemic strokes, heart attacks, atherosclerosis and also for the prevention of thrombosis after placement of intracoronary artery stents.^[1] It is administered orally as the pure (*S*)-enantiomer, since the (*R*)-enantiomer is linked to lack of antithrombotic activity and triggered convulsions at high doses in animal models.^[2] The desired enantiopure Clopidogrel is accessible through diastereomeric resolution of racemic Clopidogrel with L-camphor sulfonic acid (CSA),^[3] or the intermediate 2-chlorophenylglycine methyl ester with L-(+)-tartaric acid.^[4] Classical resolution is limited to 50% yield, unless the unwanted enantiomer can racemize. The recently discovered attrition-enhanced deracemization allows to overcome this limitation reducing the waste of the counter enantiomer in one single elegant process. Such a process is conveniently applicable to 2-chlorophenylglycinamide **1** because this compound has been proven to be a conglomerate and easy to racemize at room temperature.^[5]



Scheme 2-1: Synthetic route to Clopidogrel (**3**) employing the deracemization protocol.

The same strategy was later exploited by Wilmink *et al* to obtain a route for the synthesis of enantiomerically pure (*R*)-Prasugrel (**9**, Scheme 2-2), a structurally related analogue of Clopidogrel but with improved pharmacological properties.^[6] The 4-bromobenzylidene precursor **4a** and the benzylidene precursor **4b** were identified as conglomerates among a library of 10 imine derivatives. **4a** was successfully deracemized in butyronitrile and 2-methylbutyronitrile. Unfortunately, good yields of the deracemization process of the conglomerate **4b**, by using acetonitrile as a solvent at room temperature, were hampered by the conversion of the conglomerate to an unidentified polymorph, and to the hydrate form (the latter was formed when moisture was present, e.g. in the headspace over the reaction mixture). The two species were most likely racemic compound forming systems since they hampered the deracemization. Even if in conglomerate systems the difference in melting point between the pure enantiomers and racemic mixtures is usually 20 °C or higher, only 6 °C and 4 °C was found for compounds for **4a** and **4b** respectively. Thus, in this work it was investigated if this odd difference in melting point was also observable in the structurally related compound **1**. If so, one might suspect racemization in the melt. Racemization of compound **1** in the melt could then be exploited for its deracemization.



Scheme 2-2: synthesis of (*R*)-Prasugrel (**9**) including an attrition enhanced deracemization protocol of **4** → (*R*)-**4**.

As demonstrated by Kondepudi, deracemization can be conducted by crystallization of a melt, while stirring with a magnetic bar.^[7] The prerequisites are that the target compound must racemize in the melt and crystallize from it as a conglomerate in presence of constant stirring. While small enantiopure crystals

are obtained by means of supersaturation induced by cooling (primary nucleation), chiral amplification is promoted by fragmentation of such enantiopure crystals by means of collision and grinding under the effects of the magnetic bar and by means of the fluid shear (secondary nucleation).

In order to combat the stochastic outcome in chirality linked to primary nucleation from the racemic mixture, an excess of crystals of the desired handedness can be added.^[8] Indeed, enantiopure crystals are expected to remain solid at (or slightly above) the melting point of the racemic mixture, by virtue of their higher melting point which is usually 20 °C or higher. The enantiopure crystals suspended in the melt provide the surface for enantioselective crystal growth.

Melt crystallization, owing to its simplicity, can become an attractive method for the production of pharmaceutically interesting pure enantiomers provided that no decomposition occurs during the process. Racemization must occur selectively in the melt and not in the solid state in order to preserve the excess of enantiopure crystals gained. Finally, the excess of enantiopure crystals must survive the metastable zone (MSZ). The latter is the temperature frame between melting and crystallization from the melt. The latter always takes place below the melting point.

Racemization in the melt is known to work for compounds that exhibit atropisomerism,^[7] namely molecules with a chiral axis (single bond) whose helical sense is maintained through hindered rotation, for instance because of steric congestion.^[9] If a chiral compound that does not show atropisomerism racemizes into the melt without the need of an external catalyst, racemization reaction is most likely autocatalytic. Autocatalytic racemization might be promoted by the reversible reaction of one or more functional groups (which might act, for example, as a base) of such chiral compound with one of the substituents of the chiral center. In principle such an autocatalytic reaction can happen also in presence of solvent, provided that the solvent does not affect the reactivity. Compound **1** has both a proton bound to the chiral carbon with an enhanced acidity and a slightly basic functional group, namely the imine with its lone pair.

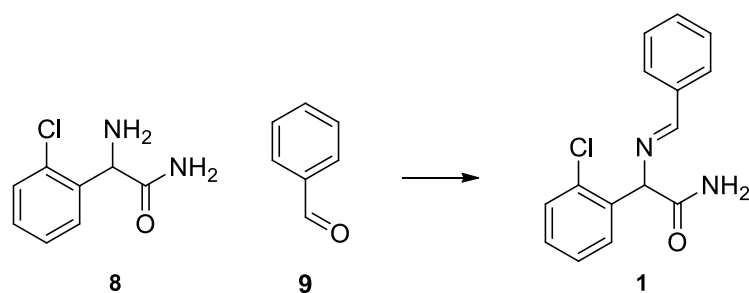
Thus, melting point determination of both racemic and enantiopure **1** was initially carried out with the aim of attempting deracemization by using a melt crystallization technique without the use of an external base catalyst. Because the temperature needed to melt compound **1** is relatively high, formation of byproduct might be expected. The solvent helps to dissipate the reaction heat. It was envisaged that a polar aprotic solvent might help to prevent the irreversible cyclization of the imine **1** to the side product already described in literature.^[10] However solubility of organic compounds increases along with the

temperature and this leads to low yields of the crystals recovered by filtration. Thus, deracemization was attempted in presence of a polar aprotic solvent like acetonitrile by using a setup where racemization is thought to take place within a heated flow tubing and the enantioselective dissolution/crystal growth process occurs simultaneously into a flask with a selective recirculation of the mother liquor between the two compartments.

2.2. Methods

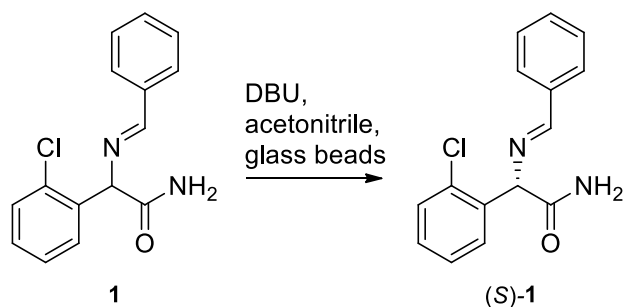
Chiral HPLC analyses were carried out on a Chiralpak IA column (4.6 x 250 mm, 5 μ m), gradient heptane/EtOH. 70/30, Flow: 0.7 mL/min with detections at 215.8 nm. DSC measurements were carried out at a ramp rate of 10 $^{\circ}$ C per minute on a DSC Q20 V24.11 Build 124 with closed pan. NMR spectra of all compounds were obtained on a Varian Mercury 300 MHz machine. All solvents were spectral grade. Chemical shifts δ of NMR spectra are reported in ppm relative to $(\text{CH}_3)_4\text{Si}$ at $\delta = 0$. With the exception of the amino amide **8**, which was already available in house, all the chemicals were purchased from Acros. Enantiomerically pure **1** used for both racemization and deracemization experiments was obtained by attrition enhanced deracemization.

2.2.1. Synthesis of 2-chlorophenylglycinamide



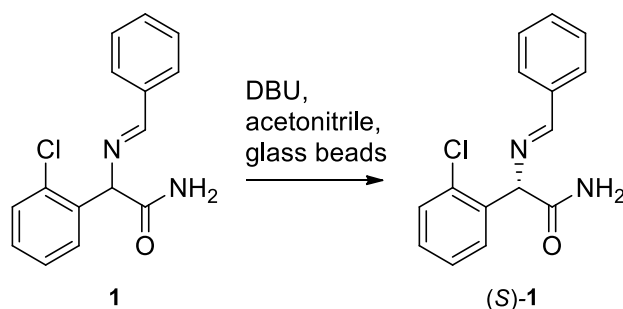
Imine **1** was synthesized according to the procedure described in literature.^[6] To a solution of racemic amide **8** (17.2 g, 318 mmol, 1.0 eq) in dichloromethane (DCM, 162 mL), benzaldehyde (10.4 mL, 102 mmol, 1.1 equiv) and Na_2SO_4 (73.4 g, 517 mmol, 1.63 equiv) were added and the mixture was stirred overnight at room temperature. The mixture was then heated with a hot water bath, and the solids were removed by filtration. The residue was washed with hot DCM (3 x 150 mL), and the combined mother liquors were concentrated in vacuo to afford a yellow/white solid. The product was washed with methyl tert-butyl ether (MTBE, 3 x 150 mL) to give imine **1** (24.4 g, 89 mmol, 96%) as a white solid. ^1H NMR (DMSO- d_6) δ 8.45 (1H, s), 7.87 (2H, dd), 7.63, (1H, dd), 7.44-7.51 (6H, m), 7.32-7.38 (2H, m), 5.43 (1H, s).

2.2.2. Deracemization of 2-chlorophenylglycinamide by attrition enhanced deracemization starting from racemic mixture



In a 50 mL round bottom flask equipped with a stirring egg, racemic imine **1** (1.260 g, 4.6 mmol) was combined with acetonitrile (14.1 mL). Glass beads (borosilicate, 2 mm, 10.3 g) were added followed by addition of DBU (207 μ L, 1.386 mmol). The mixture was allowed to grind using a stirring bar at 900 rpm at room temperature for one week. Chiral HPLC analysis revealed an $E = 99.8\%$. The suspension was withdrawn by using a glass pipette and collected by filtration under vacuum by using a glass funnel filter with P4 sintered glass disc. The resulting material was washed with MTBE (3 x 15 mL) to give (S)-**1** as a white solid (1.013 g, 3.7 mmol, yield = 80%).

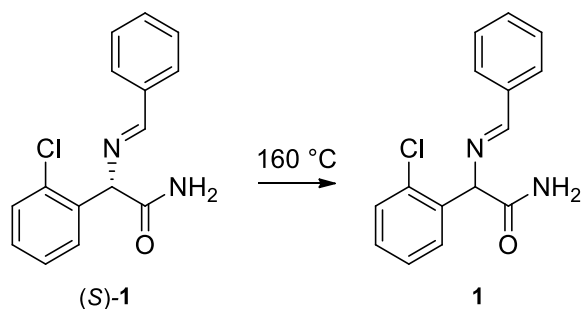
2.2.3. Deracemization of 2-chlorophenylglycinamide by using a decoupled system starting from scalemic mixture



An HPLC filter was connected to a HPLC to ensure a selective transport of the mother liquor to the racemization reactor. The racemization coil was connected from one side to an HPLC pump to the other side to the flask containing the suspension. The racemization coil was made of PFA (PerFluoroAlkoxy alkane, inside diameter = 1.0 mm, outside diameter 1/16", length = 255 cm; total internal volume of the racemization coil was 2 mL) and heated in an oil bath at 50 °C. The internal volume of the flow system was 6 mL. Both the inlet and the outlet of the flow system, together with a needle connected to the nitrogen line, pierced a septum that was used to cap the flask containing the slurry.

The flow system was flushed with MeCN at 2 mL/min for 10 minutes. The filter was submerged into a 50 mL round bottom flask containing a stirring egg, MeCN (26 mL), racemic **1** (3019 mg, 11 mmol), enantiopure (*S*)-**1** (537 mg, 1.97 mmol). The mixture was allowed to stir at 700 rpm for 15 min and glass beads (borosilicate, 2 mm, 23.4 g) were added to the mixture. The mixture was ground at 500 rpm and the 2 mL PFA coil was submerged into the oil bath at 50 °C. The mother liquor was allowed to recirculate into the flow system at 1 mL/min. After 100 hours the solid material together with glass beads was filtered and washed with MTBE (3 x 20 mL). After subtraction of the mass of the glass beads the mass of the crystalline product was 2.075 g, (yield = 68.7%, *E* = 98%).

2.2.4. Racemization of 2-chlorophenylglycinamide in the melt



A DSC pan was loaded with sample of roughly 2 mg of enantiomerically pure (*S*)-**1** and closed with the lid. The sample was heated at 10 °C/min to 160 °C and the temperature was held for 1 minute. The pan was opened after being allowed to cool down at room temperature. The pan was transferred into a 4 mL vial, submerged into 1 mL IPA and sonicated into an ultrasonic bath for 1 minute. Chiral HPLC analysis of the resulting IPA solution revealed an *E* = 1.6 %.

2.3. Results

2.3.1. Racemization of 2-chlorophenylglycinamide in the melt.

In conglomerate systems, the difference in melting point ($\Delta T_{S-rac}^f = \Delta T_S^f - \Delta T_{rac}^f$) between enantiomerically pure (*R* or *S*) and racemic mixture (*rac*) is typically 20 °C or higher. Imine **1** crystallizes as a conglomerate, as demonstrated by attrition enhanced deracemization and Single Crystal X-Ray Diffraction (SC-XRD) analysis of a crystal nucleated and grown from a racemic solution of **1**.^[5] However the melting point (T_R^f) of a first sample of enantiomerically pure compound obtained from Viedma ripening is initially found to be only 0.5 °C lower than the (T_{rac}^f) of the racemate, the latter synthesized by a procedure reported by Wilmink *et al.*^[6]

A sample obtained from Viedma ripening, with enantiomeric excess $E = 93\%$ was recrystallized by suspending it in acetonitrile for one day at room temperature with gentle stirring. After filtration, the resulting dry enantiomerically pure ($E = 99.9\%$) 2-chlorophenylglycine amide **1** was analyzed by DSC. The melting point was 156 °C ($T^f = 152$ °C), 6 °C higher than T^f of the racemate (Figure 7).

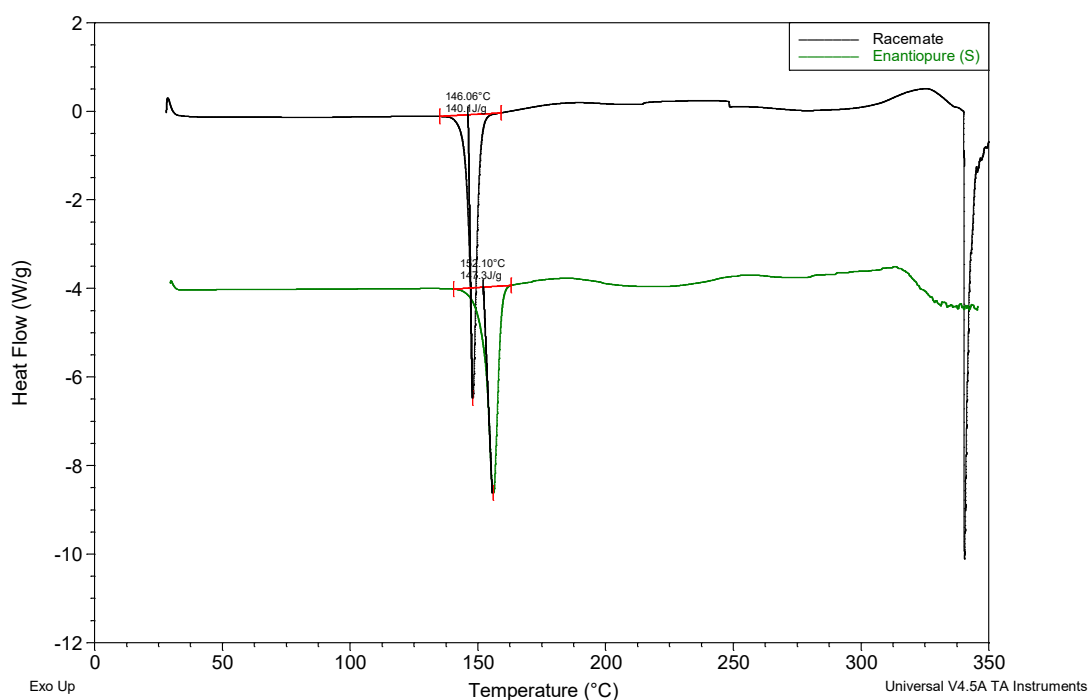


Figure 7: DSC of racemic (top) and enantiomerically pure (bottom) **1**.

These results are consistent with the difference in melting point between the pure enantiomers and racemic mixtures of two structurally related conglomerates discovered by Wilmink et al.^[6] Notably such racemic analogue compounds, according to literature, are not recrystallized in acetonitrile after the synthesis, just like racemic imine **1** analyzed in this chapter. Such racemic imines precipitated from a dichloromethane solution under vacuum by using the rotavapor. This fast crystallization could produce a crystalline form different from the one obtained through crystallization with simultaneous grinding from acetonitrile. This would justify the small temperature frame included between the melting points of the racemic and the corresponding enantiopure imines. Indeed, the pure enantiomer and racemic mixtures of such imines, analyzed by DSC, are always obtained by a recrystallization in acetonitrile in a crystallization enhanced deracemization processes. The DSC measurements shown in Figure 7 were performed once (n = 1). While the results are consistent with literature values and expected behavior for conglomerate systems, reproducibility has not been independently confirmed and should be validated in future studies.

Table 1: melting point (onset) of racemic (rac) and enantiopure (*S*) imine **1** with their relative heat of fusion (ΔH). Differences in melting points between enantiomerically pure and racemic imines (T_{S-rac}^f) are reported into the last column on the right. n.a.= not available.

Compound	T_S^f [°C]	ΔH [kJ/mol]	T_{rac}^f [°C]	ΔH [kJ/mol]	ΔT_{S-rac}^f [°C]
1	152.1	40.2	146.1	38.2	6.0
4a ^[6]	135	n.a.	129	n.a.	6
4b ^[6]	117.5	n.a.	113.2	n.a.	4.3

The existence of these two different crystal structures is supported by the DSC analysis of imine **1** with *E* = 98%, obtained by crystallization enhanced deracemization processes: an endothermic peak with onset 127 °C is present and followed by a second endothermic peak which is consistent with the melting point of the pure enantiomer.

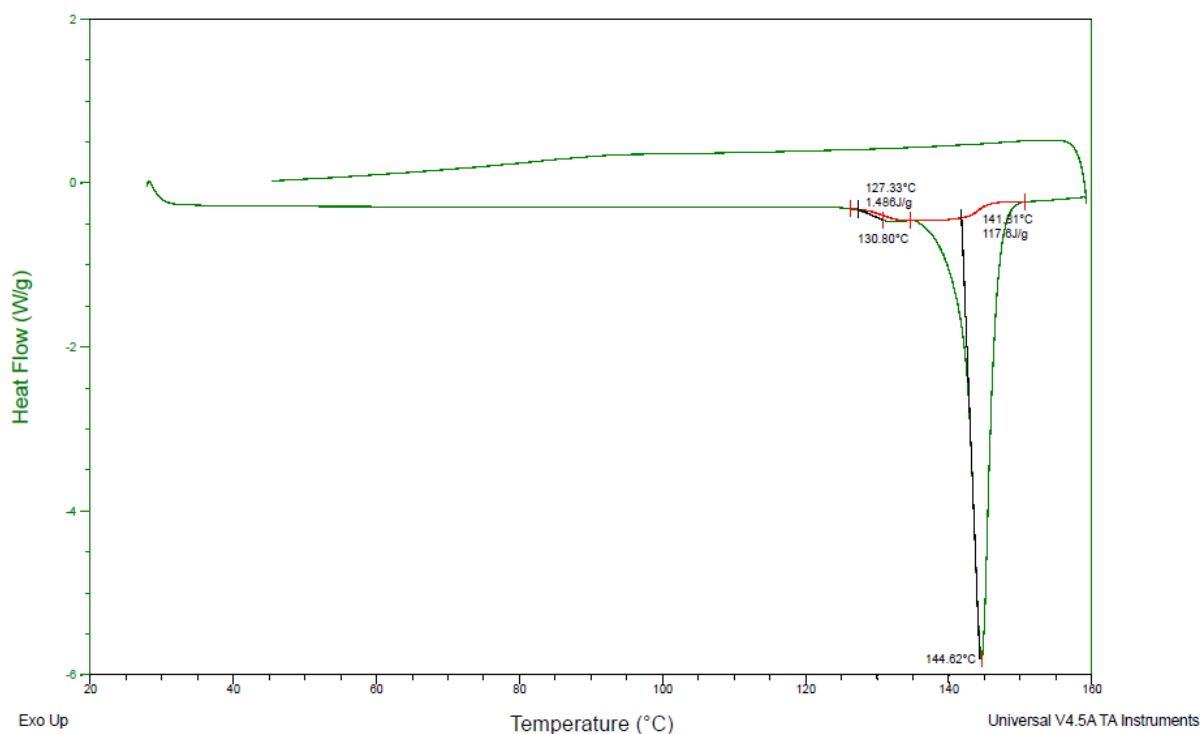


Figure 8: DSC of (*S*)-**1** *E* = 98% **1**. A small endothermic peak is detected before the melting point of imine **1**.

Notably, the endothermic peak at 127 °C is 25 °C lower than the melting point of the pure enantiomer obtained by crystallization-enhanced deracemization followed by a further isothermal recrystallization in acetonitrile. Thus, this peak at the lower temperature likely reflects the eutectic of a conglomerate system (Figure 9) because of two reasons: the first is that, in conglomerates, a difference in melting point between

enantiopure and racemic (eutectic) of 20 °C or higher is expected; the second is that this peak at 127 °C is observed with crystals formed under the same grinding conditions used to obtain the enantiopure conglomerate crystals that melt at 152 °C. The racemate melting at 146 °C probably has a different crystalline structure, which is most likely the stable one because the melting point is higher than the putative conglomerate eutectic (127 °C). Racemic **1** melting at 146 °C is obtained under different crystallization conditions than the isothermal grinding in acetonitrile and DBU used for the production of the conglomerate (*S*)-**1**. Racemic **1**, just like racemic imines **4a** and **4b**, is indeed obtained by rotary evaporation of imine **1** in presence of 0.1 equivalents of benzaldehyde (which is substituted for **4a** and **4b**) which is later removed by washing the resulting solid with MTBE. The confirmation of the existence of a second crystal form could be given by a DSC measurement of racemic and various scalemic imine **1** recrystallized in acetonitrile, together with XRPD of the material crystallized from dichloromethane, but this was not done because of time restraints.

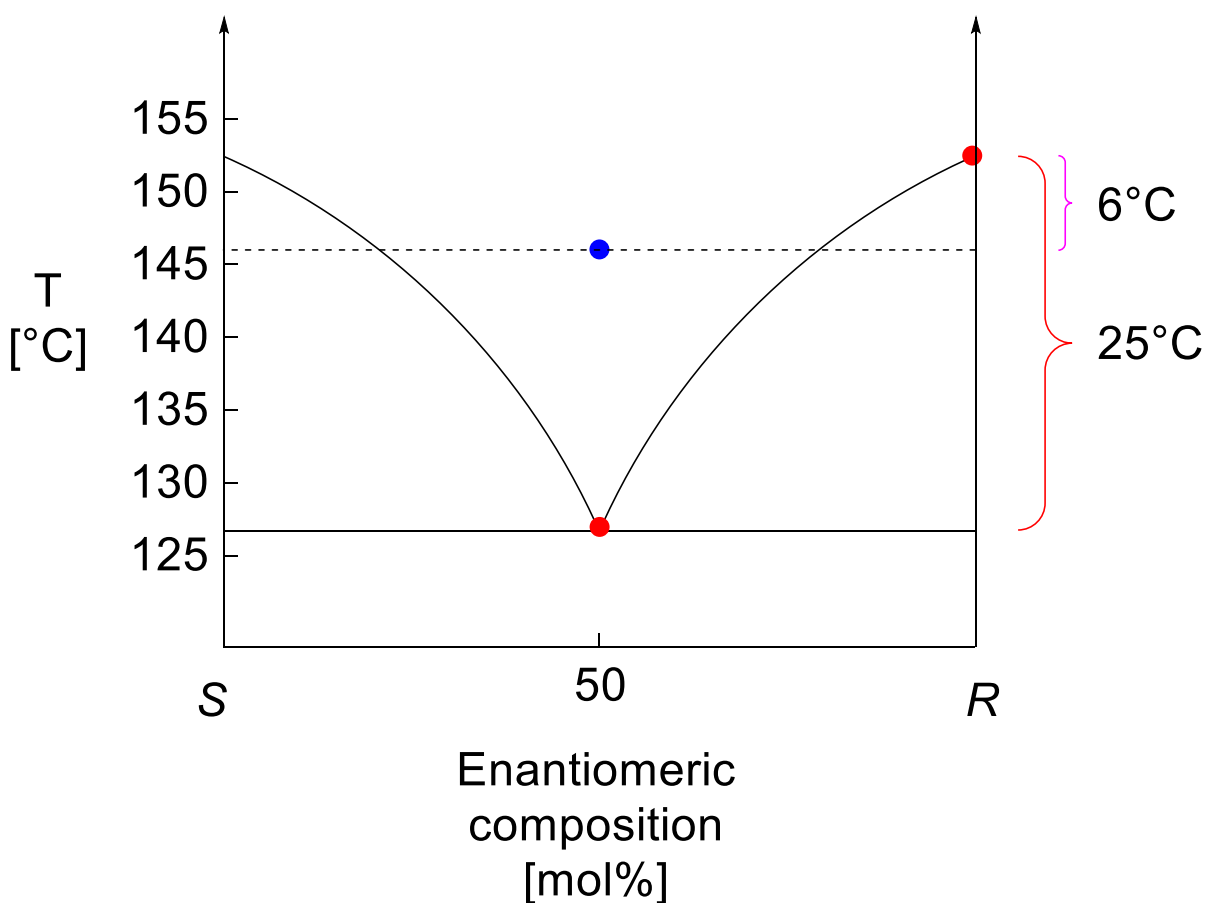
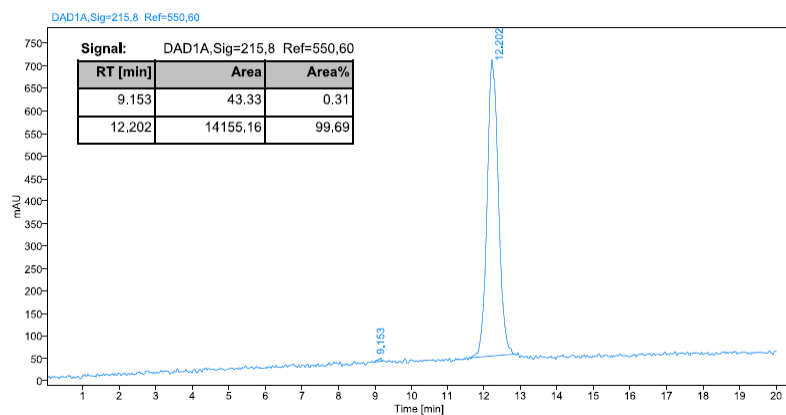


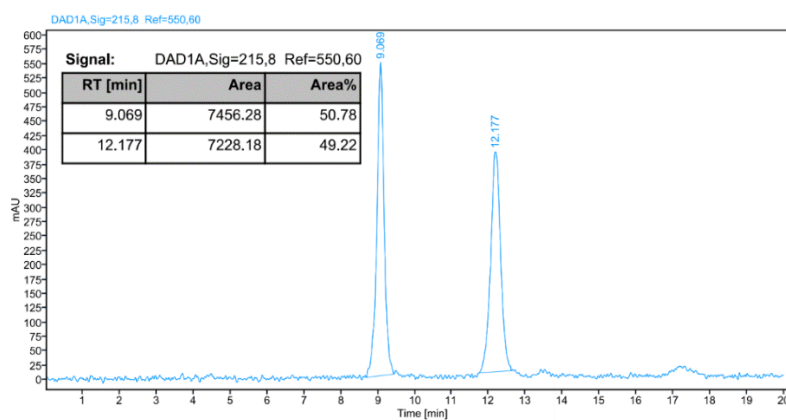
Figure 9: Proposed binary phase diagram of 2-chlorophenylglycinamide **1**, showing the melting behavior as a function of enantiomeric composition. The eutectic point (in red) at 127 $^{\circ}\text{C}$ is consistent with a conglomerate system. The blue point represents the melting temperature of a racemic sample obtained under different crystallization conditions, possibly corresponding to a distinct and more stable crystal form. The solid horizontal line indicates the melting point of the enantiopure compound (152 $^{\circ}\text{C}$), while the dashed line marks the eutectic temperature (127 $^{\circ}\text{C}$). This alternative racemic form, which melts at 146 $^{\circ}\text{C}$, may not reflect the eutectic behavior of the conglomerate system and suggests the possibility of polymorphism. This binary phase diagram is based on melting point data obtained from single DSC measurements. The eutectic and melting points were not replicated due to time constraints; therefore, the reproducibility of the phase behavior remains to be confirmed.

To investigate whether racemization occurs in the melt, enantiopure samples were subjected to melting for various times. After 1 minute in the melt at 160 $^{\circ}\text{C}$, two extra peaks (13.5 and 17 min, Figure 7b) emerge from the baseline at the chiral HPLC in addition to the enantiomers of **1** (Figure 10).

a)



b)



c)

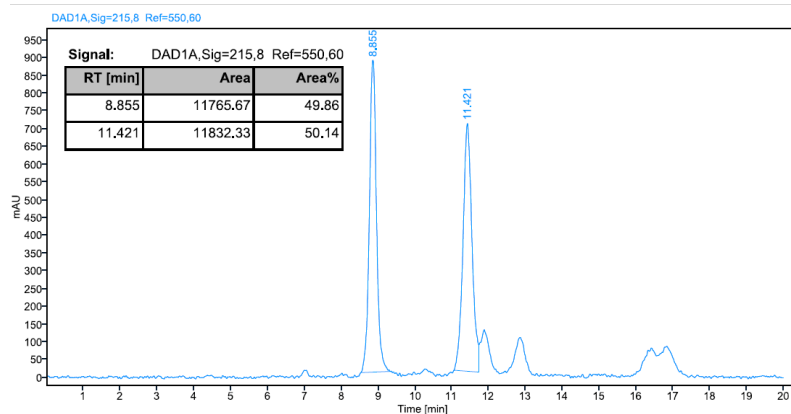
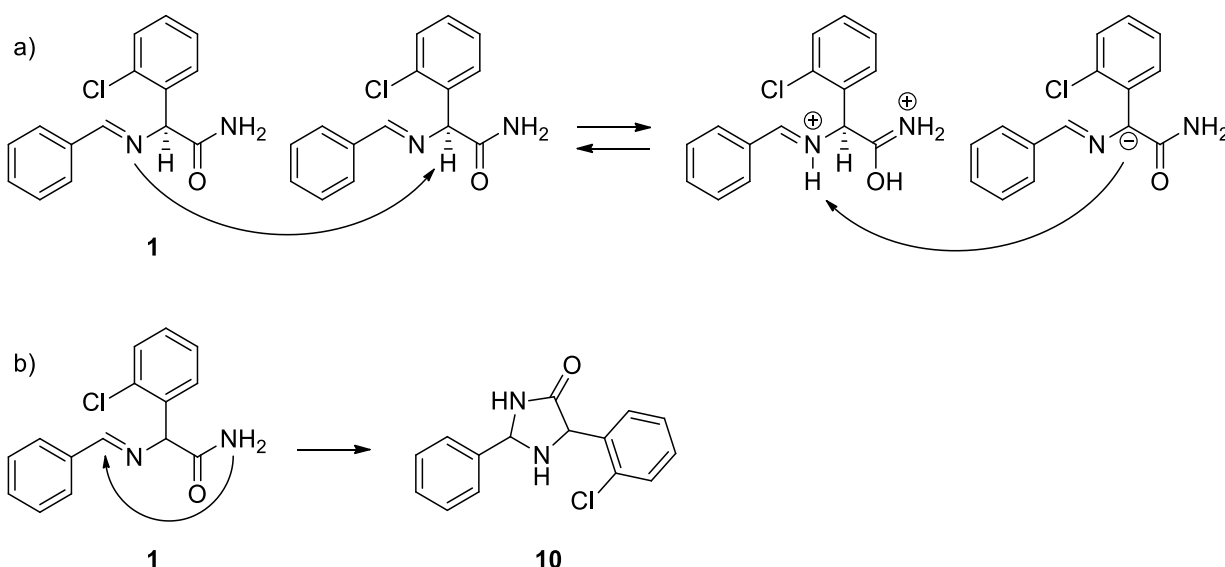


Figure 10: chiral chromatograms of the enantiomerically pure **1** before (a) and after being molten for 1 min (b) and 5 min (c) respectively at 160 °C.

When **1** is melted for 5 min (Figure 10c), four peaks with higher intensity are visible at 12, 13, 16.5 and 17.1 min respectively, leading one to think that in Figure 10b the peak at 12 min was overlapping the peak of one enantiomer of **1** and the peaks at 16.5 min and 17.1 min were collapsed in only one peak. These four peaks are consistent with an irreversible cyclization of **1** which results in a mixture of four diastereomers (with general structure **10** represented in Scheme 2-3b) with 50:50 ratio.^[10] The mechanism of racemization is probably intermolecular (Scheme 2-3a). The lone pair of the imine is free to abstract the hydrogen bound to the chiral carbon of another molecule. The same proton can land back on the chiral carbon in a random way.

DSC analyses were therefore necessary to know which temperature was needed to racemize the compound.



Scheme 2-3: a) proposed mechanism for thermally induced racemization of **1**. b) proposed byproduct formation by means of irreversible cyclization of **1** in the melt.

In principle this self-catalyzed racemization made the melt crystallization technique quite attractive. If enantiomerically pure crystals, the melting point of which is higher than the melting point of the racemate, are introduced into the melt while racemization is occurring, then crystal growth may occur in a deracemization process while the temperature is decreased below the melting point of the enantiopure, converting all the unwanted enantiomer into the desired one. In order to check the magnitude of the MSZ, a DSC of the racemate was performed: heating ramp (10 °C/min) was interrupted just above the melting point and a cooling ramp (10 °C/min) was started (Figure 11). No exothermic peaks were detected,

therefore crystallization did not occur. The lid covering the analyzed sample was removed and the mixture in the pan was a yellowish oil.

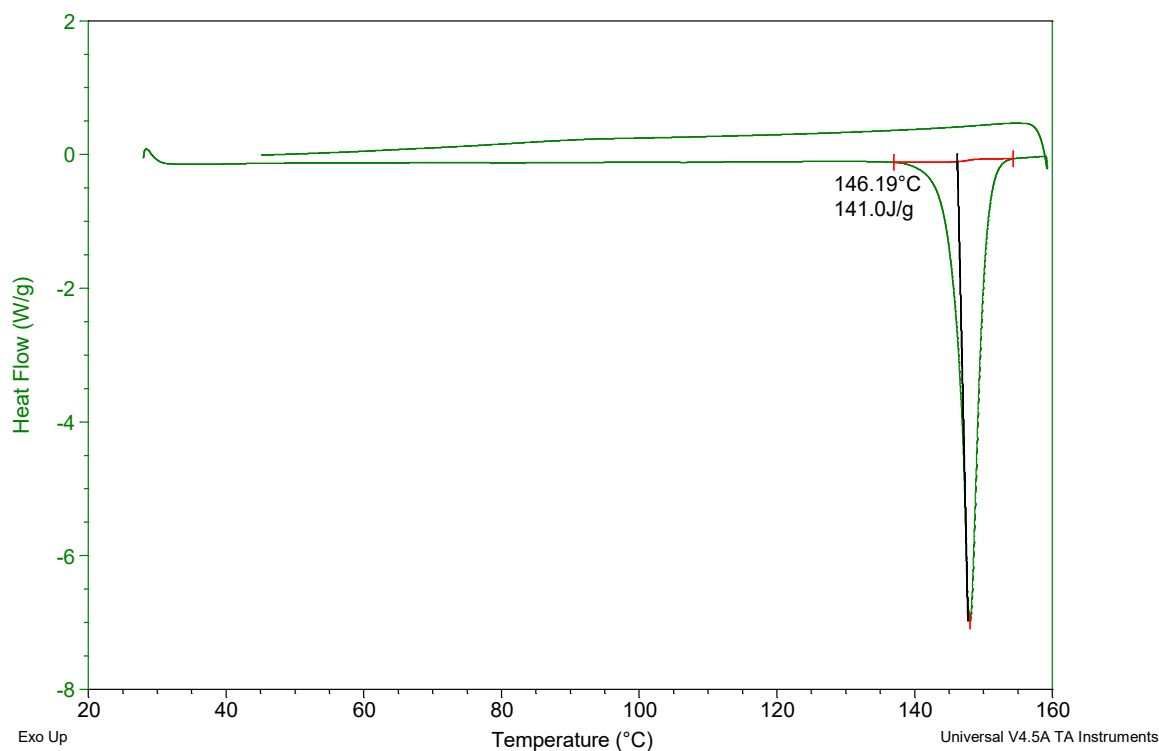


Figure 11: melting of racemic **1** followed by a cooling ramp. Exothermic crystallization event was not observed.

Nucleation might be inhibited by some degradation product (e.g. compound **10** in Scheme 2-3b). In such a case slower cooling ramps would not be useful to allow nucleation of **1** since conditions that favor the irreversible conversion of imine **1** to the cyclized product **10** would be prolonged. The introduction of seeds could have helped the crystal growth to take place. However, by melting 20 mg of racemate in an NMR tube at 160 °C and seeding with enantiomerically pure seeds of (*S*)-**1** at 137 °C during a cooling ramp of 10 °C/min, no observable crystal growth was detected. Crystals remained suspended in a yellowish oil. The mixture remained as such even after two days at room temperature. This suggests that the degradation product substantially inhibits the crystal growth of the mixture.

Compound **1** with *E* = 98% was then analyzed by DSC up to 131 °C (Figure 12) and then cooled down to observe the behavior of imine **1** at such conditions, since an endothermic peak was previously observed

at such temperature. The lid was opened and the white solid recovered from the lid was dissolved in isopropanol and analyzed by chiral HPLC. The enantiomeric excess turns out to be 64% suggesting that the molten mixture leads to racemization at the interface between melt and solid phase. Indeed, because the starting optical purity of the material used in this experiment is 98% and because the pure enantiomer was shown to melt at 152 °C, at 131 °C only the 2% of racemic **1** should be in the melt and no further melting of the remaining enantiopure fraction should occur. This unexpected racemization makes the application of the melt crystallization technique difficult because the high enantiomeric excess in the solid phase is not maintained even at temperatures below the melting point of the pure enantiomer.

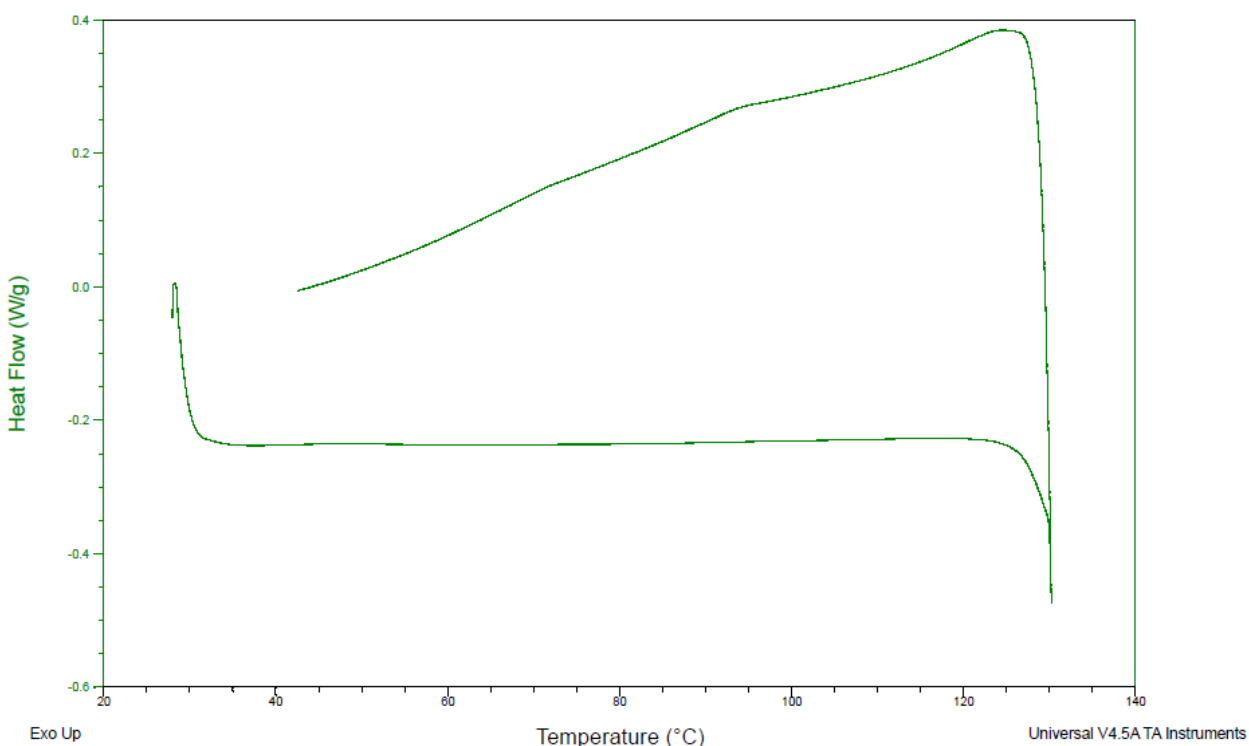


Figure 12: DSC of a sample with $E = 98\%$ heated at 131 °C where an endothermic event, probably melting of the 2% of its mass present as racemic conglomerate, was previously observed.

2.3.2. Deracemization by means of a decoupled system

Racemization in solution, which is a prerequisite for deracemization, increases in speed as the temperature increases.^[11] However as the temperature increases, the solubility increases as well. This is disadvantageous in crystallization enhanced deracemization processes, because the higher the solubility, the less is the material recovered in solid phase, thus the yield. This problem can be overcome by splitting high temperature racemization and low temperature crystallization into two separate compartments.

Recirculation of the mother liquor between the flask designated as crystallization chamber at low temperature and an external heated tubing would allow the constant availability of the desired enantiomer in solution. The desired enantiomer can then crystallize in the crystallization chamber at low temperature in good yield.

Racemization of **1** occurs in presence of DBU which is a relatively expensive base that cannot be recovered in a cost-effective manner at the end of the process. The previously demonstrated thermal induced racemization of **1** without using an external base like DBU, could occur also in organic solvents. Possibly, the use of a base-free racemization technique coupled to enantioselective crystallization could lead to an increased yield if the filtration of the deracemized product would be carried out at near room temperature.

High temperature could then be continuously applied on a fraction of mother liquor that, through the use of an appropriate filter linked to an external pipeline, is withdrawn from the thermostatted crystallization chamber, racemized in the tubing at high temperature, cooled down and pumped back into the crystallization chamber. This would allow to carry out the process without neither external base nor hot filtration, with improved yields and an easy recovery of the substrate from the mother liquor by crystallization.

A HPLC filter connected to a HPLC pump and submerged into the crystallization chamber allows the selective pumping of the liquid phase surrounding the crystals into the PFA tubing placed downstream to the pump. Crystals are allowed to remain in the crystallization flask. The central part of the PFA tubing is heated up while its extremity goes back to the crystallization chamber, once cooled down at room temperature. Such a strategy allows crystallization to occur in good yields, while the liquid phase recirculates in an external loop where heating can be applied.

The temperature in the crystallization flask has to be maintained below the temperature in the tubing and pumps which deliver mother liquor to the flow reactor in order to avoid nucleation and clogging in the flow system. Because tubing and pumps are at room temperature, the temperature in the crystallization flask is not expected to exceed 20 °C. The PFA coil reactor, with internal volume of 2 mL, are heated to 50 °C to enhance the rate of racemization.

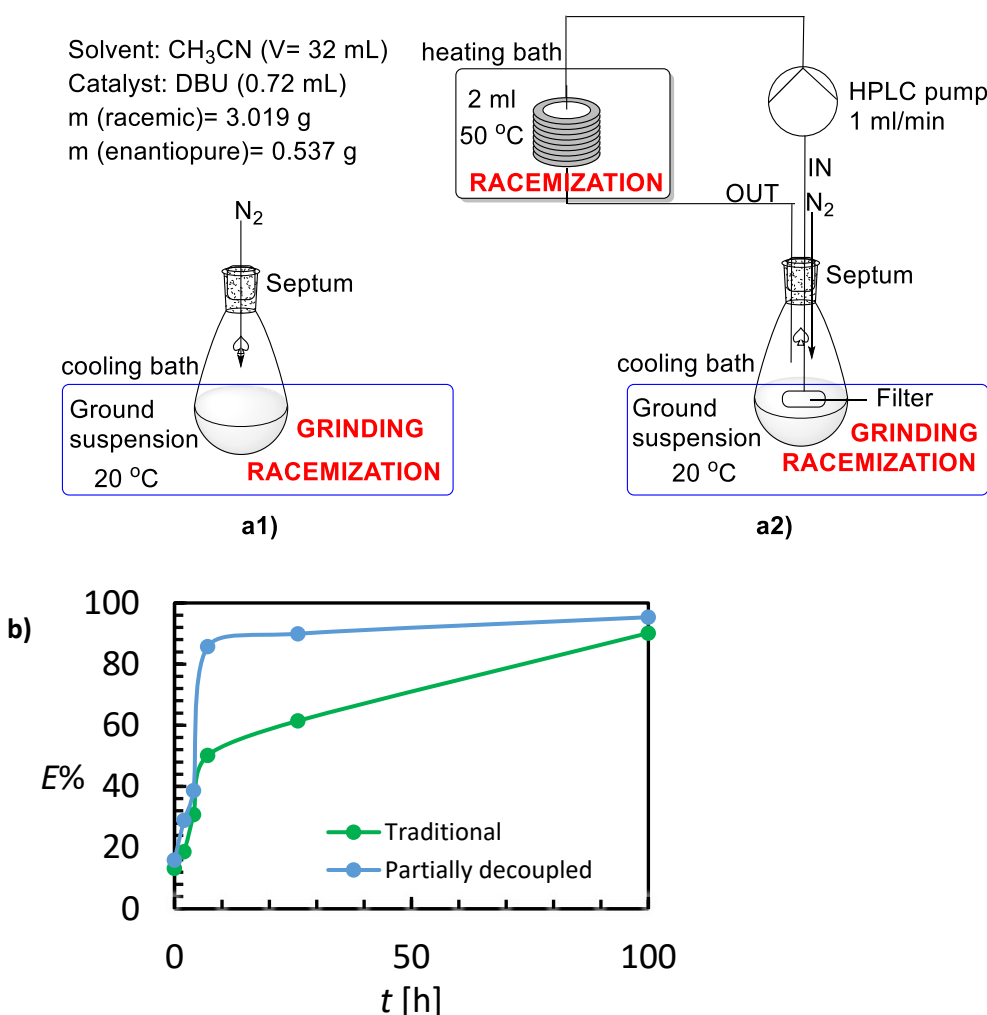


Figure 13: a1) schematic setup of a traditional Viedma ripening in batch where racemization and dissolution/crystal growth events occurs in the same flask. a2) schematic setup of a partially decoupled Viedma ripening, where racemization is enhanced through an external heated flow reactor. b) evolution of enantiomeric excess E over time of both the experiments.

After 100 hours both Viedma experiments are stopped, the solid material is filtered and washed with MTBE (3 x 20 mL). The chemically pure crystalline compound **1** is collected together with the glass beads. After subtraction of the mass of the glass beads the masses of the crystalline product is 2.153 g (yield = 71.3%, E = 90%) for the traditional one-pot Viedma ripening and 2.075 g, (yield = 68.7%, E = 98%) for the partially decoupled Viedma ripening where the racemization is enhanced by using an *ex-situ* flow reactor. In addition to the higher E the deracemization time was also considerably reduced from 26 to approximately 10 hours.

Racemization of **1** observed in the melt in absence of DBU leads one to think that racemization might also occur in conventional solvents without need of an external base. Here the deracemization in conventional

solvent without DBU is attempted by using a decoupled flow system. Because of time restraints racemization is not tested and deracemization was tested directly. By using a flow system in loop, the same flow system as depicted in Figure 13, was employed, but with the addition of a 100 bar Back Pressure Regulator (BPR). The BPR was placed downstream to allow the warming of the solution of imine **1** in acetonitrile at 100°C, thus above the boiling point without affecting the flow rate, in order to increase the chances of collision between substrate molecules. Attrition-enhanced deracemization (Viedma ripening) was preferred over Temperature Cycles Induced Deracemization (TCID) and Second Order Asymmetric Transformation (SOAT) by crystallization from a seeded solution because of the risk of the nucleation of the counter enantiomer during the cooling ramp. Indeed, because thermally induced racemization is expected to have an intermolecular mechanism, the lower temperature achieved in TCID or SOAT would have led to lower concentration in the flow system and, as a consequence, to a slower racemization rate. Viedma ripening instead largely relies on attrition at constant temperature, thus a slow racemization rate does not represent a threat to the outcome of the experiment, provided that serious decomposition does not occur.

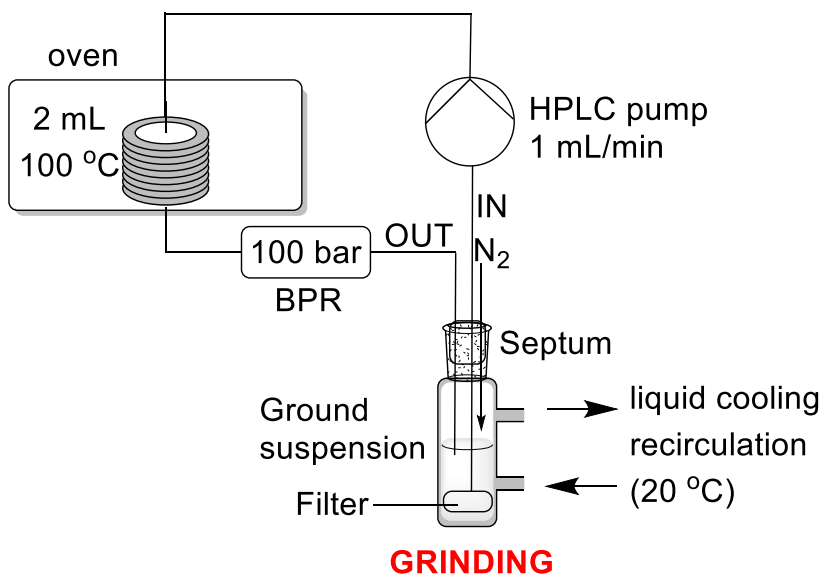
The 2 mL racemization reactor is placed in the oven at 100 °C. The total volume (18 mL) used in this experiment was kept as low as possible in order to allow a faster racemization of the whole mother liquor. Thus, the reaction was conducted in a thermostatted tube because its shape allows the filter to be completely submerged with a minor amount of solvent in comparison to a round bottom flask. In this experiment only 12 mL were left in the jacketed tube thermostatted at 20 °C, thus 6 mL were in part of the flow system for a total volume of 18 mL. A suspension was achieved with 450 mg of racemic imine **1**. With 100 mg of (*S*)-**1** (*E* = 99.9%) an initial enantiomeric purity of the suspended solid was measured to be 33% *E* after one hour of recirculation of the mother liquor through the flow system at 1 mL/min with simultaneous grinding with glass beads (7.764 g) at 250 rpm using a magnetic bar. The experiment was conducted under nitrogen atmosphere. An increase in enantiomeric excess of the solid phase was observed over time (Figure 14) but at the end of the Viedma experiment all the solid **1** was completely dissolved and no crystallization was observed when the grinding was turned off. Possibly the temperature in crystallizer increased leading to dissolution of the crystals. Because solubility of the racemate is twice than the one of the pure enantiomer, the enantiomeric excess increased upon progressive dissolution of crystals of both handedness in equal amount (50% R and 50% S)

a)

Solvent: CH₃CN (V = 18 mL)

m (racemic) = 0.450 g

m (enantiopure) = 0.100 g



b)

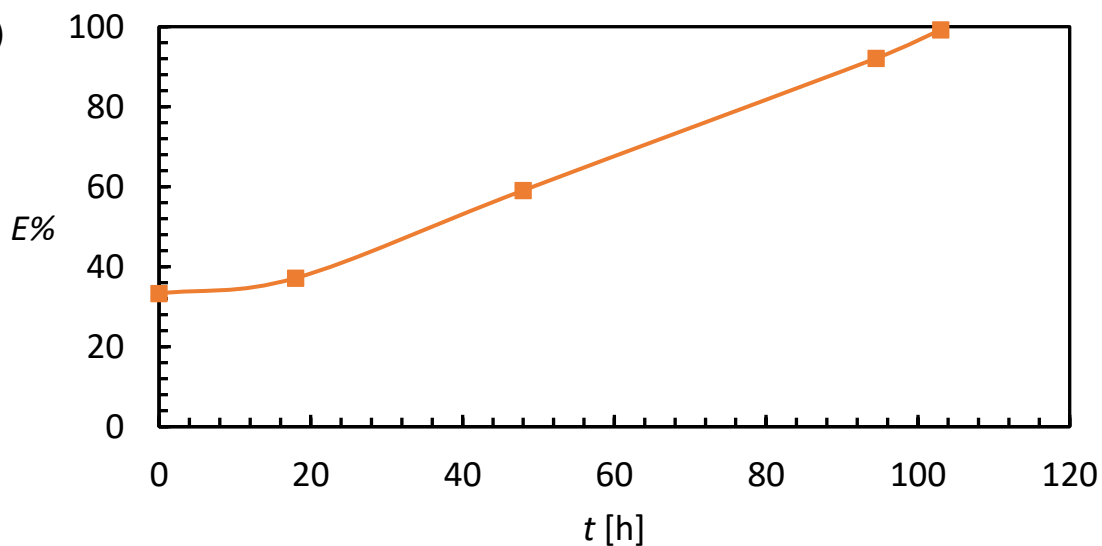


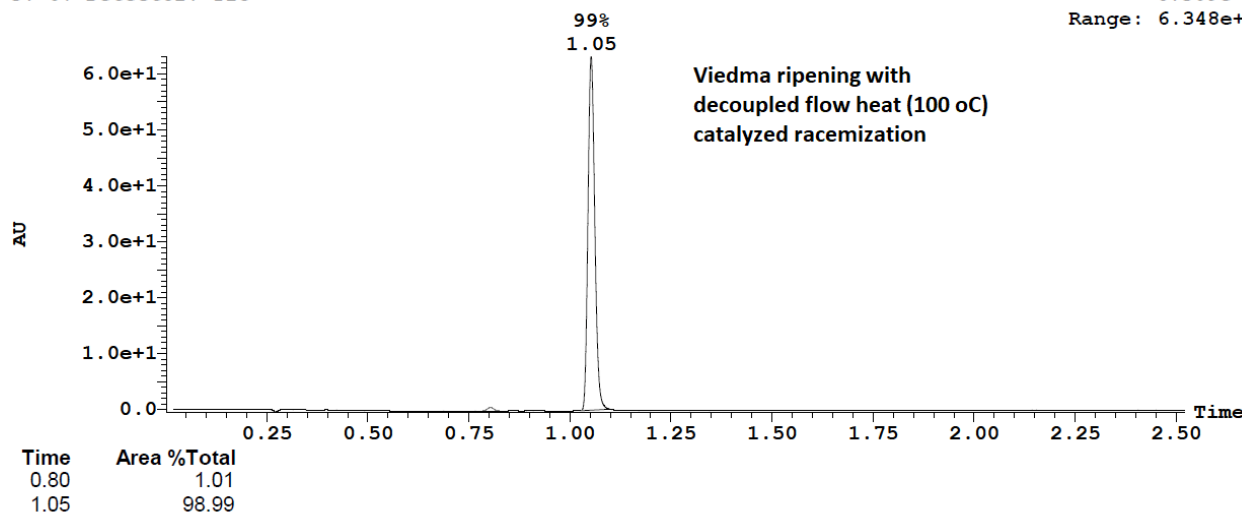
Figure 14: a) schematic setup for the flow-based deracemization of imine **1** at 100°C. The experiment was conducted in the absence of a catalyst, utilizing a 100 bar Back Pressure Regulator (BPR) to maintain solution phase. b) evolution of enantiomeric excess over time in a decoupled Viedma ripening experiment without the aid of an external base.

The mother liquor was analyzed by HPLC-MS in the end of the experiment (Figure 15). Conversely to a DBU catalyzed deracemization shown in Figure 13, only one peak corresponding to the imine **1** is observed, thus the mother liquor remains clean and could be recycled.

3: UV Detector: TIC

6.309e+

Range: 6.348e+



3: UV Detector: TIC

5.106e+1

Range: 5.622e+1

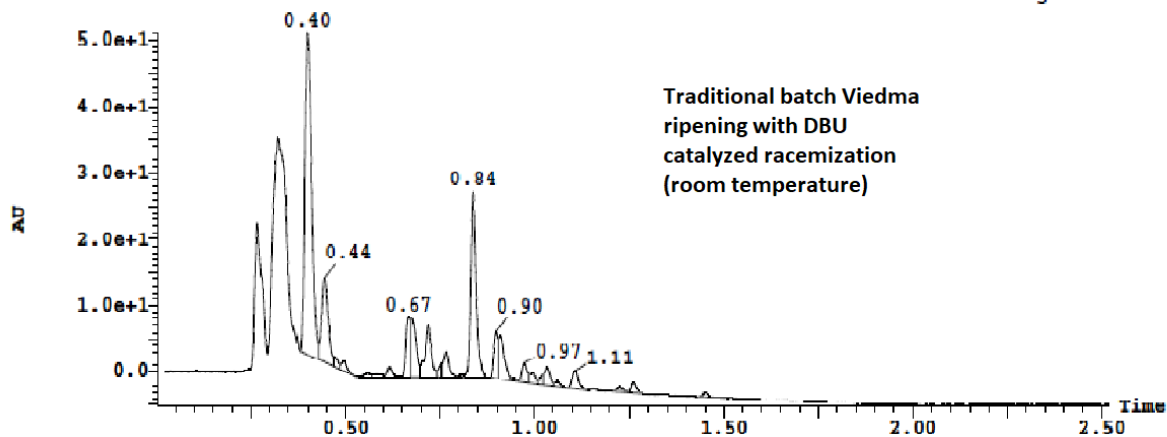


Figure 15: comparison between DBU free decoupled Viedma ripening after 95 hours with racemization coil heated at 100 °C with a 100 bar BPR with residence time (τ) = 2 min (top) and traditional one-pot Viedma ripening (bottom) after 100 hours at room temperature.

2.4. Discussion

The reason why two melting points of enantiomerically pure imine **1** were obtained is still unclear. Likely a crystal form of imine **1** different from the one described by van der Meijden et al^[5] has been identified by DSC. This crystal form is obtained by crystallization from a solution of racemic imine **1** in dichloromethane under vacuum in presence of 0.1 equivalents of benzaldehyde followed by washing with TBME (procedure described by Wilmink et al)^[6]. Imine **1** obtained through this procedure should also be analyzed by XRPD and the resulting data should be compared with the results obtained by DSC and XRPD of racemic **1** recrystallized in acetonitrile.

DSC measurements of scalemic mixtures of analogues imines **4a** and **4b**, identified as potential Prasugrel intermediates by Wilmink et al,^[6] should be performed to observe if an analogue behavior is observable at DSC.

The reason why imine **1** melted at 160 °C turned into an oil that does not crystallize out a room temperature should be also investigated. Turbidity measurements in a xylene solution at different concentrations of imine **1** (thus different temperatures) should be carried out with and without an inert atmosphere. In case nucleation of **1** would result in inhibition without inert atmosphere then it is possible that inhibition is caused by the cyclized product **10**. In such case the melting procedure itself should be conducted under inert atmosphere.

At 131 °C enantiopure (*E* = 98%) molten mixture led to partial racemization in the solid phase. As a consequence, the application of the melt crystallization technique becomes difficult. The identification of a MSZ of racemic **1** recrystallized in acetonitrile is of crucial importance to determine if racemization of the solid occurs even at lower temperatures.

The limited difference in yields of 2.5% between the two DBU catalyzed deracemization experiments with and without external racemization loop at higher temperature suggests that the amount of decomposition in the mother liquors was not significant. If more substrate would decompose in the liquid phase, more of the suspended solid would have dissolved, thus reducing the solid yield. On the other hand, the decoupled racemization at higher temperature resulted in a faster deracemization under Viedma conditions, most likely as the result of faster racemization in the high temperature racemization loop. The experiment in which a temperature of 100 °C in the decoupled racemization loop, used to try without the use of DBU as racemization catalyst, resulted in complete dissolution of the solid material and Viedma

ripening could not be proven. DBU free racemization studies in flow are needed and crystallization of the material exposed to racemizing conditions must be demonstrated.

2.5. Conclusion

Various alternative crystallization-enhanced deracemization techniques were probed for the compound N-benzylidene-2-chlorophenylglycinamide (**1**). Deracemization of compound **1** through a melt crystallization technique still remains challenging because of the lack of crystallization of **1** from the melt even in presence of enantiopure seeds.

An alternative setup for the Viedma ripening experiment using flow reactor to enhance racemization allowed the deracemization of compound **1**. External racemization in loop in presence of DBU in the liquid phase was shown to accelerate the deracemization without any clogging of the system. This setup can be applied to other compounds that require more harsh conditions to racemize so that racemization relies uniquely on the flow reactor. Attrition enhanced deracemization of compound **1** without the use of an external base like DBU by using a decoupled flow system has not been demonstrated. Racemization studies have to be carried out and the kinetics should be determined in order to find the appropriate process conditions. TCID and SOAT might provide alternative options to carry out deracemization of compound **1**.

2.6. References

- [1] G. L. Plosker, Katherine A Lyseng-Williamson, *Drugs* **2007**, 67, 613-646.
- [2] R. A. Badorc, D. Fre´hel, **1989**, US Patent no. 4847265
- [3] L. Wang, J. Shen, Y. Tang, Y. Chen, W. Wang, Z. Cai, Z. Du, *Org. Process Res. Dev.* **2007**, 11, 487.
- [4] S. Eswaraiyah, Raghupathi Reddy, A.; Goverdhan, G.; Lokeswara Rao, M., **2007**, U.S. Patent 2007225320
- [5] M. W. van der Meijden, M. Leeman, E. Gelens, W. L. Noorduyn, H. Meekes, W. J. P. van Enckevort, B. Kaptein, E. Vlieg, R. M. Kellogg, *Organic Process Research & Development* **2009**, 13, 1195-1198.
- [6] P. Wilmink, C. Rougeot, K. Wurst, M. Sanselme, M. van der Meijden, W. Saletra, G. Coquerel, R. M. Kellogg, *Organic Process Research & Development* **2015**, 19, 302-308.
- [7] D. K. Kondepudi, J. Laudadio, K. Asakura, *Journal of the American Chemical Society* **1999**, 121, 1448-1451.
- [8] H. Ishikawa, K. Ban, N. Uemura, Y. Yoshida, T. Mino, Y. Kasashima, M. Sakamoto, *European Journal of Organic Chemistry* **2020**, 2020, 1001-1005.
- [9] E. L. Eliel, S. H. Wilen, L. N. Mander, in *Stereochemistry of organic compounds*, New York (N.Y.) : Wiley, **1994**, p. 1142.

- [10] W. L. Noorduin, T. Izumi, A. Millemaggi, M. Leeman, H. Meekes, W. J. P. Van Enkevort, R. M. Kellogg, B. Kaptein, E. Vlieg, D. G. Blackmond, *Journal of the American Chemical Society* **2008**, *130*, 1158-1159.
- [11] E. J. Ebbers, G. J. Ariaans, J. P. Houbiers, A. Bruggink, B. Zwanenburg, *Tetrahedron* **1997**, *53*, 9417-9476.

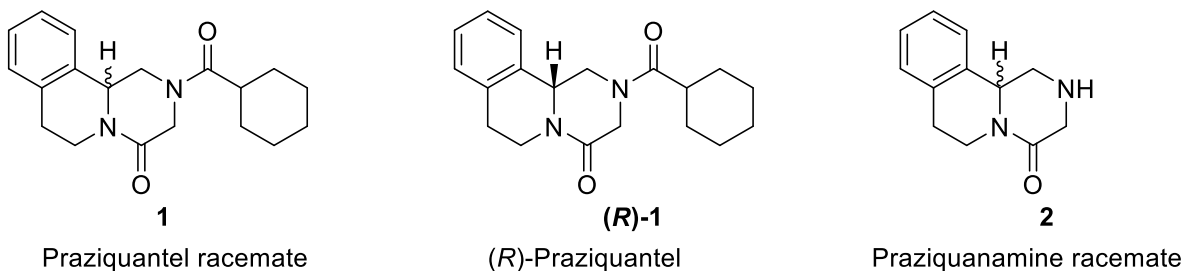
Chapter 3: Deracemization of a conglomerate derivative of Praziquantel:
A route to enantiomerically pure (*R*)-Praziquantel.

An efficient crystallization-enhanced deracemization method for conversion of the racemate to the desirable (*R*)-enantiomer of Praziquantel has been developed by coupling incompatible racemization and crystallization processes. By a library approach a derivative of Praziquantel that crystallizes as a conglomerate has been identified. Racemization occurs via reversible dehydrogenation over a palladium on carbon (Pd/C) packed column at 130 °C, whereas deracemization is achieved by alternating crystal growth/dissolution steps with temperature cycling between 5-15 °C. These incompatible processes are combined by means of a flow system resulting in complete deracemization of the solid phase to the desired (*R*)-enantiomer in 98% enantiopurity. Such an unprecedented deracemization by a decoupled crystallization/racemization approach can readily be turned into a practical process, and opens new opportunities for the development of essential enantiomerically pure building blocks that require harsh conditions for racemization.

3.1. Introduction

Table 2

Praziquantel (**1**, Biltricide, Scheme 3-1) is widely used for treatment of schistosomiasis, caused by infection by blood flukes.^[1] About 200 million people suffer from the infection, especially in less developed countries.^[1] The drug is thought to affect the permeability of membranes of the parasite towards calcium ions. A dose of the pure (*R*)-enantiomer (Scheme 3-1) is about five times more effective than the same dose of the racemate ^[2] although the cheaper latter is generally used for treatment. In addition, the inactive (*S*)-enantiomer causes a strongly bitter taste. Also, since the (*S*)-enantiomer is inactive, a large dose of racemic **1** is required to obtain the therapeutic effect, thus large tablets have to be administered, but they are difficult to swallow for infants. These disadvantages lead to low compliance in patients. It would therefore be desirable to administer only the (*R*)-enantiomer.



Scheme 3-1: Racemic praziquantel **1** is currently used in commercial dosage forms; (*R*)-**1** is the active enantiomer (eutomer); racemic praziquanamine precursor **2**.

The maximum yield of diastereomeric resolution is 50%. Pure enantiomers of Praziquantel can be obtained via classical resolution of precursor Praziquanamine **2** (Scheme 1) or its N-benzoyl derivative.^[3] Praziquantel has also been resolved by diastereomeric co-crystal formation with L-malic acid.^[4] Recently, **1** has been resolved on semipreparative scale using simulated moving bed chiral chromatography.^[5] An efficient method to convert the racemate to enantiomerically pure (*R*)-Praziquantel is of obvious interest. There are now new emerging alternative crystallization-assisted deracemization technologies in which the combination of racemization with crystallization allows one to obtain a single enantiomer in up to 100% yield.^[6] However, there are several challenges to overcome in order to arrive at a working crystallization-assisted deracemization.

We aim to apply a crystallization-enhanced deracemization protocol in the synthetic route of racemic Praziquantel in order to produce enantiopure (*R*)-Praziquantel in a convenient and cost-effective way. First, a conglomerate is required^[7]. Praziquantel^[8] and previously known intermediates such as praziquanamine (**2**, Scheme 3-1) crystallize as racemic compounds. In addition, a suitable method for *racemization* of the chiral carbon in the solution is required. Although Praziquantel can be racemized, harsh conditions are required.^[3b, 9] Finally, the system of conglomerate and solvent and the racemization in solution must be compatible.^[3b, 8, 9b-e] In order to successfully develop a crystallization-assisted deracemization for Praziquantel, the above described three challenges have to be overcome.

In the method of Temperature Cycles Induced Deracemization (TCID)^[6e, 6f] crystal growth events are induced by means of controlled cooling. Together with enantioselective secondary nucleation events^[10] in the presence of an initial bias in the solid in favor of the desired enantiomer, the solution is depleted of this preferred enantiomer more than its unwanted counterpart, leading to an enrichment of the mother liquor in the counter enantiomer. Under racemization conditions in solution, the unwanted enantiomer is therefore converted into the desired one, allowing progressive conversion to the desired enantiomer in the solid phase. The eventual remaining unwanted enantiomer can be further dissolved by a controlled increase in temperature according to the solubility of the racemate which tends to be twice as soluble as the pure enantiomer. As a consequence, at every cycle enantiomeric excess increases.^[11] The desired enantiomer remains thus in excess in the solid phase. This sequence is repeated until quantitative yields of enantiopure product are achieved.

The process originally developed by Viedma (coined Viedma ripening by others^[6a-d]) can be started with an initial bias in the solid in favor of the desired enantiomer in a suspension. But the process is isothermal: dissolution/crystal growth events occur simultaneously and are generated by means of induced

supersaturation mainly through grinding which is attained by stirring glass beads or by applying ultrasound to the suspension.^[6a, 12]

Crystallization Induced Asymmetric Transformation (CIAT, often referred to as Second Order Asymmetric Transformation, abbreviated SOAT)^[6g], unlike the previously described techniques, needs only one dissolution step to dissolve all the unwanted enantiomer, while the desired enantiomer is present as seeds in the solid phase. Similar to TCID, supersaturation is induced by means of a controlled cooling ramp. If the crystallization is well balanced with the solution racemization, a simple filtration in the end of the process provides enantiopure product. These processes are very versatile and they are described to work under light,^[13] intermolecular redox,^[14] base,^[6b-d] and acid^[15] catalyzed racemization, for neutral molecules and for salts. In some cases they were even combined with the synthetic step that generate the conglomerate, allowing synthesis and deracemization to occur in one pot.^[16]

3.2. Methods

3.2.1. Conglomerate search

3.2.1.1. Synthesis of derivatives

The synthesis of the racemic amide derivatives started by slowly adding the acyl chloride (1.1 eq) to a solution of racemic **2** (1.0 eq, 200mg) and trimethylamine (1.5 eq, 150 mg, 0.21 mL) in DCM (5 mL) submerged in an ice-water bath. Enantiomerically pure amide derivatives were synthesized by the same procedure using enantiomerically pure (*R*)-**2** as starting material. The mixture was allowed to stir overnight. Full conversion of **2** to the desired product was observed by HPLC-MS. Water (1.5 mL) was added to quench the reaction mixture. The resulting biphasic mixture was allowed to stir for 1 hour. Water was removed and the organic layer was washed with an equal volume of saturated aqueous solution of sodium carbonate, 0.5 M HCl solution and brine (3 times each washing). The organic layer was dried over sodium sulfate and solvent removed by means of a rotavapor. Aryl derivatives that still contained traces of aryl chloride or their corresponding acid were suspended in 3 mL tert-butyl methyl ether (TBME) on the glass filter, crushed and stirred with a spatula and filtered under vacuum. All the pure derivatives were dissolved in hot toluene and allowed to cool down to room temperature to obtain crystalline material so as to make sure that all the derivatives underwent the same crystallization conditions. The solids were collected by filtration.

Chiral SFC (Supercritical Fluid Chromatography) analyses were carried out on a Phenomenex Lux Cellulose 4 column (3.0 x 150 mm; 3 μ m) with a carrier solution of supercritical CO₂ and methanol in a gradient

mode for separation of **1** and **3u**. Racemic and enantiomerically pure **1** and **2** were kindly supplied by Merck KGaA, Darmstadt, Germany. Pd/C was purchased from Sigma Aldrich and Strem.

3.2.1.2. Characterization of Derivatives

The 30 crystalline derivatives, suspended in toluene in NMR tubes, were pre-screened by SHG as a suspension of crystals in toluene according to a previously described procedure.^[17] SHG is a technique that relies on nonlinear optics. Crystals were subjected to irradiation by a pulsed Nd:Yag laser (1064nm).

In order to confirm the positive SHG hits, the eutectic composition was determined. The racemate was suspended in toluene and allowed to stir for one hour at room temperature. Enantiomerically pure crystals were added and the slurry was allowed to stir for at least 2.5 hours. Samples of each compound were withdrawn and filtered through PTFE syringe filters. The isolated mother liquors were then diluted in isopropyl alcohol (IPA) and analyzed by chiral HPLC to determine their enantiomeric excess.

Reflections for crystallographic determinations were measured on a Bruker D8 Quest diffractometer with sealed tube and Triumph monochromator ($\lambda = 0.71073 \text{ \AA}$). The software package used for the intensity integration was Saint.^[18] Absorption correction was performed with SADABS.^[19] The structures were solved with direct methods using SHELXT.^[20] Least-squares refinement was performed with SHELXL-2014^[21] against $|F_o|^2$ of all reflections. Non-hydrogen atoms were refined freely with anisotropic displacement parameters. Hydrogen atoms were placed on calculated positions or located in difference Fourier maps. All calculated hydrogen atoms were refined with a riding model.

DSC measurements were carried out at a ramp rate of 10 °C per minute on a DSC Q20 V24.11 Build 124. XRPD diffractograms of the racemic and the enantiopure form were recorded by using a Bruker D8 Advance Diffractometer. The melting points (T^f) values are reported as the onset of the DSC signal.

3.2.2. Racemization

Activation of the racemization catalyst (Pd/C 10%) with hydrogen could have been conveniently performed by using an H-cube (Thalesnano), a commercially available flow hydrogenator. However, the used model of the H-Cube did not allow temperatures greater than 100 °C. Also, traditional commercially

available CatCarts from Thalesnano did not allow the racemization to occur with a decent flow rate. To overcome these problems, the H-Cube was equipped with a stainless-steel column (4.6 x 250 mm) filled with 1356 mg of Pd/C 10%. The dead volume (1.6 mL), which in a packed bed reactor is the volume between the solid particles of catalyst, was measured by the toluene volume obtained by pumping water through the packed bed column prefilled with toluene which was collected in a graduated cylinder. Activation of the catalyst with H₂ was performed when the column was warmed up to 130 °C into an external oven. During activation, the Back Pressure Regulator (BPR) of the H-Cube was set at 10 or 30 bar to dissolve H₂ generated *in situ* upstream of the racemization column. Also, the use of back pressure allows the solvent to remain in the liquid phase whenever its boiling point is lower the actual temperature, thus ensuring a reliable flow rate.

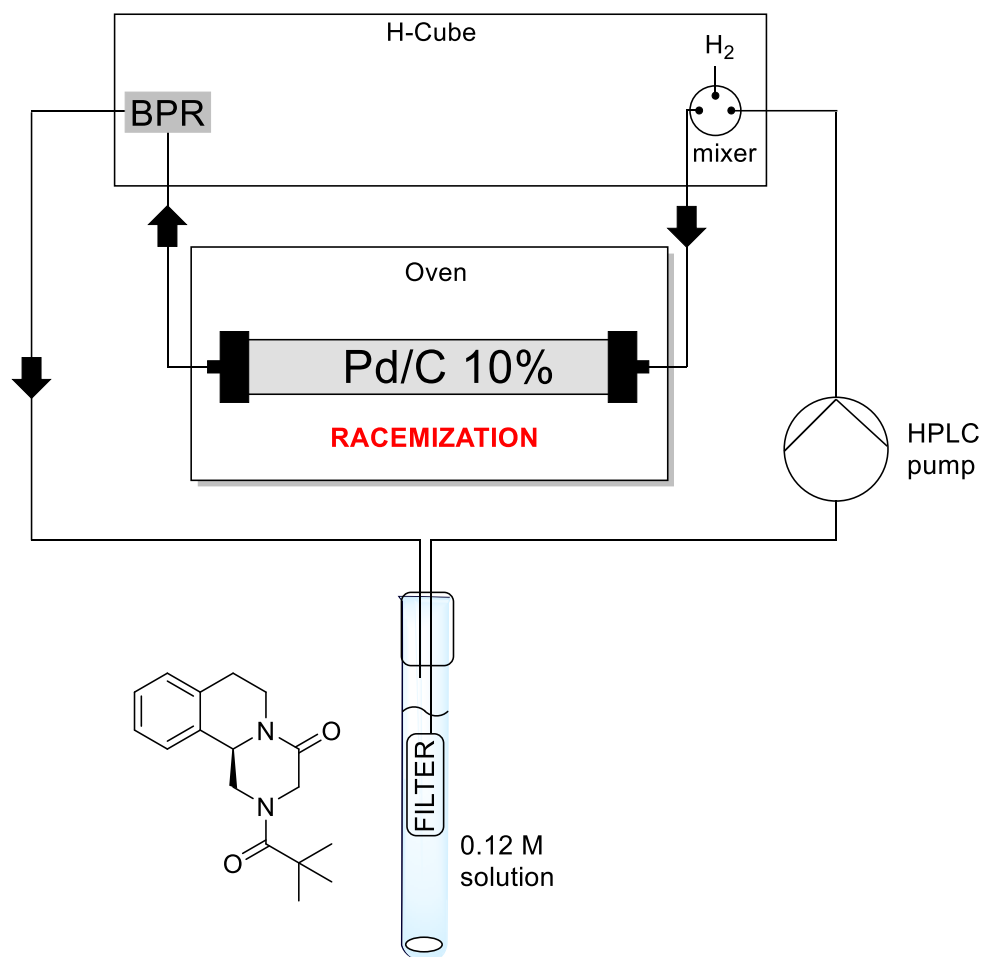


Figure 16: schematic representation of the system used to test racemization in the recycle.

A HPLC filter was connected to the inlet to stop passage of solid and allow selective racemization of the mother liquor. Both the inlet and the outlet of the flow system were placed into the test tube in order to maintain the volume of the mother liquor in the crystallization flask/reactor constant. Both the inlet and outlet were provided with a septum used to cap the neck of the flask, in order to avoid solvent evaporation.

The system consisting of HPLC pump, H-Cube, packed bed column with 1582 mg of Pd/C 10% and stainless steel tubing had a volume of 7.1 mL which at the start was flushed with toluene. A solution of racemic **3u** (1575mg) and (*R*)-**3u** (175 mg) in toluene (50 mL) was prepared in a 100 mL round bottom flask. The solution was pumped through the system to replace the toluene. Part of the outcoming solution (25 mL) was discarded as it was diluted with the toluene used to flush the system. The remaining solution (17.9 mL) was transferred into a test tube equipped with a magnetic stirring egg, leaving 7.1 mL in the racemization system. The solution in the test tube was recycled through the racemization system by pumping the solution through a column by using the HPLC pump (minimum flow rate = 0.01 mL/min, maximum flow rate 3.00 mL/min). An HPLC filter was connected to the inlet of the recycle to ensure that no solid particles were pumped through the system. Both the inlet and outlet were provided with a septum that was used to cap the neck of the flask, in order to avoid solvent evaporation.

3.2.3. Deracemization

The setup is the same described for the racemization experiments, but the test tube was replaced with a jacketed tube connected to a thermostat.

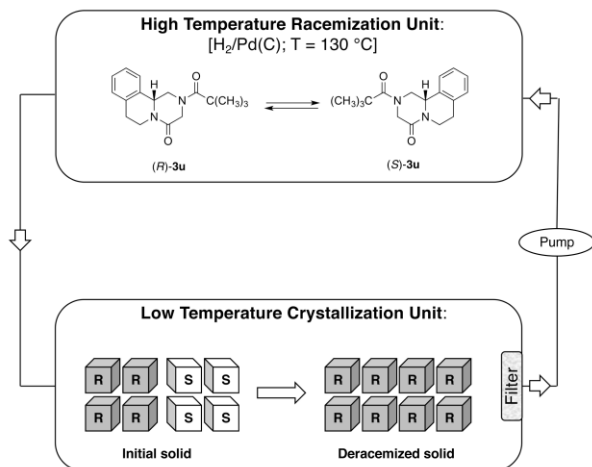


Figure 17: schematic representation of the setup used for SOAT and TCID procedures. The crystallization unit consists in a thermostatted jacketed flask.

3.2.3.1. SOAT

The flow system was flushed with toluene. In a 20 mL jacketed reactor equipped an oval magnetic stirring bar, racemic **3u** (1000 mg) was introduced and toluene (15 mL) was poured in. The racemate was completely dissolved at 50 °C and the temperature was set at 16 °C. No precipitate was observed, even after 1 hour. The jacketed flask was capped with a septum and perforated with the inlet and the outlet tubing so that the filter was completely submerged into the slurry. The mixture was allowed to stir at 200 rpm for 2 hours while the mother liquor was recirculated in the flow system at 1.0 mL/min. Seeds (79 mg) of enantiomerically pure **3u** were then added. The flow rate was set at 0.8 mL/min and the cooling ramp shown in Figure 18a was started. Hydrogen production was turned on with a BPR set at 30 bar for 80 minutes. The slurry was filtered off achieving **3u** as a white solid.

3.2.3.2. TCID

The thermostat was programmed so that each temperature cycle has the profile shown in Figure 18b. The flow system was flushed with methanol. A thermostatted jacketed flask ($T = 15\text{ }^{\circ}\text{C}$) equipped with an oval magnetic bar was filled with MeOH (12 mL). Racemic **3u** (1925 mg) was introduced into the flask. The jacketed flask was capped with a septum, perforated with the inlet and the outlet tubings so that the filter was completely submerged into the slurry. Stirring (200 rpm) was turned on and the mother liquor was allowed to recirculate in the flow system at 1 mL/min for 4 hours. (R)-**3u** (216 mg) was introduced into the flask and the mixture was allowed to stir an additional hour. The pump was set at 0.8 mL/min and the

Back Pressure Regulator was set at 10 bar. The packed bed reactor was placed in the oven at 130 °C. Hydrogenation production was cyclically turned on 5 minutes before and turned off at the beginning of each cooling ramp (segment 2 Figure 18b). After 10 temperature cycles, the mixture was filtered through a P4 glass filter to provide white crystalline **3u**.

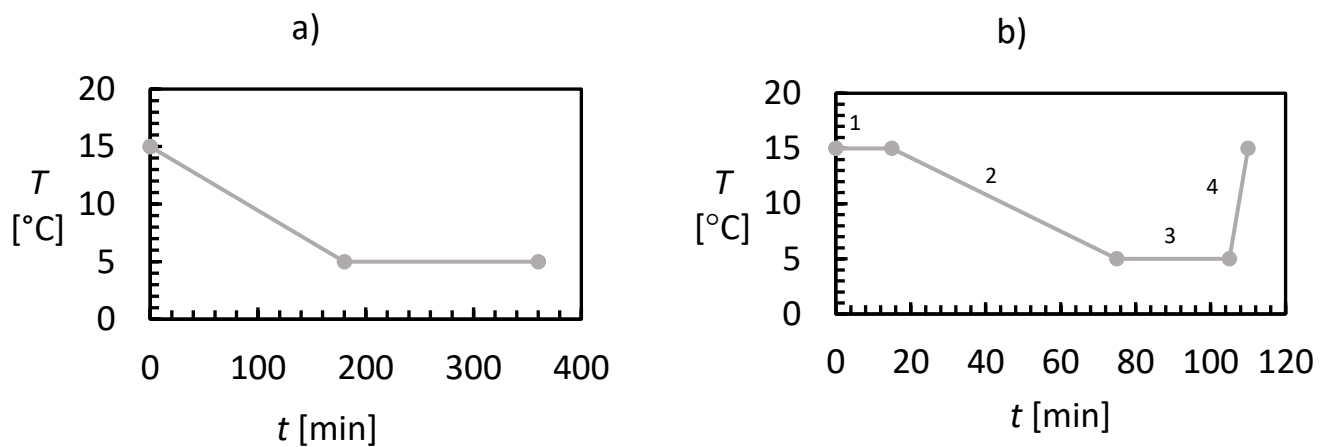
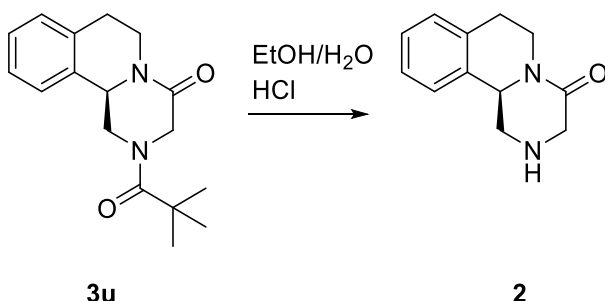


Figure 18: a) temperature ramp adopted during the SOAT experiment. b) Ramp profile adopted during TCID experiment.

3.2.4. Conglomerate hydrolysis



Scheme 3-2: Hydrolysis of **3u**

A suspension of **3u** (265 mg) in a mixture of ethanol (6 mL) and 1 M HCl (aq, 11 mL) was stirred and heated at reflux until the solution became clear. The resulting mixture was allowed to stir for 16.5 hours and allowed to cool down at room temperature. The pH was adjusted to 12.4 with 5N NaOH and the basified reaction mixture was extracted with DCM (3 x 30 mL). The combined organic layers were washed with brine, dried over sodium sulfate and concentrated under reduced pressure. Compound **2** was obtained as a pale-yellow solid (173 mg, yield = 92.4%, $E = 97.5\%$ at 260.8 nm). The pH of the reaction mixture of the hydrolysis of (*R*)-**3u** was monitored by using a pH meter (InoLab pH 7170). NMR spectra of all compounds were obtained on a Varian Mercury 300 MHz machine. All solvents were spectral grade. Chemical shifts δ of NMR spectra are reported in ppm relative to $(\text{CH}_3)_4\text{Si}$ at $\delta = 0$. Enantiomers of **2** were separated by using Chiralcel OJ-H column (4.6 x 250 mm, 5 μm) with a carrier solution of heptane/ethanol/ Et_2NH (60/ 40/ 0.2).

3.3. Results

3.3.1. Conglomerate search

Currently, rules about how to design a conglomerate do not exist. The incidence of occurrence of conglomerates based on experience described in the literature seems to be in the range of 5-10%. A library of derivatives of Praziquanamine was prepared using reversible reactions for the synthesis. These were characterized through several analytical techniques described in the literature.^[6b, 6d, 22] The library was first tested by a high-throughput screening technique like Second Harmonic Generation (SHG) which can spot candidates with high chances to crystallize as conglomerates. SHG screening was performed in part by AMOLF institute (Amsterdam) using a microscope detector and RUG (Groningen) using a spectrophotometer detector. Positive hits are further characterized by Diffraction Scanning Calorimetry, X-Ray Powder diffraction (XRPD), eutectic composition and Single Crystal X-Ray Diffraction (SC-XRD) for unambiguous determination of a conglomerate system.

For a proper deracemization, the conglomerate should be chemically stable to racemization conditions in order to avoid decomposition. Praziquanamine was identified as a suitable starting material for library generation because it is racemizable^[9a] and its reversible functionalization with acyl halides allows formation of several different derivatives without affecting the optical purity.^[3a] Thus, in order to find a conglomerate intermediate of Praziquantel, a covalent library of 30 crystalline derivatives was prepared by reaction of both racemic and enantiomerically pure intermediate praziquanamine (**2**) with various acyl and aryl chlorides available in house to provide crystalline derivatives. Most of these were selected with the aim of generating derivatives stable to reversible hydrogenation conditions at the high temperature and pressure conditions needed to racemize the precursor **2**.^[9a] Owing to this consideration, sensitive groups (e.g.: nitro, esters, chlorides, alkenes, alkynes, benzyl groups) were mostly avoided. Furthermore, the reactants are selected with the criteria of showing similarities in their structure in order to facilitate the comparison among other derivatives to observe how the presence of a substituent can influence the crystallization behavior. Such derivatives can be easily hydrolyzed to **2** without loss of optical purity. Second harmonic generation (SHG) is used for preliminary screening on the library of racemic derivatives **3**. Conglomerates (non-centrosymmetric crystal structure) are expected to give a positive signal.^[23] The following analytical methods were used to confirm/refute a positive SHG signal.

1. DSC: if the melting point of the enantiomerically pure crystals is at least 20 °C higher than the one from the crystals from a racemic mixture, then the compound is likely a conglomerate

2. X-Ray Powder Diffraction (XRPD): for a conglomerate the spectra of the two enantiomers should be identical.
3. Eutectic composition: when enantiomerically pure crystals are added to a slurry of racemate, at equilibrium conglomerates will always provide a racemic mother liquor as the solubility of (*R*) crystals is equal to that of the (*S*) crystals.
4. Single Crystal X-Ray Diffraction (SC-XRD): the single crystal structure is the ultimate proof for conglomerate formation when crystallized from a racemic mixture. It needs, however, a single crystal of sufficient quality and size which is often difficult to obtain.

3.3.1.1. First indication by Second Harmonic Generation

SHG is a technique that allows one to detect non-centrosymmetric structures using only a few milligrams of crystalline samples of the racemate.^[17] Conglomerates as well as about 5% of all the racemic compounds crystallize in non-centrosymmetric space groups. Such structures emit light after absorption from a laser source.^[23] In this study samples were irradiated in their mother liquor because it helps to dissipate the energy of radiation preventing decomposition. Also, the presence of the solvent helps to reduce the risk of false positives or negatives linked to the formation of the crystalline form at the thermodynamic equilibrium which can solvate or desolvate. For instance a solvate might transform to a solvent free crystal or collapse to amorphous material upon drying on air after filtration.

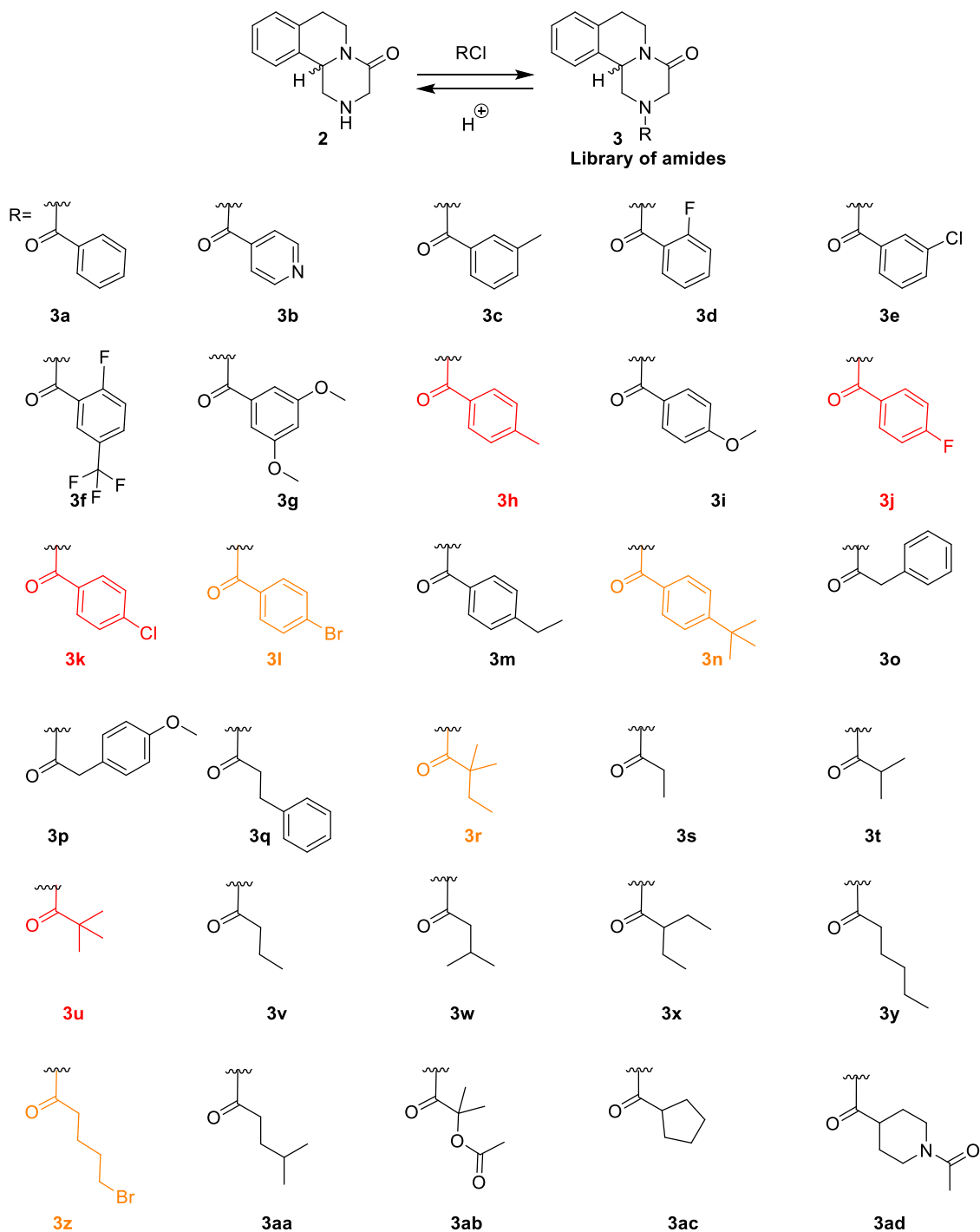


Figure 19: reversible derivatization of **2** in order to generate candidates for conglomerate screening. SHG allows screening for conglomerates of the derivative solids suspended in toluene. Strong signals (in red): **3h**, **3j**, **3k**, **3u**. Weak signals (in yellow): **3l**, **3n**, **3r**, **3z**. The remaining derivatives gave no signal. After further characterization only **3u** was recognized as a conglomerate.

Figure 19 shows the derivatives of racemic praziquanamine and their SHG responses. Most of the derivatives contain functional groups unsensitive to hydrogenation as this reaction is involved in the planned deracemization process. However, some of them do contain sensitive functional groups as the primary goal was to identify a conglomerate with which even preferential crystallization might be possible.^[7a] Among the derivative shown, compounds **3l**, **3n**, **3r**, **3z** give a weak signal upon irradiation. According to literature, the weak signals are considered “spurious light” and they are not considered relevant.^[17] Compounds **3h**, **3j**, **3k**, **3u** give a strong signal, indicating a high chance that these compounds crystallize as conglomerates.

Compound **3h** (Figure 19) was irradiated both as a dry powder and suspension in toluene (Figure 20). In both cases the solid turned bright giving a strong signal. This result indicates that **3h** crystallizes in a non-centrosymmetric structure, thus with a high chance to be a conglomerate. It is also possible to hypothesize that **3h** maintains the same crystal structure both as dry powder and as a suspension in toluene.

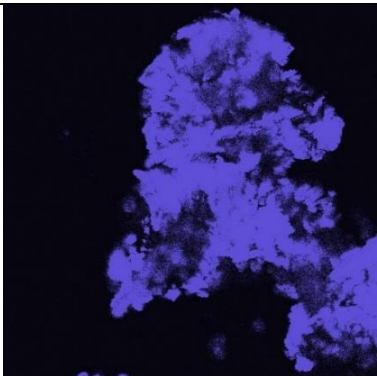
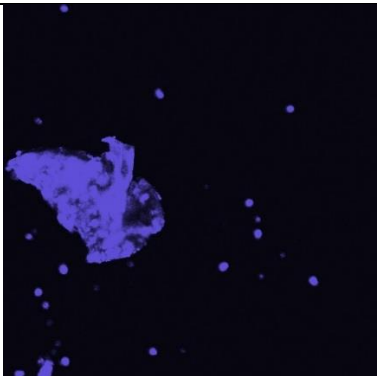
	Dry powder	Suspension in toluene
3h		

Figure 20: example of crystalline samples screened at SHG. The picture shows irradiated crystals without (left column) and with (right column) addition of toluene. In both cases a strong emitted light is detected.

3.3.1.2. Further Confirmation of Conglomerate Formation

3.3.1.2.1 DSC

DSC measurements can indicate whether the compound crystallizes as a racemic compound or as a conglomerate.^[24] For a conglomerate system the difference in melting point (T^f) between enantiomerically pure (*R* or *S*) and racemic mixture (*rac*) is typically $\Delta T^f = T_R^f - T_{rac}^f = 20$ °C or higher. For racemic compounds, ΔT^f varies with the couple of enantiomers and it can also be negative. Typical binary phase diagrams of conglomerates and racemic compounds are represented in Figure 3 in Chapter 1 where the main differences are the consistency of $\Delta T^f \geq 20$ °C for conglomerates and the presence of two eutectic points (Eu, Eu') rather than one in case of racemic compound systems.

Racemic Praziquantel melts at 136 °C (heat of fusion, $H = 25.7$ kJ/mol), while the pure enantiomer melts at 111 °C ($H = 18.5$ kJ/mol), resulting in $\Delta T^f = -25.6$ °C.^[8] Such a large difference in melting point between racemic and enantiomerically pure **1** indicates that Praziquantel is quite a stable racemic compound, consistent with the SHG indication. For **2**, both racemic and enantiomerically pure praziquanamine melt at 118-119 °C suggesting a racemic compound system, consistent with SHG indication.^[9a, 25] Compound **3h**, positive to SHG, shows a $\Delta T^f = 3$ °C. This suggests that **3h** is not a conglomerate, but rather a racemic compound crystallizing in a non-centrosymmetric space group.

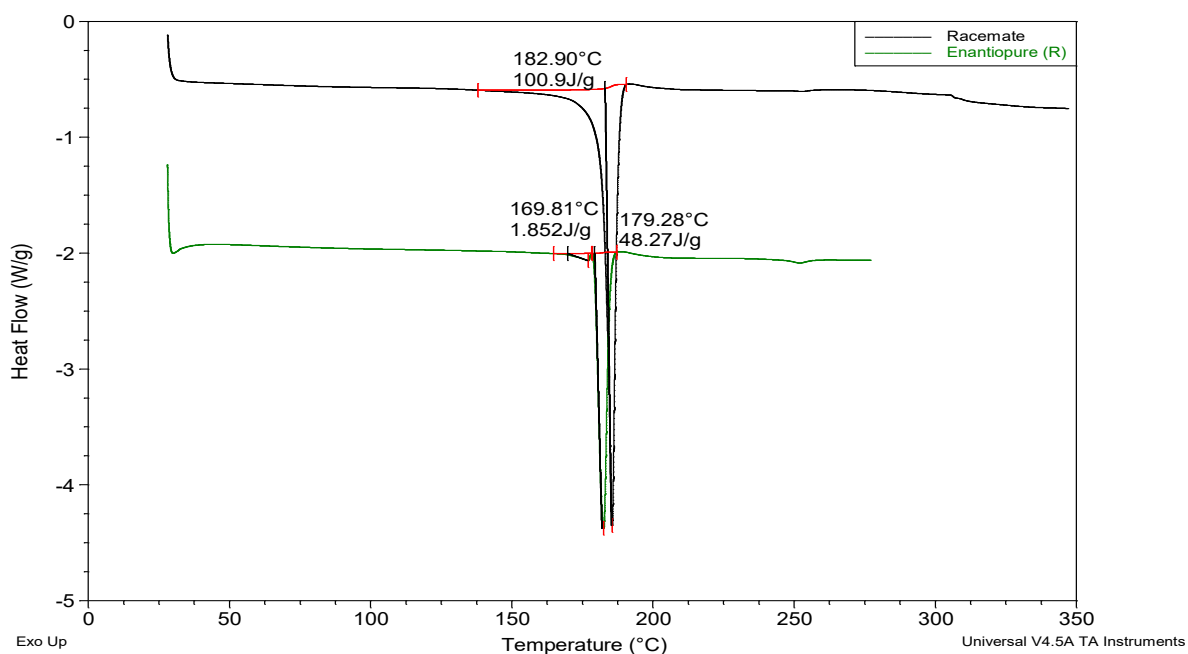


Figure 21: Stacked DSC of racemic and enantiomerically pure **3h**. It is important to note that these DSC measurements have an associated error, and reproducibility can be challenging, especially with only single ($n = 1$) readouts that have not been repeated.

The difference in melting points between enantiomerically pure (*R*)-**3j**, (*R*)-**3k**, (*R*)-**3u** and their corresponding racemic mixtures suggest that such compounds are conglomerate, and these results are consistent with their positive signal to SHG. However further analyses are necessary to determine if **3j**, **3h** and **3u** crystallize as conglomerates.

Table 3: onsets of the melting temperatures T_{rac}^f and T_R^f and their relative enthalpies ΔH and ΔH_A of fusion for some racemic (*rac*) and enantiopure (*R*) derivatives, respectively. All DSC measurements reported were conducted once ($n = 1$). While the observed melting point differences support the identification of potential conglomerates, further replicates are necessary to confirm the reproducibility of these thermal behaviors.

Compound	T_{rac}^f [°C]	ΔH_{rac} [kJ/mol]	T_R^f [°C]	ΔH_R [kJ/mol]	ΔT_{R-rac}^f [°C]
1 ^[8]	110.6	18.5	136.2	25.7	-25.6
2 ^[9a, 25]	118-119	22.4	118-119	20.1	0
3a	122.9	14.5	158.7	24.2	-35.9
3h	179.3	15.4	183.0	29.3	-3.7
3i	211.6	30.0	206.5	36.3	5.2
3j	201.7	28.0	179.8	28.2	21.9
3k	234.3	23.0	212.9	32.6	21.4
3u	179.4	29.4	147.3	23.6	32.2

In Figure 22, the measured melting temperatures of the racemic mixture are plotted against that of the enantiopure compound. The melting temperature T_{rac}^f of a conglomerate system ($x = 0.5$) can be predicted from the melting temperature T_R^f and heat of fusion of the enantiopure compound using the van 't Hoff equation:

$$\ln x = -\frac{\Delta H_{rac}}{R} * \left(\frac{1}{T_{rac}^f} - \frac{1}{T_R^f} \right)$$

where x is the mole fraction of the single enantiomer in the mixture. Using this, the boundary lines between racemic compound system and conglomerate system are drawn in Figure 22 using various realistic values of the heat of fusion. Above the boundary line, an experimental pair of melting temperatures [$T_{rac}^f(x_R = 0.5)$, $T_R^f(x_R = 1)$] indicates a conglomerate system, below it a racemic compound system. Praziquantel (orange point) is known to be a racemic compound and as expected gave negative response to SHG. Praziquantel **1** and other compounds negative at SHG like **3a** and **3i** lie pretty far from the conglomerate region. Three out of four positive hits at SHG, namely **3u**, **3j** and **3k**, are positioned in the racemic compound region of the plot, indicating that they might be false positives in the SHG analysis. The compound **3u** is the only derivative that has melting temperatures potentially indicating a conglomerate system, although the measured heat of fusion is lower than the minimum heat of fusion of

30 kJ/mol needed for compound **3u** to be a conglomerate system. This might be explained by the relatively large confidence intervals of experimental heats of fusion.

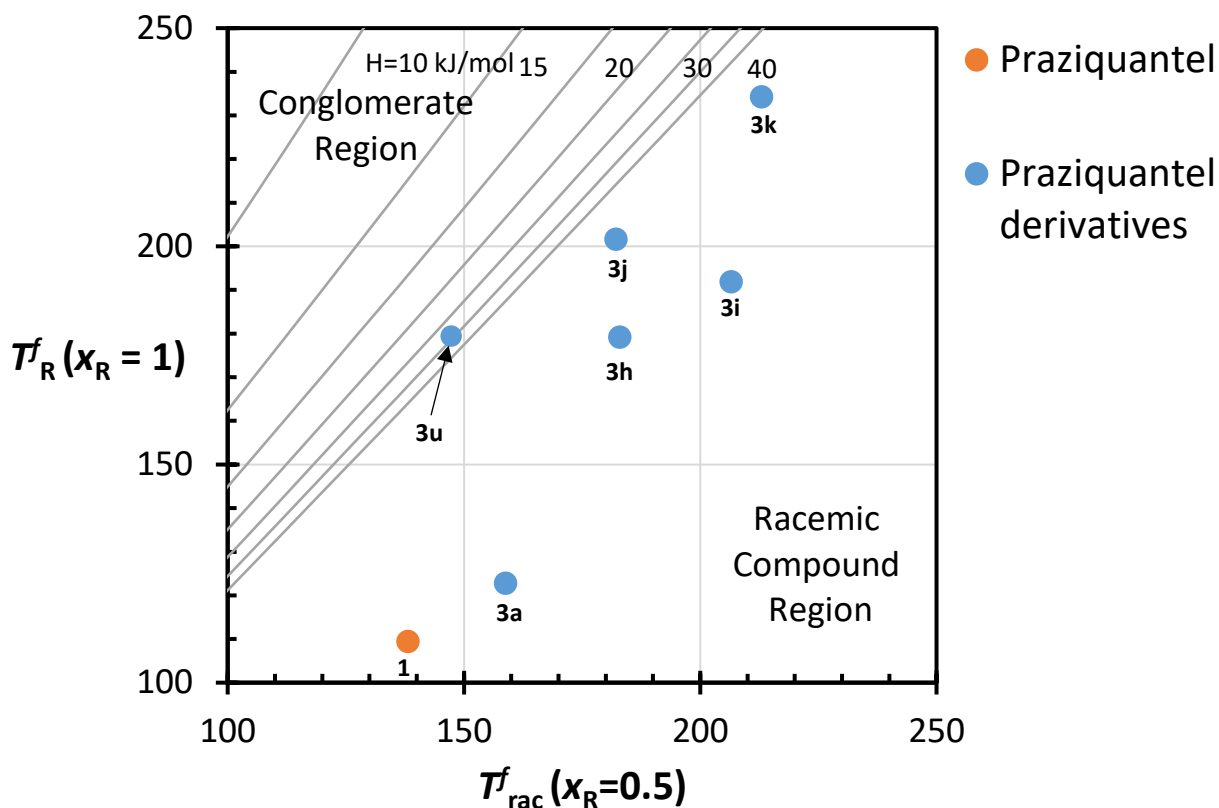


Figure 22: melting temperature of racemic and enantiopure compounds as a function of the heat of fusion H of the enantiopure compound. $T_{rac}^f(x_R=0.5)$ is the melting temperature of the racemate, $T_R^f(x_R=1)$ is the melting temperature of enantiopure compound.

3.3.1.2.2 XRPD

The XRPD patterns obtained from the racemic and enantiopure **3h** do not overlap (Appendix, Figure 46), strengthening the theory that **3h** is a racemic compound crystallizing in non-centrosymmetric space group, consistent with the positive SHG signal. Similarly, the diffractograms of racemate and enantiopure of derivative **3j** differ (Appendix, Figure 47), contrasting SHG indications.

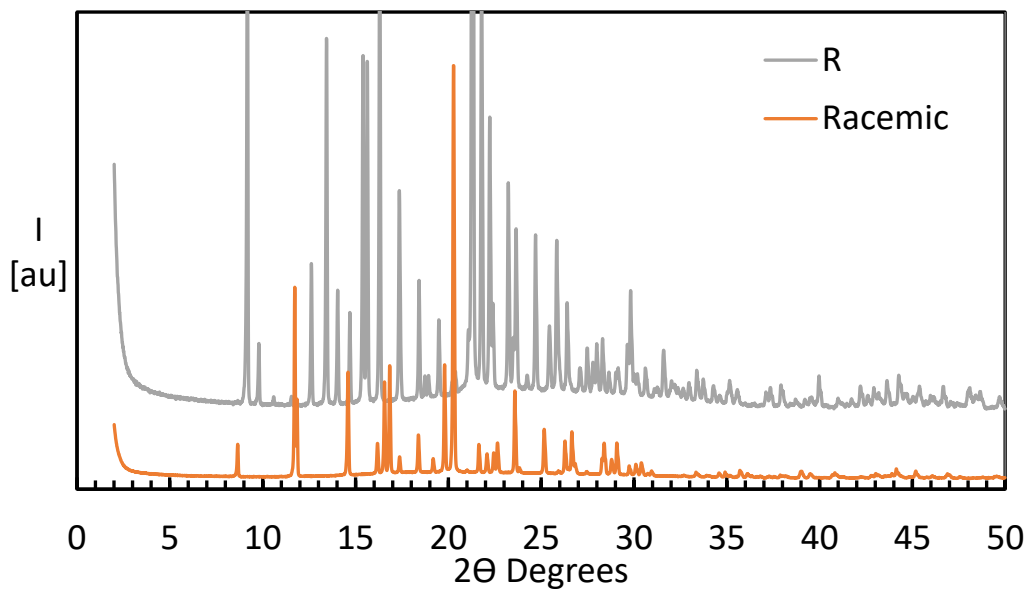


Figure 23: stacked XRPD diffractograms of derivative **3h**.

The diffractograms of racemate and enantiopure of derivative **3k** differ (Appendix, Figure 48), although many peaks overlap. This result indicates possible racemic compound formation which is in contrast with previous SHG indications. Because crystals of good quality for SC-XRD are difficult to obtain from a racemic solution of compound **3k**, the eutectic composition is used as method of choice to determine if **3k** is a conglomerate and thus suitable for crystallization-enhanced deracemization techniques.

However, Figure 24 shows that XRPD patterns of the racemate of **3u** and the enantiomerically pure (*R*)-**3u** overlap, giving a further confirmation that this compound forms a conglomerate system.

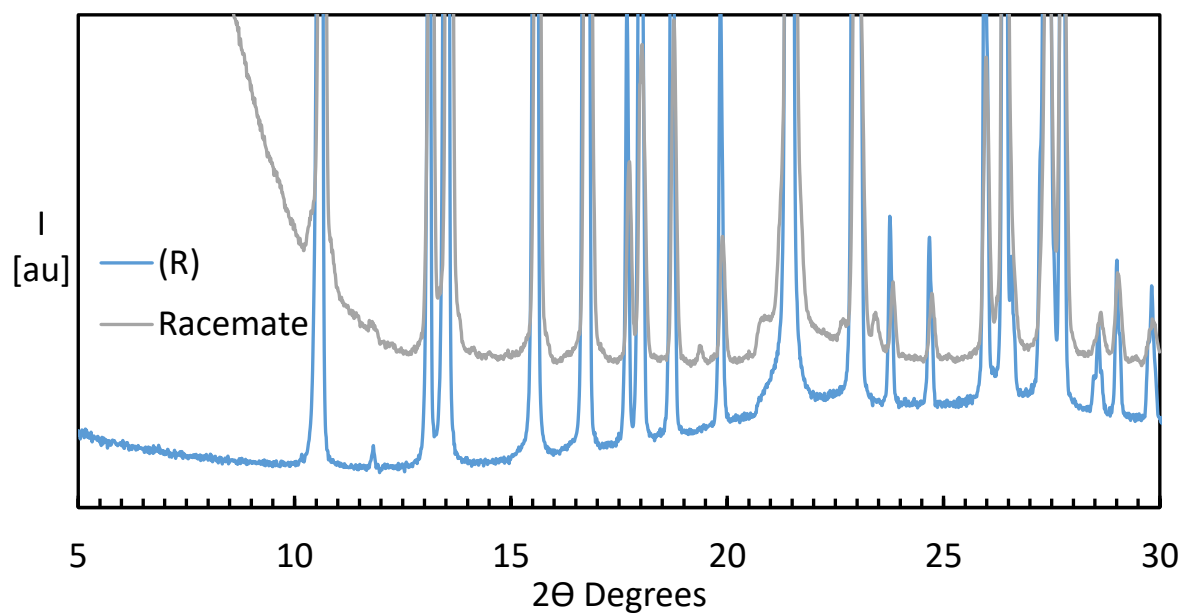


Figure 24: XRPD patterns of enantiopure (blue) and racemic (grey) derivative **3u**.

3.3.1.2.3 Eutectic composition

Figure 25 represents isothermal ternary phase diagrams for a conglomerate (left) and a racemic compound system (right). The dashed arrow 1 represents the dilution of the mass of crystalline racemate until the achievement of a racemic slurry. The dashed arrow 2 represents the addition of enantiomerically pure R-crystals. Depending on whether it is a conglomerate or a racemic compound system the solution concentration of the established equilibrium is different. In a conglomerate system adding small amounts will not change the initial eutectic concentration E_u from its racemic composition. The enantiomeric excess in the solution therefore remains 0. However, in the solid the enantiomeric excess is high as all excess crystallizes out. In a racemic compound system adding a small amount of enantiopure compound R will have it all dissolve, leaving the crystals in the suspension at racemic composition. However, the solution composition will contain an excess of R. Adding large amounts of enantiopure crystals, in presence of attrition (for instance given by the magnetic stirrer against the glass walls), might result in the enrichment in the opposite enantiomer to the one in excess in the solid phase. Indeed, grinding can prevent the system from reaching the thermodynamic equilibrium by slightly increasing the solubility. This factor, combined with a large surface of enantiopure crystals suspended, encourages enantioselective crystal growth which depletes such enantiomer from the mother liquor. Determining the eutectic composition indicates conglomerate formation. The “dilution line” (in orange) connecting the apex of the solvent and the eutectic point (E_u) gives the enantiomeric excess of the mother liquor at the intersection with the SR line. Such an intersection represents the eutectic composition which tells if the compound crystallizes as a conglomerate (if its value equals 0% E) or a racemic compound (if its value is above 0% E). The “tie line” (in green) passing through the eutectic and the point and the blue point gives the enantiomeric excess of the filtered cake at the intersection with the SR line.

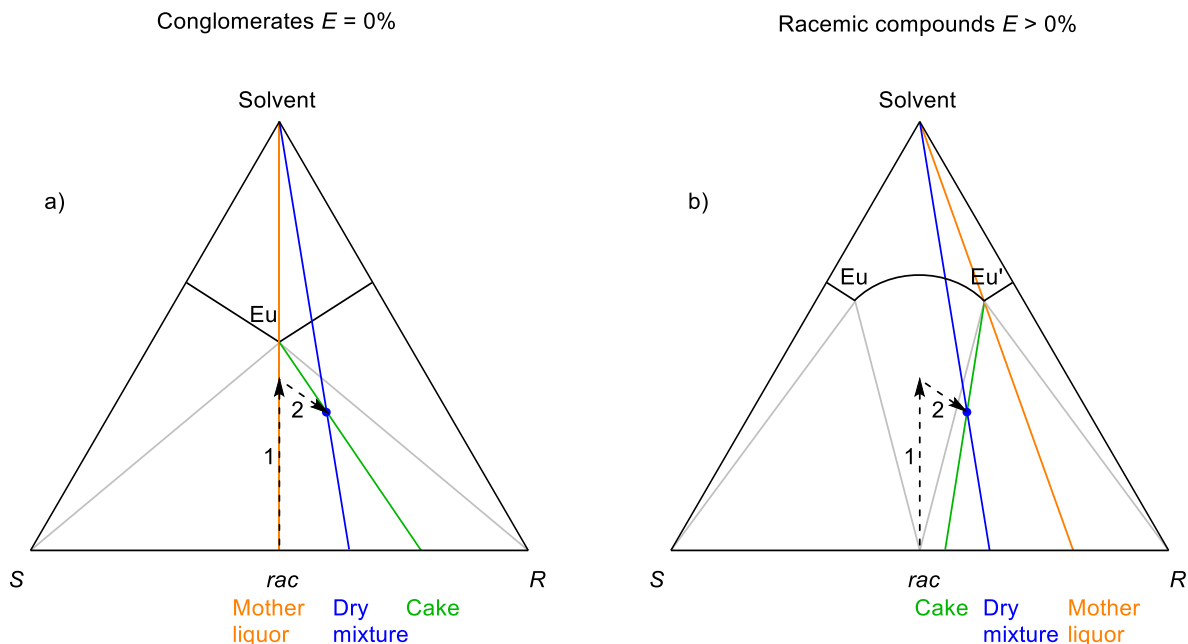


Figure 25: Isothermal ternary phase diagrams for a conglomerate (left) and a racemic compound system (right). The dilution of a dry racemic mixture to a thermodynamically stable suspension is represented by arrow 1. Following addition of enantiopure crystals is represented by the dashed arrow 2. Filtration of the slurry results into a mother liquor which composition is defined as eutectic and corresponds to the intersection of the orange line and SR line. Such value is indicative of the crystallization behavior of the couple of enantiomers.

According to the guidelines described above, the eutectic composition was measured for the compounds that give positive response to SHG s at room temperature and the results are listed in Table 4. From the information gained from such experiment a first estimation of the solubility can be obtained. At the end of the experiment, the data can be linked as follows:

$$m_{RS}^{sol} = m_{RS}^F \frac{E^F - E^{cr}}{E^{sol} - E^{cr}}$$

Where m_{RS}^{sol} is the amount of chiral compound in solution after experiment, m_{RS}^F is the overall amount of chiral compound (mixture of both enantiomers), E^F , E^{cr} , E^{sol} are the enantiomeric excesses overall, in crystal phase and in solution. Concentration of pure enantiomers R is:

$$c_R^{sol} = \frac{1}{2} c_{RS}^{sol} (1 + E^{sol}) = \frac{m_{RS}^F}{V} \frac{E^F - E^{cr}}{E^{sol} - E^{cr}}$$

Where V is the volume of solvent.

Table 4. Results of the eutectic measurement. The letter among parenthesis indicates the enantiomers in excess. The solvent used is toluene. A second measurement in methanol has been carried out for **3u** in methanol once *E*% of the mother liquor close to 0 has been observed in toluene.

Compound	<i>rac</i> [mg]	<i>R</i> [mg]	<i>E</i> % dry mixture	Solvent [mL]	<i>E</i> % mother liquor	<i>E</i> % cake	Estimated solubility [mg/mL]
3a	40	10	20	2 (toluene)	44 (<i>R</i>)	4 (<i>R</i>)	10
3h	30	9	23	2 (toluene)	36 (<i>R</i>)	3 (<i>R</i>)	12
3i	30	8	21	2 (toluene)	48 (<i>R</i>)	16 (<i>R</i>)	3
3j	40	10	20	1 (toluene)	67 (<i>R</i>)	19 (<i>R</i>)	1
3k	40	13	24	2 (toluene)	29 (<i>R</i>)	22 (<i>R</i>)	8
03u	30	8	21	0.5 (toluene)	2 (<i>S</i>)	51 (<i>R</i>)	43
3u	92	27	23	1 (methanol)	2 (<i>S</i>)	39 (<i>R</i>)	48

The results strongly suggest that only derivative **3u** forms a conglomerate system both in toluene and in methanol because the mother liquor of the stirred mixture is close to racemic. The mother liquor is slightly enriched in the counter enantiomer both in toluene and in methanol, possibly owing to the attrition of the magnetic stirring egg against the glass walls of the crystallization vial in presence of an enantiomeric excess in the suspended solid (51% (*R*)-**3u** in toluene and 39% (*R*)-**3u** in methanol). This result could be explained by the fact that the samples are withdrawn soon after turning off the stirring plate so that a small deviation from the thermodynamic equilibrium could be given by the grinding by action of the magnetic stirrer. All the other compounds behave as racemic compounds as the enantiomeric excess in the solution is much larger than 0% *E*. Both in racemic compounds and conglomerates, the *E* of the suspended solid (cake) and mother liquor indicate in which region of the phase diagram the composition is located, thus if the *E* of the mother liquor corresponds to the intersection of the orange dilution line passing through the eutectic point (*Eu*) and *SR* line at the (near) thermodynamic equilibrium (Figure 25b). This indicates that for compounds **3i**, **3j**, **3k**, **3u** the samples (blue point) of the slurry were withdrawn within the region *rac-Eu-R*: both the solution and the solid have a significant enantiomeric excess of *R*. The solution then has eutectic composition and the measured enantiomeric excess in the solution then is a good estimate for the enantiomeric excess in the eutectic. This is not certain for compound **3a** and **3h** as the enantiomeric excess in the solid is close to 0% *E*. These samples may come from the region *rac-Eu'*-

R but very close to the gray line or within the region Eu-*rac*-Eu', while in this case this might mean that integration of the chromatographic peaks was not precise enough.

Also, Table 4 shows that the solubility of **3u** is larger than the other derivatives. Solubility of **3u** in methanol turned out to be higher than **3u** in toluene.

3.3.1.2.4 Evidence (SC-XRD)

SC-XRD analysis shows that racemic derivative **3u** crystallizes in orthorhombic chiral non-centrosymmetric $P2_12_12_1$ space group (Figure 3-11). In the same crystalline unit a Van der Waals interaction links two molecules of **3u**: one interaction connects the proton covalently bound to the chiral center to C09. The carbon of the cyclic amide (C13) forms an interaction with the C12 of an adjacent molecule. Finally, a short contact exists between the oxygen of the cyclic amide and the hydrogen bound to the methylene bridge (C10). The predicted XRPD, obtained from SC-XRD measurement, corresponds to the experimental one, indicating the presence of the same crystal form.

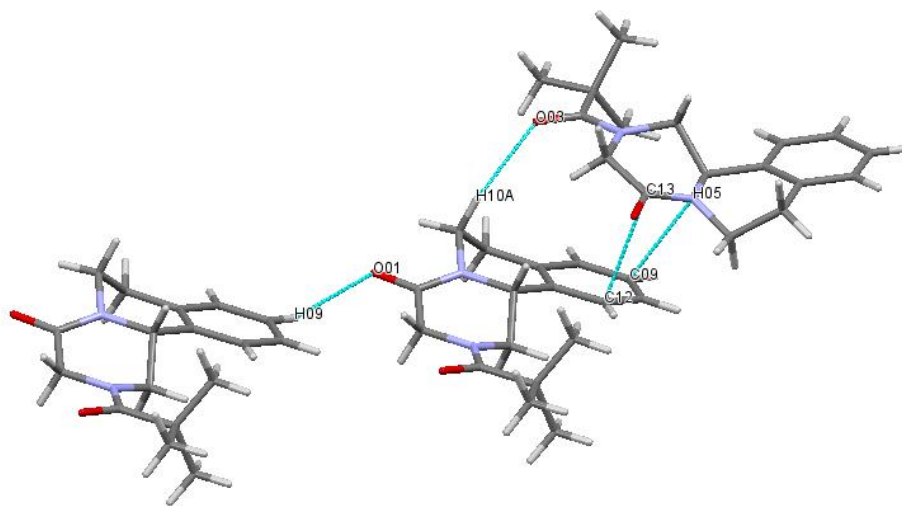


Figure 3-11: single crystal representation of **3u** (left). Representation of short contacts (in blue) within the same crystalline unit

SC-XRD measurement (Figure 3-12) evidenced that racemic derivative **3h** crystallizes with the monoclinic achiral non-centrosymmetric space group (*Pc*) and this is consistent with the positive signal observed by SHG. H09 establishes two Van der Waals interactions with the carbons C05 and C19 of an adjacent molecule. Other two Van der Waals interactions are present between the oxygen of the cyclic amide and

H17B and H21A respectively, which are bound to two methylene protons bound. The proton bond to the chiral center forms a hydrogen bond with the oxygen O02 of an adjacent molecule.

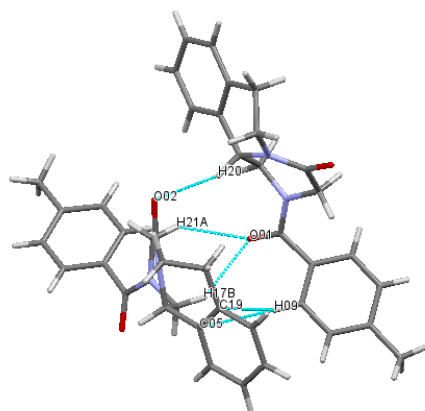


Figure 3-12: 3D representation of compound **3h**

SC-XRD measurement showed that **3j** crystallized from racemic mixture (Figure 3-13) has space group: P21/c (achiral centrosymmetric), monoclinic. This is one of the most common space groups in the family of racemic compounds, thus a further indication that a “non SHG” signal was detected during the pre-screening. A Van der Waals interaction is formed between C16 and the methylene proton of C19 of an adjacent molecule. The proton H15 establish a Van der Waals interaction with the oxygen O01 of the adjacent molecule. The corresponding carbon C10 gives a hydrogen bond with the C08 of an adjacent molecule.

Crystals obtained from a solution of enantiomerically pure **3j** showed a P₂₁2₁2₁ space group (Figure 29). In the same crystalline unit, three molecules are connected to each other with hydrogen bonds: the first molecule the proton bound to the chiral carbon is linked to C12 and C19 of a second molecule while the oxygen of the non-cyclic amide is linked to the hydrogen vicinal to the fluorine (bound to C13 or C15).

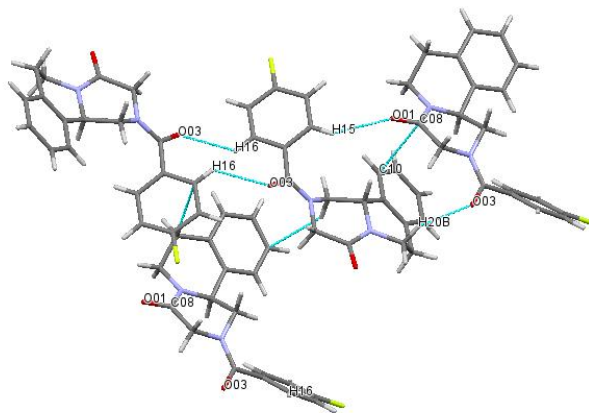


Figure 3-13: 3D representation of compound **3j** crystallized from a racemic mixture.

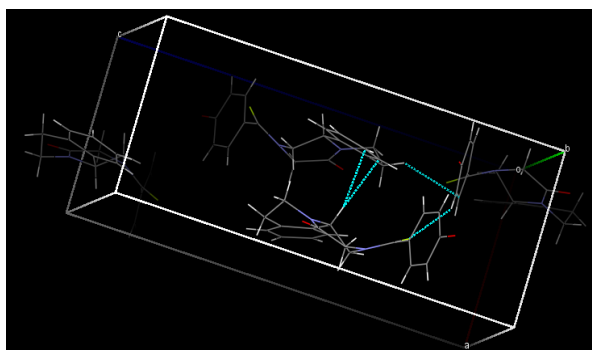
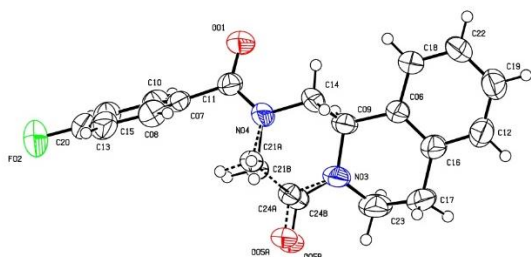


Figure 29: 3D representation of compound **3j** crystallized from enantiomerically pure solution. The dotted lines means that there are two conformations for that moiety, one or the other is present. The ratio is about 70 (continue) / 30 (dotted).

Attempts to obtain from the racemic **3k** single crystals of sufficient size and quality for an SC-XRD analysis were unsuccessful.

Table 5: Summary of the screening results. Results consistent with a conglomerate system are represented as “+”. Not available data are reported as “n.a.”. “Crystal structure” is determined on crystals obtained from racemic solutions.

Compound	SHG	DSC	XRPD	Eutectic composition	Crystal Structure
1	-	- [8]	-	n.a.	- [26]
2	-	- [25]	- [25]	n.a.	n.a.
3a	-	-		-	n.a.
3h	+	-	-	-	-
3i	-	-	-	-	-
3j	+	-	-	-	-
3k	+	-	-	-	n.a.
3u	+	+	+	+	+

3.3.2. Racemization

Racemization of the intermediate praziquanamine in presence of Pd/C and H₂, as reported in literature ^[9a], has some disadvantages for use in the deracemization. The high reaction temperatures (130 °C) required for racemization would lead to extremely high solubilities leading to a low yielding deracemization process or clear solutions. Because of the high pressure (24 bar), the system has to be kept closed for maintaining steady reaction conditions, thus kinetic would be difficult to monitor. Hot filtration would be required at the end of the experiment to prevent nucleation of the counter enantiomer that could hamper the enantiomeric excess. The heterogeneous catalyst could hamper crystallization and furthermore it needs to be isolated from crystalline product. Such isolation step would need particular precaution because the catalyst is pyrophoric. The racemization rate described for praziquanamine is furthermore very low: the complete racemization of enantiopure (*S*)-**2** at 130 °C takes 48 h.

All these disadvantages could be easily overcome by conducting the Pd/C catalyzed racemization in a packed bed reactor under flow conditions. During a crystallization enhanced deracemization experiment the solution could be selectively pumped from a thermostatted flask at low temperature through the packed bed reactor. The racemized solution could return then into the jacketed flask. The racemization rate must be checked in the crystallizer in order to check if the reaction is adequately fast.

The use of a packed bed reactor under flow conditions offers several advantages. The typically long reaction times in batch are often accelerated when transferred to flow. This is by virtue of the contact surface area between reaction mixture and the solid supported catalyst which is significantly higher in flow rather than in batch conditions. Also, the use of back pressure regulators (BPR) would allow attainment of high pressure conditions in a safe manner with a reproducible flow rate. Finally, the catalyst does not need to be isolated afterwards because it is safely confined in the stainless-steel reactor.

With this setup we set out to test the feasibility of this racemization, which should occur in the order of few minutes with a model compound. First, the racemization of enantiomerically pure Praziquantel **1** was tested. Praziquantel is the cyclohexyl amide of praziquanamine and its reactivity is expected to be similar to that of an amide derivative of praziquanamine. We found that in a traditional racemization in a Berghof reactor enantiomerically pure (*R*)-praziquantel (*E* = 99.9%, 2 M) can be partially racemized in toluene to a final enantiomeric excess of *E* = 38.9% within 24 hours. However, the racemization was not clean according to ¹H-NMR and HPLC-MS: an achiral intermediate as well as unidentified byproducts were detected.

The racemization of enantiopure Praziquantel was further conducted in flow at 0.56 M concentration with a packed bed reactor (internal volume = 2 mL) to observe if such conditions were applicable to a near saturated solution at room temperature with a residence time (τ) in the actual packed bed of 0.25 min and 0.5 min respectively. The product was collected downstream to the column and the solution was nearly racemic (results are summarized in Table 6). Traces of the achiral intermediate were observable at 6.75 ppm and at approximately 2.35 ppm in the ^1H -NMR spectrum (Figure 30). The mass of M-2 detected at HPLC-MS is a further confirmation of the presence of this intermediate.

Table 6: Screening of racemization conditions in 5 different runs starting with an enantiopure solution with a concentration of 0.56 M. Reacted **1** is collected downstream to the column. τ = residence time, which is the time spent by a single molecule into the flow reactor. T = temperature, P = pressure. Compound (*R*)-**1** has a starting E = 99.9%?

Entry	Flow rate [mL/min]	τ [min]	T [°C]	P [bar]	final E
1	0.5	0.25	130	10	2.5%
2	1.0	0.50	130	30	8.1%
3	0.5	0.25	150	10	3.7%
4	0.5	0.50	150	30	3.3%
5	1.0	0.25	150	10	3.3%

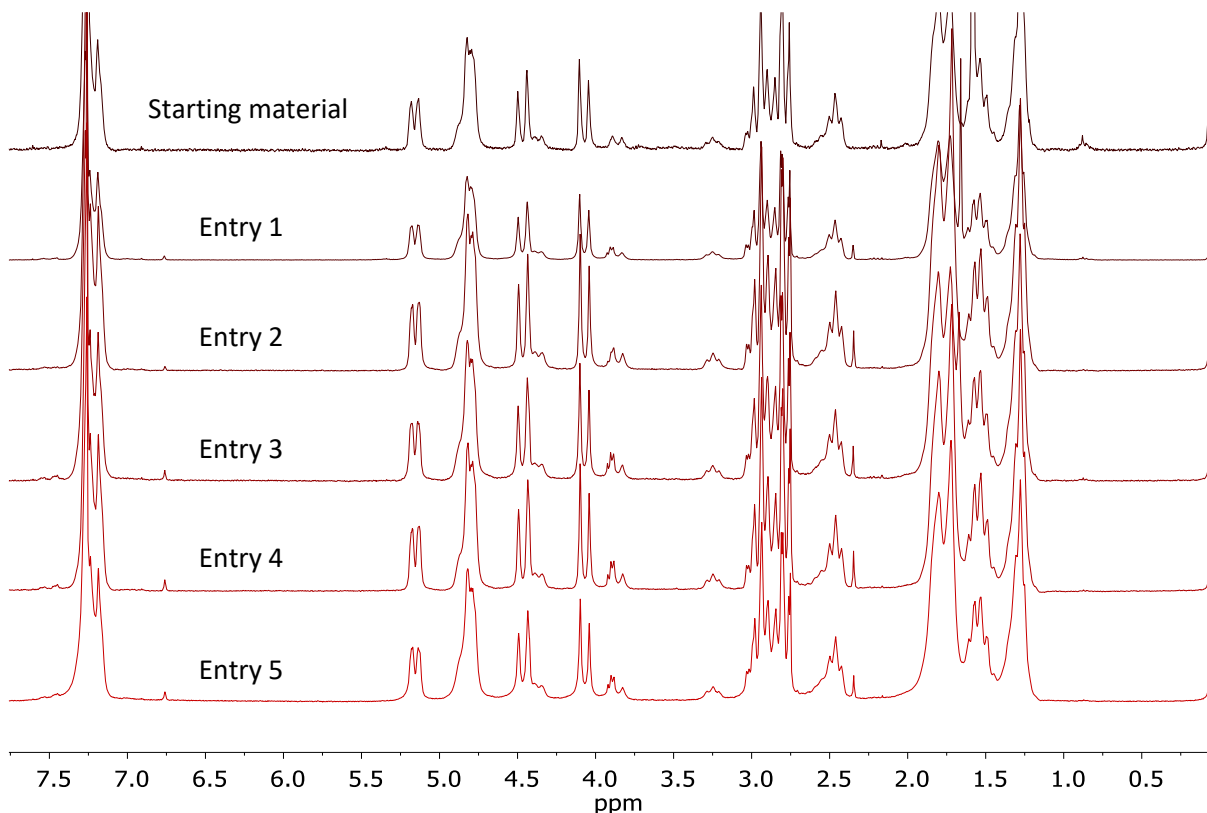


Figure 30: ^1H NMR of the reacted **1** after a first pass through the packed bed column in the screening described in Table 6.

Subsequently, racemization studies and optimization were carried out for derivative **3u**, which is the real target of the deracemization. It was demonstrated that a solution 0.18 M of enantiopure **3u** racemizes under the same reaction conditions to those used for Praziquantel. Thus, racemization was studied by

recycling the mother liquor to establish the overall racemization rate of the whole solution to simulate the behavior of the liquid phase of a crystallization enhanced deracemization. It is important to mention that the speed of racemization is dependent on the total volume/dead volume ratio: the lower this ratio, the faster is the racemization of the whole solution.

The earlier studies were performed at low concentrations of (*R*)-**3u** in order to obtain general observation without using too much enantiopure compound. It was observed that if H₂ was continuously delivered to the catalyst, then a plateau in enantiomeric excess was reached. The moment the H₂ supply was interrupted the racemization proceeded quickly (Figure 31). HPLC-MS analysis further shows that once the H₂ supply was interrupted, the amount of achiral intermediate increased over time (Figure 32).

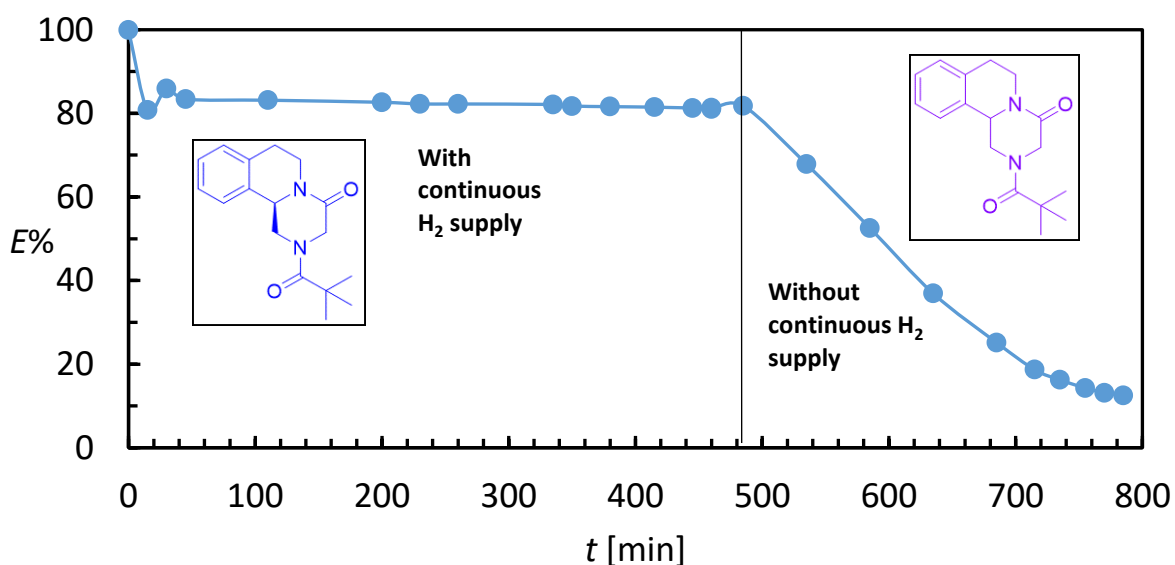


Figure 31: racemization of **3u** in loop in presence and in absence of continuous H₂ supply at 130 °C and 30 bar with a total volume/dead volume ratio = 20.1.

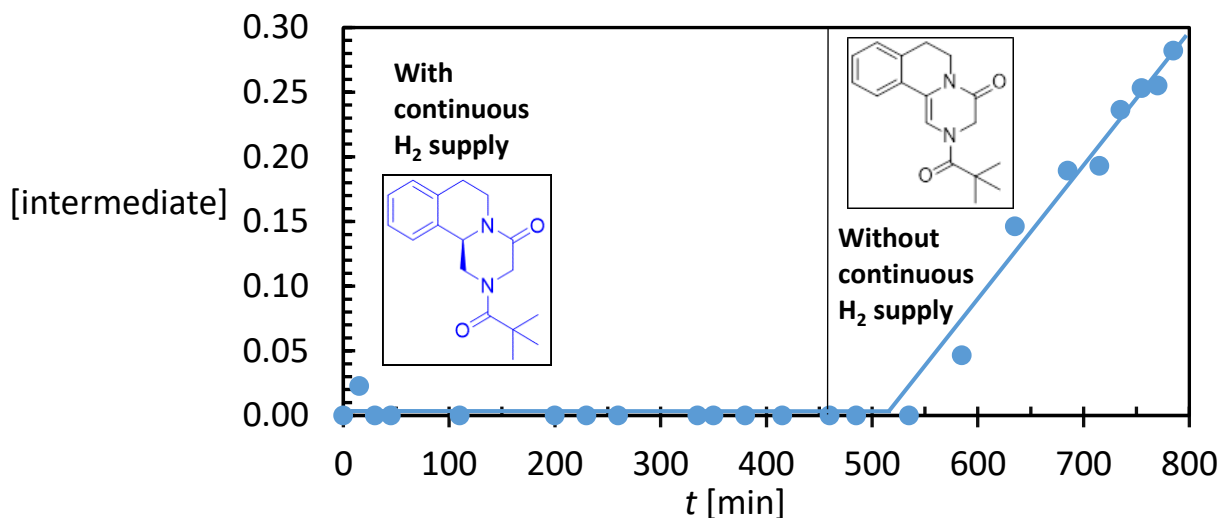


Figure 32: Concentration of achiral intermediate over time. The concentration is quantified by the ratio of the absorbances of the intermediate and **3u** detected in the Total Ion Current (TIC) Chromatogram.

Interestingly the first drop in E (second point of Figure 31) corresponds to the formation of the achiral intermediate (second point in Figure 32). After this first point, a plateau in E is reached, which means that no further racemization is occurring. This is probably linked to the coordination of the supported palladium to H_2 . In this way the oxidation state of the palladium switches from 0 to 2 and subsequently $Pd(0)$ becomes $Pd(II)$, which cannot perform the dehydrogenation necessary for the racemization reaction. This plateau region in Figure 31 corresponds to the disappearance of the achiral intermediate in the mixture which is hydrogenated to re-form racemic **3u**.

When hydrogenation is interrupted at 460 min, racemization turn accelerates as soon as some traces of intermediate are formed (535 min). This happens probably because of desorption phenomena^[27] which converts $Pd(II)$ into $Pd(0)$ with release of H_2 . Such desorption phenomena take roughly 90 minutes to produce a boost in racemization. This suggests that the H_2 desorption phenomena are slower than H_2 absorption ones. Such absorption phenomena are linked to the flow rate of H_2 delivered by the H-cube (H_2 flow rate data not available).

When the same recycle is performed with a column packed with fresh, not pre-activated catalyst with a total volume/dead volume ratio equal to 16.9, thus even more advantageous in comparison to the experiment shown in Figure 31, racemization is much slower (Figure 33). Thus, H_2 pre-activation seems necessary to obtain a fast racemization.

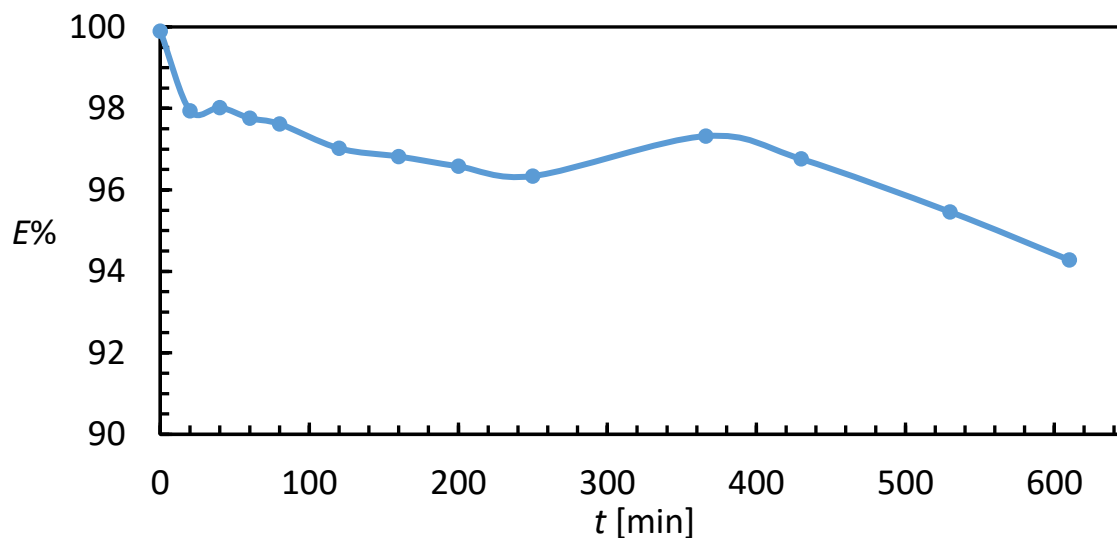


Figure 33: racemization of **3u** in loop absence of external H₂ supply at 130 °C and 30 bar with a total volume/dead volume ratio = 16.9.

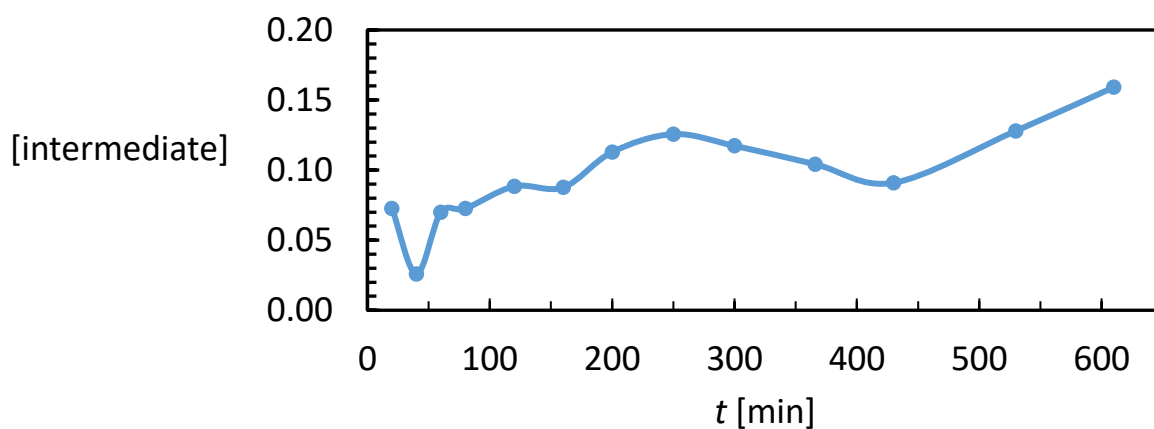


Figure 34: formation of achiral intermediate over time. The y axis reports the ratio of the absorbance of the intermediate and the absorbance (Abs) of **3u** detected in the Total Ion Current (TIC) Chromatogram.

Finally, the racemization rate was monitored by using the same racemization loop but with concentrations of **3u** similar to the one expected during a deracemization experiment (Figure 35) during which, in absence of racemization, a small enantiomeric excess (usually lower than 10%) in the unwanted enantiomer would be generated. The highest temperature during a deracemization experiment was planned to be

maintained at 15 °C so that the solution pumped through the flow system would warm up to room temperature remaining undersaturated in order to avoid nucleation. Racemization is meant to be tested at the highest concentration achievable during the process. The concentration of palladium remains constant over time and since the catalytic sites are limited, the highest concentration is considered the most critical for an efficient racemization. At a higher concentration a larger fraction of the catalytic sites will be occupied. Beyond a certain threshold concentration all catalytic sites would effectively be occupied. Over this threshold concentration, which has not been determined, the racemization rate is expected to slow down. Since the solubility of the mixture is affected by the enantiomeric excess, the racemization rate was determined by racemizing a near saturated solution at 15 °C with *E* 10% in toluene (Figure 35). The half-life was found to be about 31 min. Thus, racemization occurs relatively quickly for a recycled highly concentrated solution of **3u** provided that the catalyst is pre-activated with H₂ and the ratio between the solution to be racemized (total volume) and the internal volume of the packed bed reactor equipped with catalyst (dead volume) is adequate. In this specific experiment the total volume/dead volume ratio was 15.6.

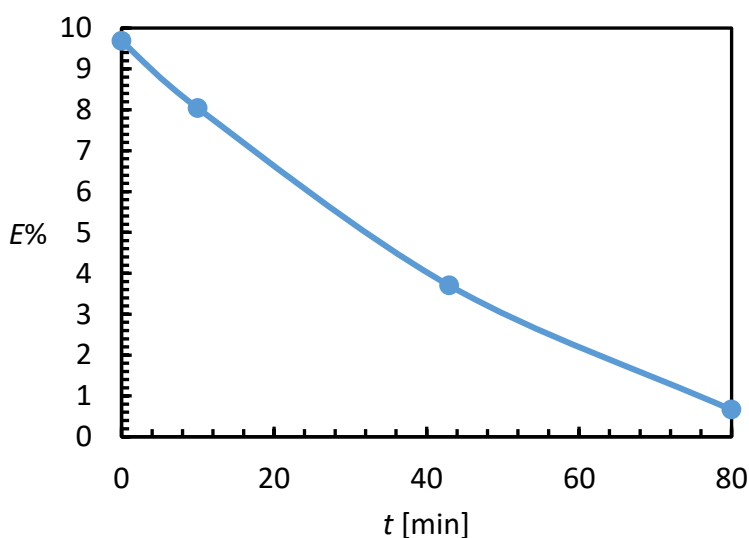


Figure 35: racemization of a 0.12 M solution of **3u** 10% *E* in toluene at 130 °C.

Palladium catalyzed racemization of compound **2** and derivatives relies on two reactions, namely dehydrogenation and hydrogenation, with two different reaction constants. Both reactions are not enantioselective and they are identical in rate for both enantiomers.

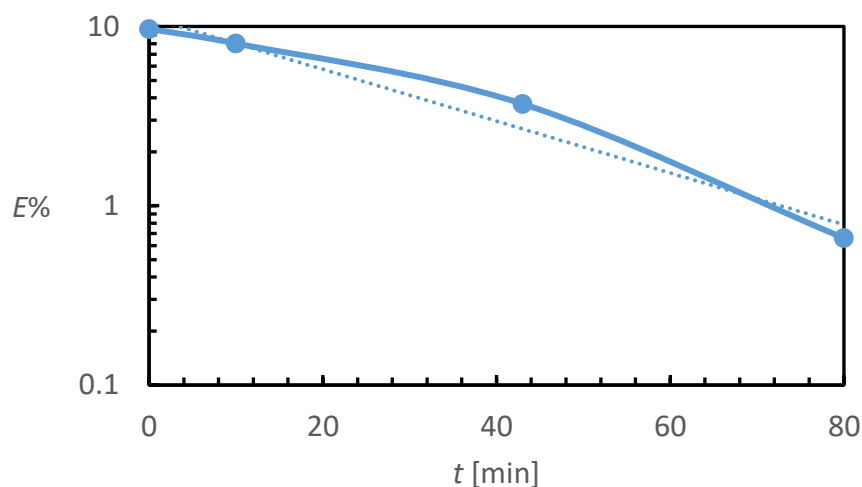


Figure 36: Racemization of a 0.12 M solution of **3u** 10% *E* in toluene at 130 °C in a log-normal plot. The decrease in enantiomeric excess can be approximated by a straight line. This suggests with a certain approximation a first order kinetic.

This racemization does not seem to exactly follow first order kinetics. Thus, it is not possible to determine the racemization rate in a precise manner. The racemization rate should be measured as a function of all components such as H₂ concentration, amount of catalyst and substrate. However, the hydrogen concentration absorbed on the catalyst surface as a function of time is unknown.

3.3.3. Deracemization

Deracemization was first attempted in a decoupled Viedma ripening mode. This Viedma ripening technique can start from a racemic suspension but the deracemization speed is much higher when the enantiomeric excess E exceeds the threshold of 5-10%. During Viedma ripening dissolution/crystal growth events take place while racemization is occurring in solution. These events are promoted by applying grinding which can occur by stirring in the presence of glass beads, by applying ultrasound or by using a combination of both.^[12] This grinding decreases the average particle size. In a suspension at constant temperature, smaller crystals tend to dissolve while larger ones grow. Therefore, in a polydisperse suspension, crystallization and dissolution occur simultaneously, establishing an equilibrium. A bias in the distribution of the enantiomeric excess over the size of the crystals then is driving the E of the suspended crystals towards 100%.^[6a, 28]

Because Pd/C catalyzed racemization of conglomerate **3u** can be conveniently performed only in a packed bed reactor, the racemization and grinding processes were decoupled. A tubing equipped with a filter was submerged into the slurry, thermostatted at 15 °C. Such tubing, connected to the pump allowed to deliver the solution to the H-Cube equipped with a packed bed column and thus to achieve *ex-situ* racemization.

However, in all the experiments performed, the yield was insufficient to establish if deracemization occurred, because the mass of the enantiomer in excess never exceeded the mass of the seeds introduced (Figure 37 and Figure 38). E seemed to increase when grinding and racemization were applied. However when grinding was stopped E decreased. It is possible to assume that the grinding led to enhanced dissolution of racemic **3u**. The mass of the suspended racemic **3u** decreased over time while the (*R*)-**3u** in excess did not decrease by virtue of lower solubility, thus the E measured in every sample was every time higher.

The same problem was encountered when a thermostatted ultrasonic bath was used to replace the grinding provided by the glass beads. Dissolution of the material was easily detected by eye and clogging events occurred in the tubing very quickly and the process could not be carried out.

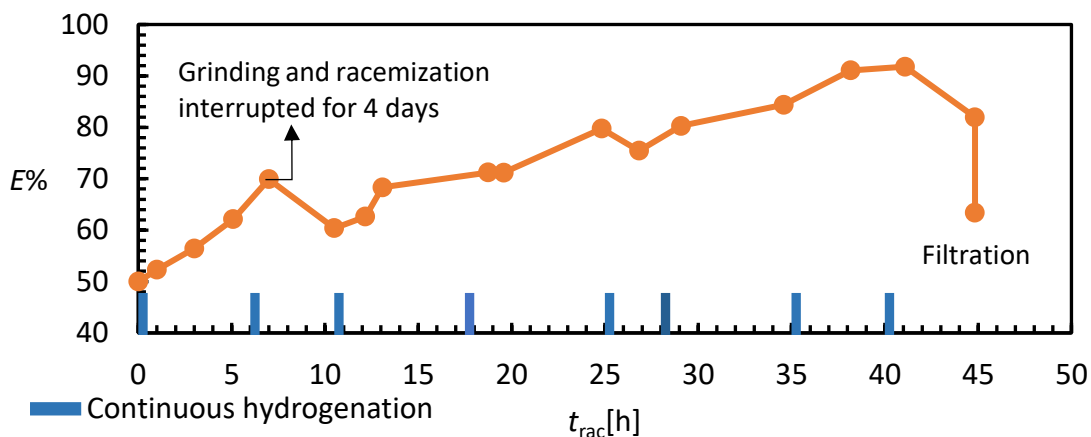


Figure 37: deracemization through decoupled Viedma ripening with *ex situ* racemization starting from high initial E . After that the fifth sample was withdrawn oven, pump, H-Cube and stirrer were turned off. A line is added to guide the eye.

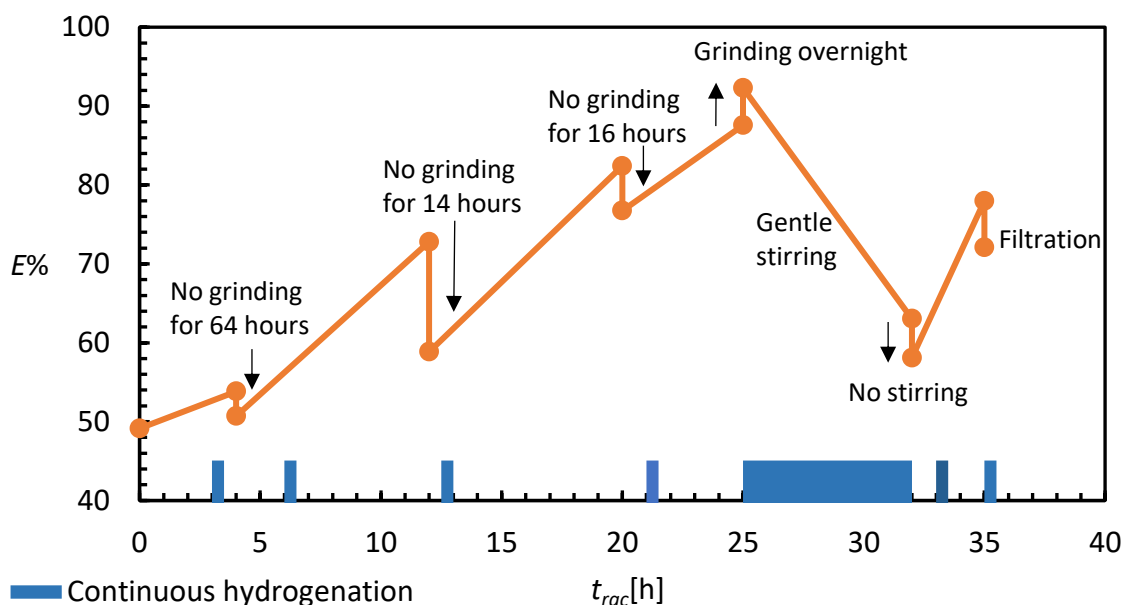


Figure 38: deracemization through decoupled Viedma ripening with *ex situ* racemization starting from high E . t_{rac} represents the time during which the mother liquor was continuously pumped through the packed bed column. The blue stripe at the bottom, represents the time during which the packed bed column was continuously hydrogenated at 130 °C and 30 bar. Where arrows are drawn, the heating of the racemization column was switched off. A line is added to guide the eye.

Dissolution and crystallization may occur at different rates. Usually, the latter is slower than the first. This might explain why the yields were all the time so low. The grinding could have hampered the crystal growth, leading to the formation of small particles that passed the filter.

Other techniques in which the dissolution/crystal growth process rely on the variation of temperature of the crystallization chamber, like Temperature Cycling Induced Deracemization (TCID) and Second Order Asymmetric transformation (SOAT) seemed to overcome these limitations.

During a SOAT experiment, a nearly saturated solution is seeded with a fraction of enantiomerically pure crystals. A cooling ramp is then applied to allow homochiral crystal growth on the surface of pre-existing crystals. Racemization in solution prevents high supersaturation (and therefore subsequent primary nucleation) of the counter enantiomer. During a TCID experiment a slightly enantiomerically enriched suspension is subjected to temperature cycles to promote dissolution and crystal growth events in different timeframes while racemization occurs in solution.

With a first SOAT approach, starting with 2971 mg racemic **3u** and 290 mg enantiopure **3u** in toluene at 15 °C cooling with a temperature ramp over 3 h provided 710 mg crystalline **3u**, *E* 88.9%, corresponding to a net achievement of 342 mg new (*R*)-**3u**. The mother liquor was still enriched in (*S*)-**3u** (*E* 11.4%) indicating that equilibrium had not been reached under these conditions. The total volume/dead volume ratio (41.3) was much higher than the one used for the racemization test, however the available thermostatted glassware was too large therefore too much solution was required to cover completely the filter in order to prevent air to enter the system and thus causing blockages of the flow system. From the solubility phase diagram in Figure 39a) it is possible to see that the solution was still undersaturated at the beginning of the experiment and this explains the low yield achieved. The use of smaller jacketed tube-shaped reactor allowed the stirring to occur by means of a magnetic bar in presence of the filter that could have been completely submerged in the slurry while maintaining a much lower total volume/dead volume ratio corresponding to 12.8 (Figure 40). In this experiment a higher starting concentration was used.

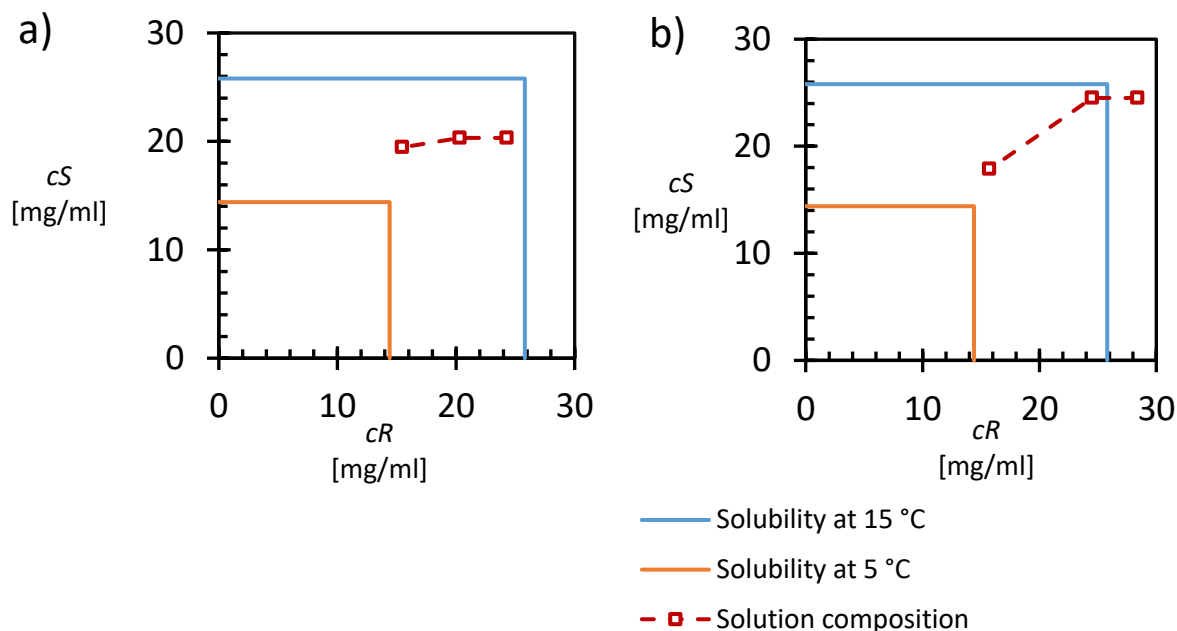


Figure 39: solubility diagrams. The blue line represents the solubility at 15 °C, the orange line represents the solubility at 5 °C. The dotted line represents the variation of concentration in the liquid phase during the deracemization process. a) SOAT experiment performed with total volume/dead volume ratio = 41.3 b) SOAT experiment performed with total volume/dead volume ratio = 12.8.

In both the SOAT procedures the final solution concentration does not correspond to the apex of the solubility line at 5 °C drawn in orange. This is probably because the thermodynamic equilibrium was not reached yet. In the second experiment the filtration occurred closer to the thermodynamic equilibrium in comparison to the first experiment. The higher concentration used could have allowed the achievement of the thermodynamic equilibrium faster than in the first experiment. Results of both experiments are summarized in Table 7.

Table 7: results of SOAT procedure.

Mass of RS [mg]	Mass of R seeds ($E = 100\%$) [mg]	Mass of harvest collected [mg]	E (harvest)	Mass of R including seeds [mg]	Mass of R excluding seeds [mg]
2971	290	710	88.9%	631	341
1000	79	394	91.8%	362	283

TCID mode is advantageous because multiple cycles may be carried out with a single filtration in the end. Two TCID experiments were carried out using a total volume/dead volume ratio corresponding to 11.9, thus similar to the one used in the most successful SOAT approach. Complete deracemization was achieved by TCID (Table 8, Figure 40). Mother liquor is racemic. Recharging would allow virtually total conversion of the racemate to the desired enantiomer. The collected crystalline product was analyzed by Brightlab BV to check the palladium contamination which was determined to be lower than 0.1 mg/kg.

Table 8: TCID Induced Deracemization of **3u**. Temperature ramp: 15.0 °C → 5.0 °C; the reaction was run in methanol; τ = 2 min, flow rate 0.8 mL min⁻¹ ; 1356 mg activated Pd/C 10% catalyst; total volume/dead volume reactor = 11.9 cooling rate = 5 °C min⁻¹.

Mass of RS [mg]	Mass of R seeds (E = 100%) [mg]	Initial E in suspension	Suspension density [mg/mL]	Mass of harvest collected [mg]	E (harvest)	Mass of R including seeds [mg]	Mass of R excluding seeds [mg]
2029	216	19	72	888	97%	858	642
1925	216	23	72	854	98%	834	618

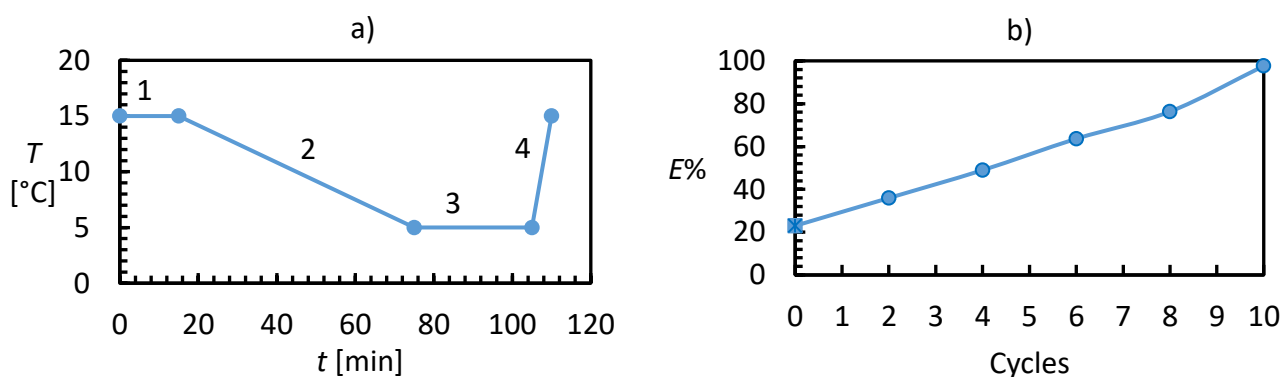


Figure 40: a) Temperature cycle profile adopted during the TCID experiment. b) Enantiomeric excess of the collected crystals of **3u** as a function of number of cycles. Square represents a sample withdrawn at 15 °C while circles represent sample withdrawn at 5 °C.

3.4. Discussion

The entire process of conglomerate search is schematically represented in the workflow drawn in Figure 41. First, the Praziquantel intermediate praziquanamine **2** is identified as a suitable starting material for the development of a crystallization-enhanced deracemization procedure. Later Praziquantel, available within the CORE Network, is used as a model compound for early racemization studies to establish a fast and clean racemization method. Then, with racemization conditions in hand, the search for conglomerates can start by synthesizing several Praziquantel analogues and analyzing them by using a combination of analytical methods. Once the conglomerate is identified, suitable conditions to racemize Praziquantel are tested on the conglomerate. Finally, the conglomerate is deracemized exploiting racemization conditions combined with crystallization techniques to allow selective crystallization of the desired enantiomer while converting the unwanted enantiomer in solution.

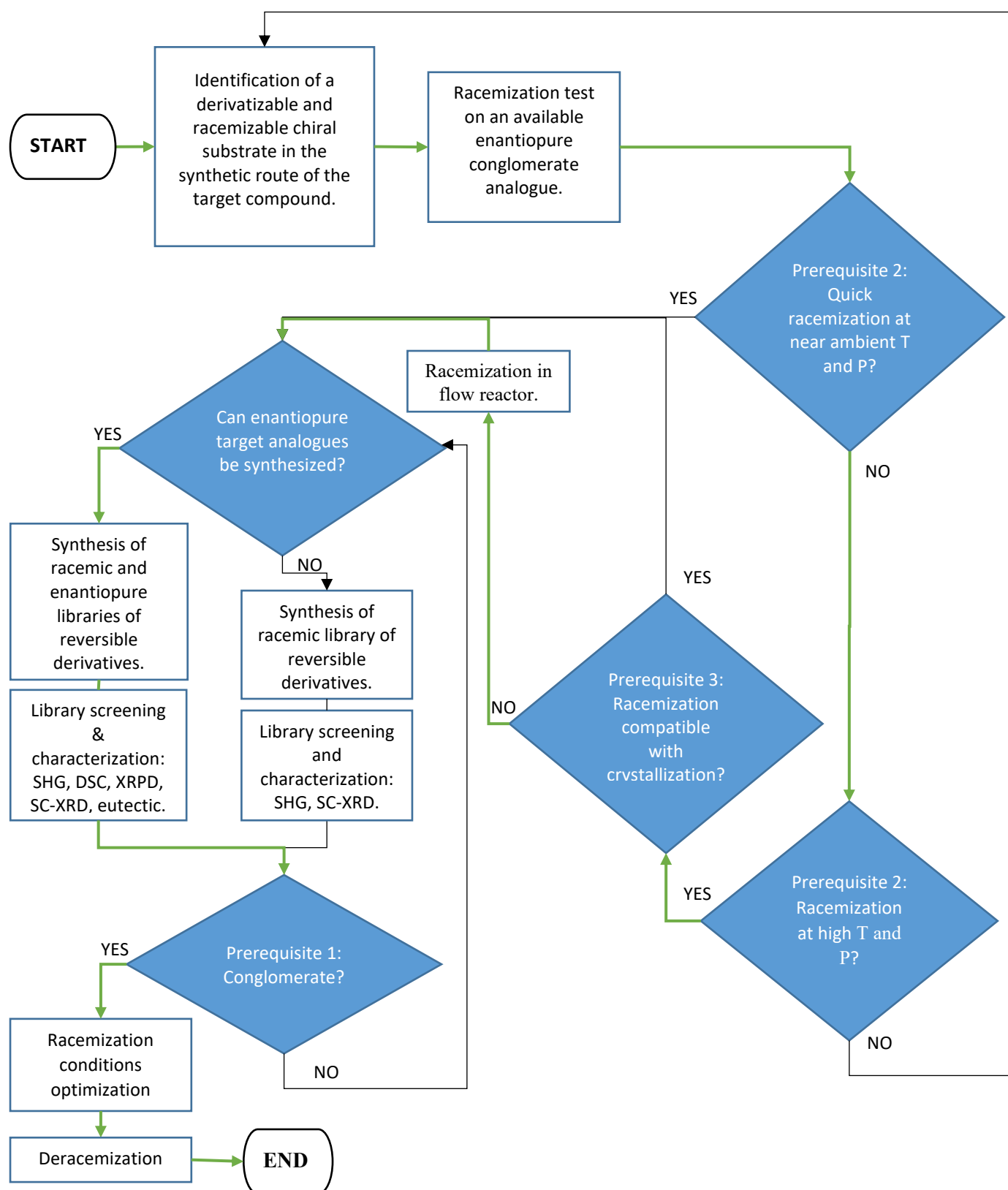


Figure 41. General workflow for conglomerate based crystallization-enhanced deracemization. The specific strategy for deracemization of Praziquantel follows the gray arrows.

3.4.1. Conglomerate search

So far it is not possible to predict a conglomerate structure. We chose to prepare a covalent library of compounds that can readily be reconverted to the parent. Salts and co-crystals can also be used to prepare libraries, but we expected racemization to be easier and cleaner with neutral compounds.

SC-XRD is a very powerful technique that requires only racemate, but so far it requires long analysis times and expensive apparatus. Also, in order to produce crystals suitable for SC-XRD analyses, particular crystallization conditions are needed and they might not correspond to the crystallization conditions adopted during resolution/deracemization experiments. Polymorphism and meta-stable racemic compounds have to be taken into account.

When also enantiomerically pure material is available, methods like XRPD and eutectic determination are of primary importance, however calibration curves for polarimeter and developing methods for chiral HPLC are time consuming, thus this is why it is important to have a high throughput screening technique like SHG.

3.4.2. Racemization

The racemization has a redox mechanism and occurs through dehydrogenation/hydrogenation catalyzed by Pd/C. This mechanism is facilitated when the chiral center is activated by an aryl moiety. Racemization without pre-activation of hydrogen is not really effective, whereas saturation of the catalyst with hydrogen does not allow the dehydrogenation to take place. Results suggest that at the condition used, the hydrogen is partially released by the catalyst, most likely dissolved in the solvent, thus several activations are needed when the racemization needs to occur for long time. An optimal activation frequency was found to be one activation each two hours.

3.4.3. Deracemization

Knowing the residence time is not enough to apply this racemization method to crystallization-assisted deracemization techniques, in particular when temperature ramps are applied. The ratio between the total volume and the dead volume and the system plays a key role in preventing primary nucleation of the counter enantiomer.

3.5. Conclusion

Deracemizations using Viedma ripening and related technologies are usually restricted to cases where racemization and crystallization occur under mutually compatible conditions. The present work marks, to the best of our knowledge, the first example of the use of flow systems together with Second Order Asymmetric Transformation (SOAT) and Temperature Cycling Induced Deracemization (TCID) in order to decouple the crystallization and solution racemization. This work recognizes flow chemistry as an enabling technology in the field of crystallization-enhanced deracemization, which enables two different previously incompatible process conditions to work simultaneously. By using a packed bed reactor connected to a hydrogen source it has been possible to selectively racemize the solution *ex-situ* at high temperature while allowing a cooling crystallization to occur at low temperature. In this way enantiomerically pure Praziquantel can be obtained through crystallization-enhanced deracemization. The technology described in this chapter should be applicable to other medicinally interesting chiral compounds that racemize only under harsh racemization conditions. A fast racemization method was developed for Praziquantel analogues which can be applied for the racemization of the mother liquor in crystallization-assisted deracemization. This method is based on flow heterogeneous catalysis through a packed bed column. As often observed, reaction times were accelerated in flow, especially when utilizing immobilized catalyst packed in fixed bed reactor. This is by virtue of the contact surface area between reaction mixture and the solid supported material which is significantly higher in flow rather than in batch conditions. Indeed, this reactor type affords a significantly higher effective molarity of the catalyst/reagent. In flow, small volumes (dead volume) of substrate solution are in contact with a high surface of catalyst, while usually the opposite situation occurs in batch. Also, leaching of palladium, which is a very common problem when these palladium-based catalysts are used, was found to not represent a threat in the collected crystalline product. Thus, this racemization methods combined with controlled cooling crystallization is compatible with Good Manufacturing Practice (GMP) protocols for pharmaceuticals which have restrictions in terms of toxicity from heavy metals. Only one suitable conglomerate has been found among the library of 30 derivatives of praziquanamine. Three aryl derivatives with similar molecular structures gave strong positive SHG signals, but were found to behave as racemic compounds when suspended in toluene. These false positives show that SHG needs to be supported by other measurements. However, SHG can be conveniently used as a fast pre-screening tool, when a large number of racemic derivatives is available. The decoupling strategy in crystallization-enhanced deracemization should also be possible for racemization methods beyond transition metal catalysts such as enzymatic or light induced racemization.

The obtained conglomerate derivative of praziquanamine, once deracemized, can be converted back to praziquanamine without loss of optical purity.

3.6. Appendix

3.6.1.1. DSC

Compound **3h**

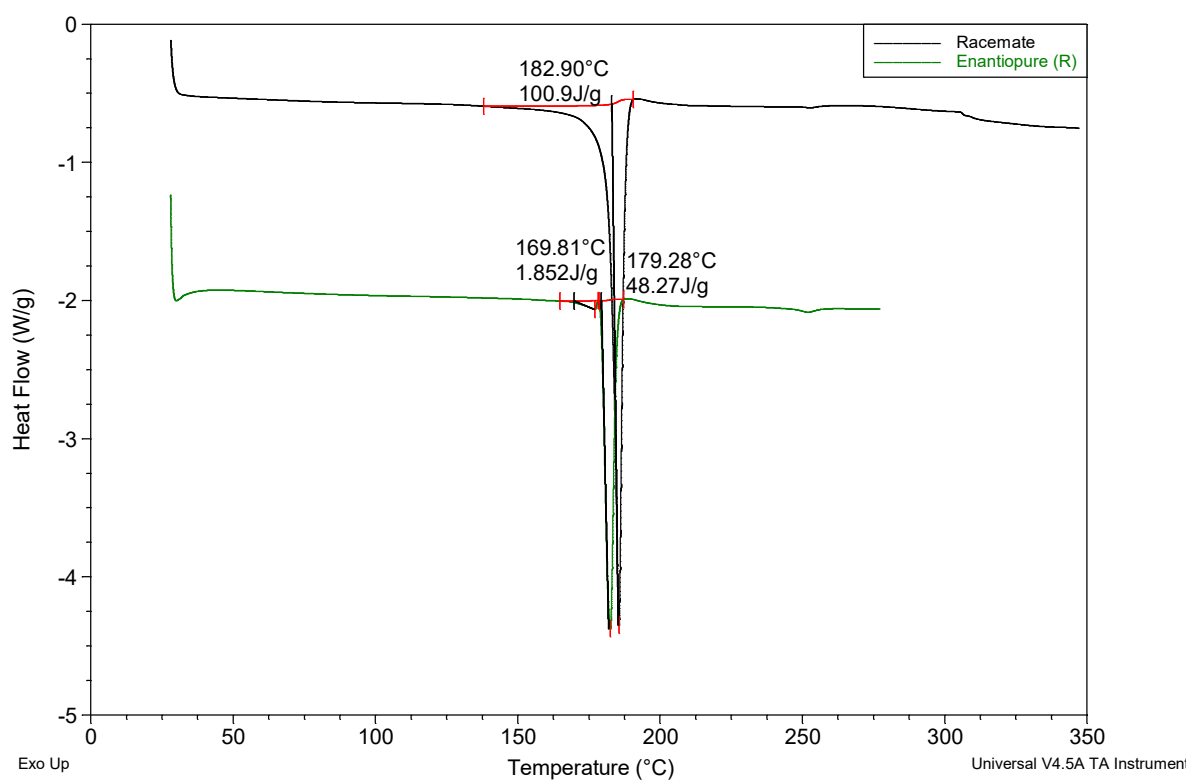


Figure 42: Stacked DSC of racemic and enantiomerically pure **3h**. ΔT^f (*R-RS*) = -3 °C. This difference does not suggest a conglomerate.

Compound **3j**

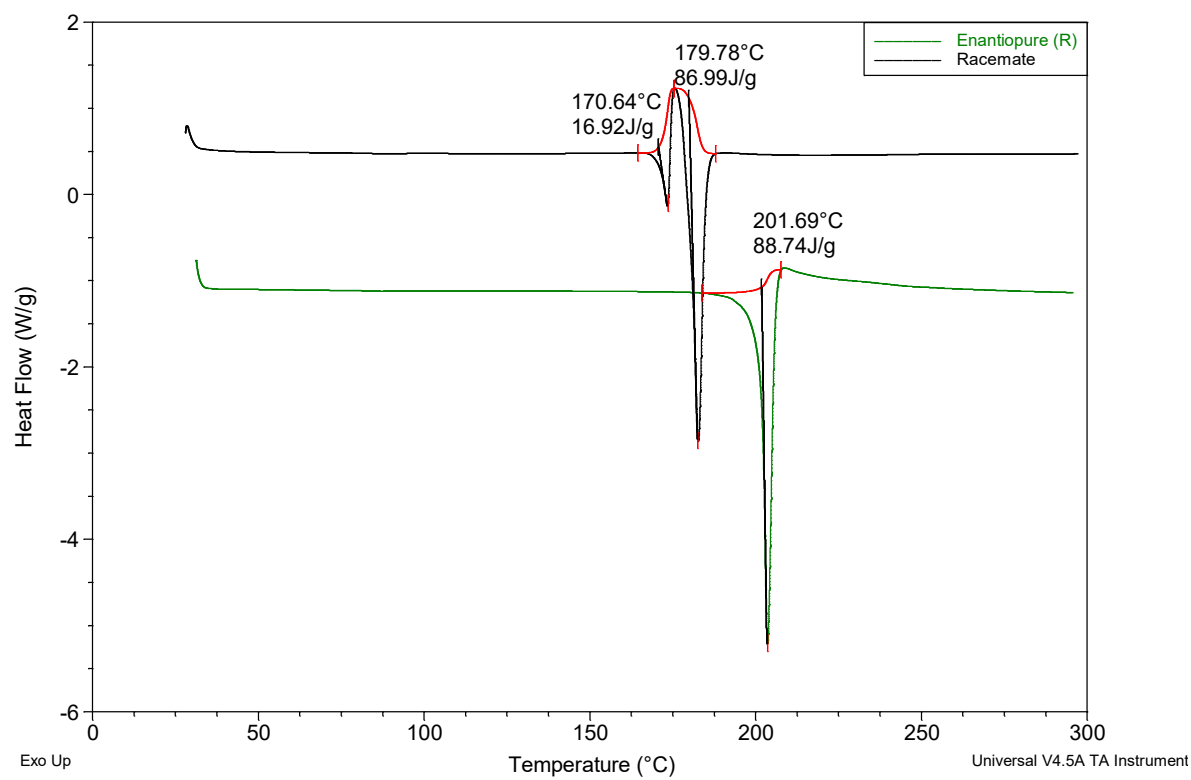


Figure 43: Stacked DSC of racemic and enantiomerically pure **3j**. ΔT^f (*R-RS*) = 19.6 °C. This difference suggests a conglomerate.

Compound **3k**

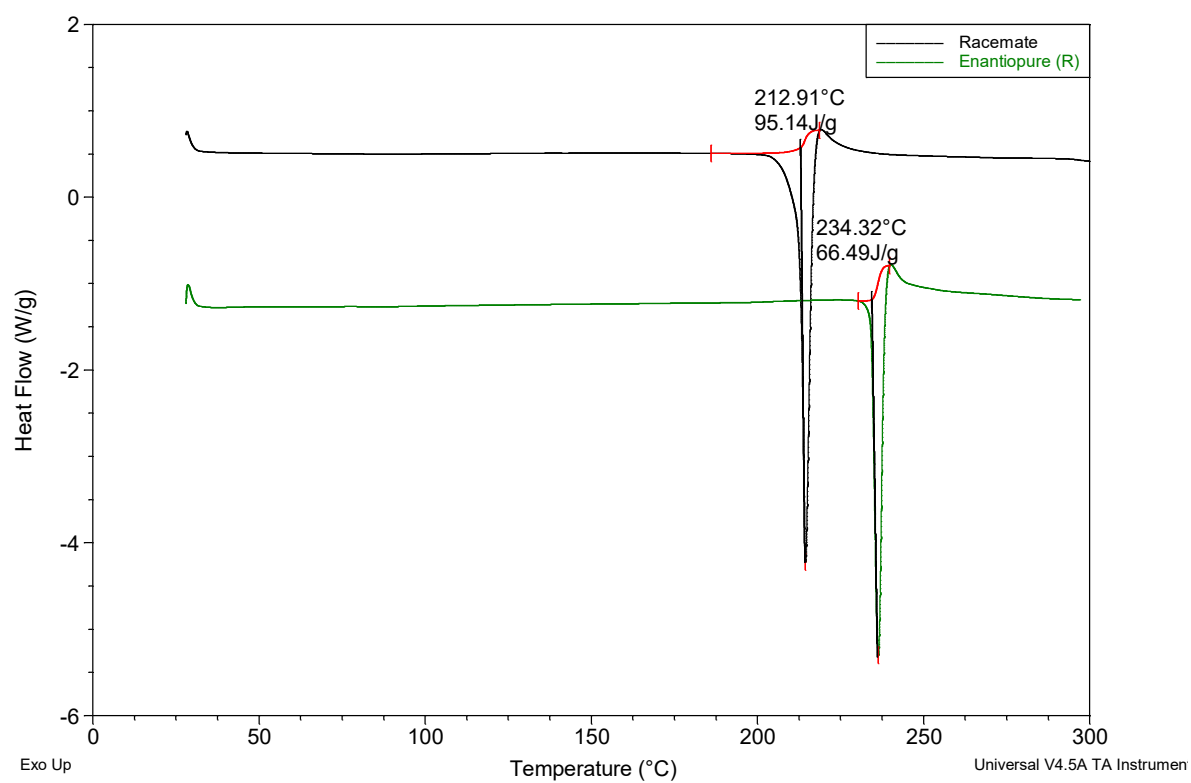


Figure 44: Stacked DSC of racemic and enantiomerically pure **3k**. ΔT^f (*R-RS*) = 19.6 °C. This difference suggests a conglomerate.

Compound **3u**

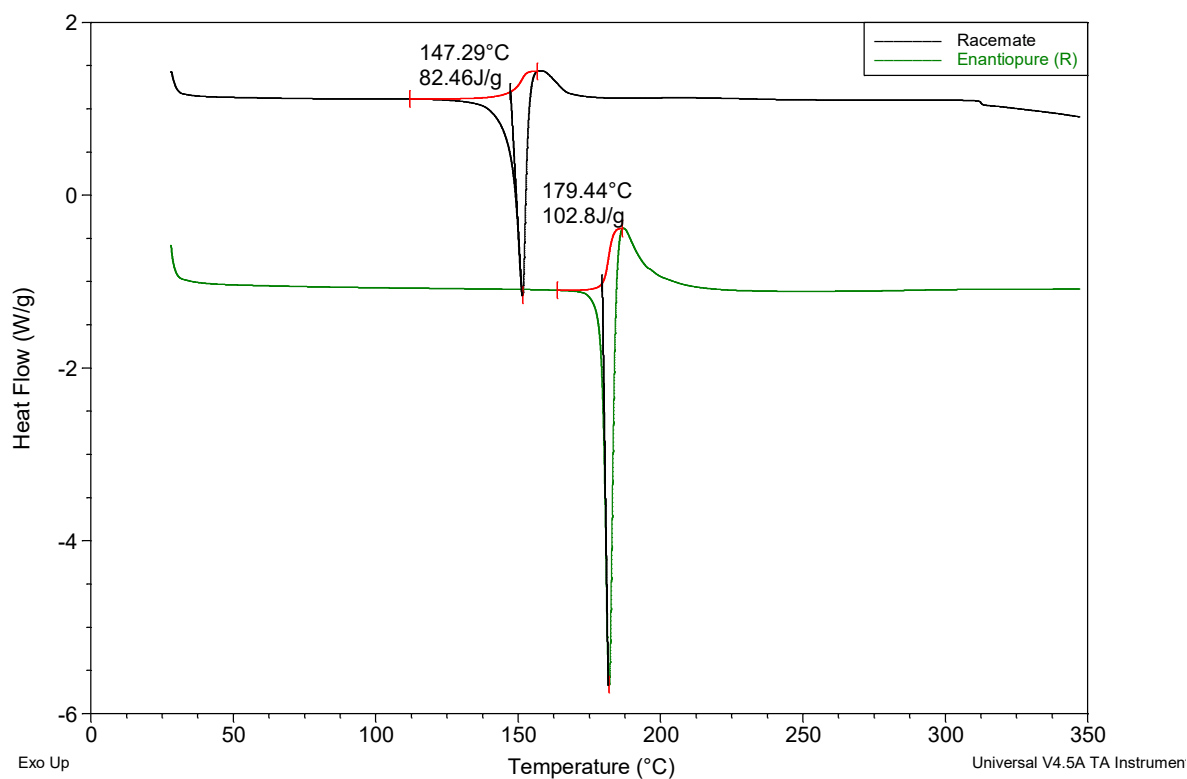


Figure 45: Stacked DSC of racemic and enantiomerically pure **3u**. ΔT^f (*R-RS*) = 32.1 °C. This difference suggests a conglomerate.

3.6.1.2. XRPD

Compound **3h**

Figure 46 shows that XRPD patterns of the racemate and the enantiomerically pure (*R*)-**3i** do not overlap, giving a further confirmation that such derivative forms a racemic compound system. The predicted XRPD, obtained from SC-XRD measurement corresponds to the experimental one, indicating the presence of the same crystal form.

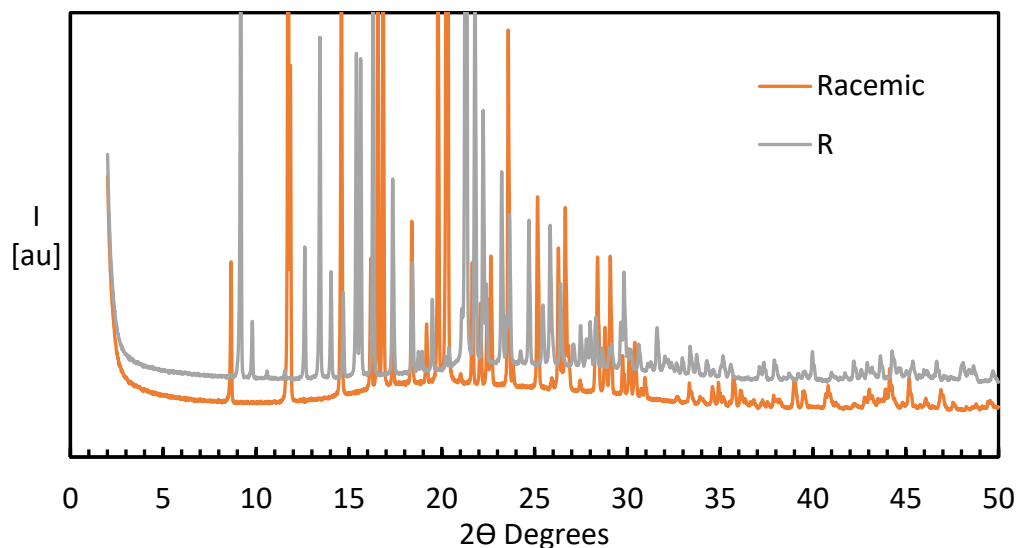


Figure 46: stacked XRPD patterns of derivative **3h**.

Compound **3j**

The experimental diffractogram (Figure 47) of the racemate (top black curve), matches nicely with the predicted powder diffractogram from the single crystal model (blue curve). A minor amount of the enatiopure crystal form is also present (~5%).

The experimental diffractogram of the enatiopure sample, matches mostly with the predicted powder diffractogram from the single crystal model (red curve). The additional diffraction peaks, indicate that a second, unidentified crystalline phase is also present.

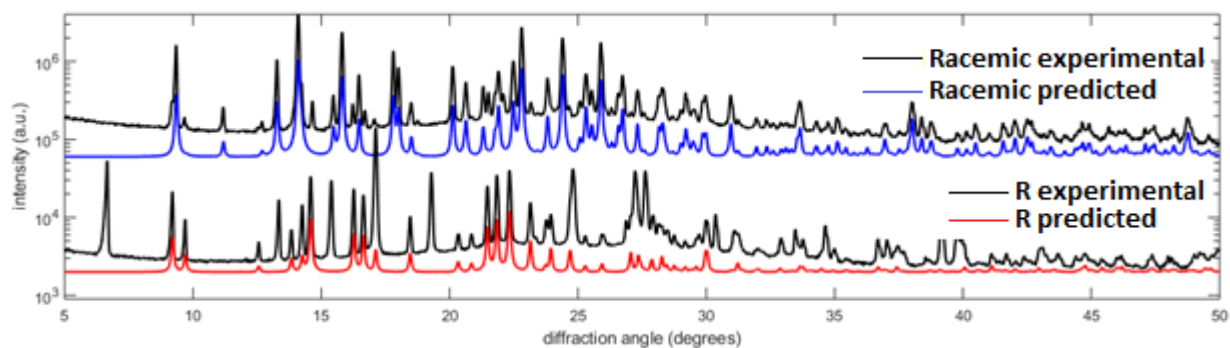


Figure 47: stacked XRPD patterns of derivative **3j**.

Compound **3k**

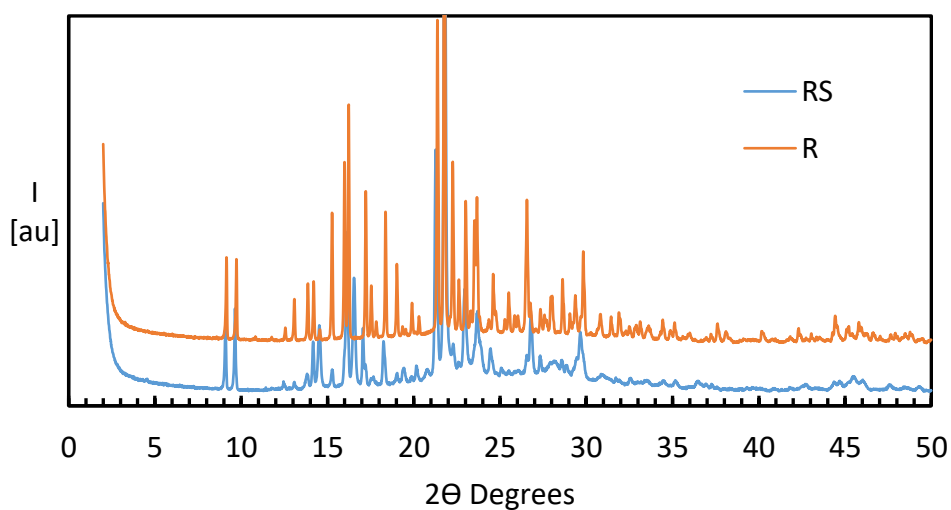


Figure 48: stacked XRPD patterns of derivative **3k**.

The diffractograms of racemate and enantiopure of derivative **3k** differ (Figure 48). Although many peaks overlap this indicates a racemic compound.

Compound **3u**

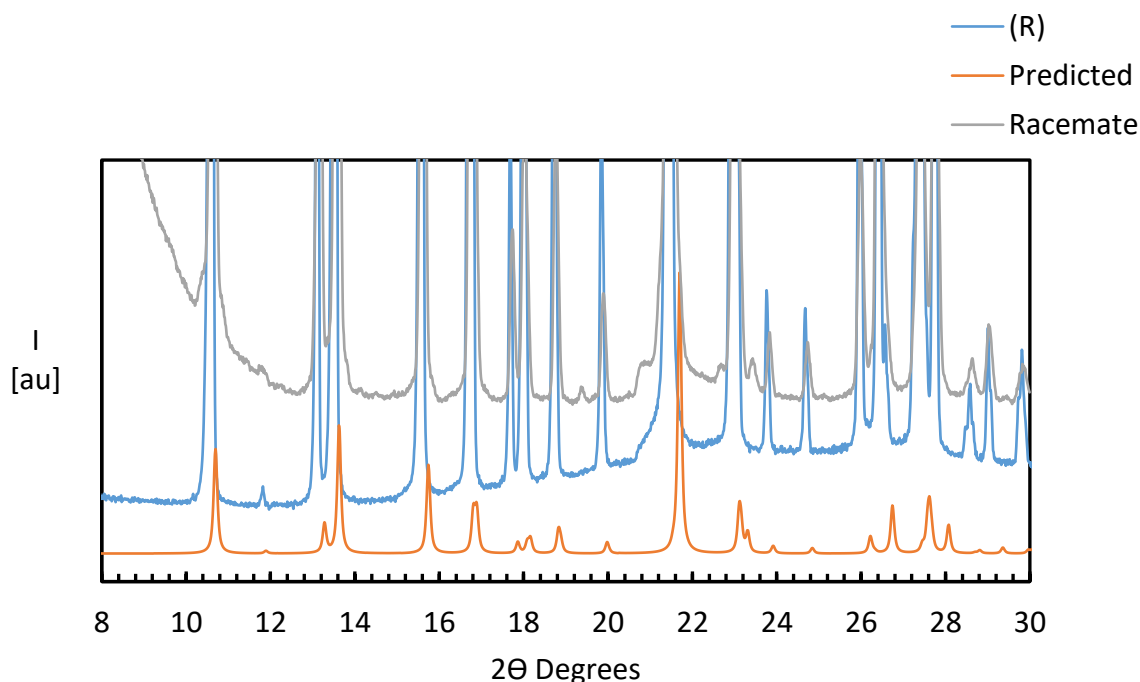


Figure 49: stacked XRPD patterns of derivative **3u**.

Figure 49 shows that XRPD patterns of the racemate and the enantiomerically pure (*R*)-**3u** overlap, giving a further confirmation that such compound forms a conglomerate system. The predicted XRPD, obtained from SC-XRD measurement corresponds to the experimental one, indicating the presence of the same crystal form.

3.6.2. References

- [1] H. Liu, S. William, E. Herdtweck, S. Botros, A. Dömling, *Chemical Biology & Drug Design* **2012**, *79*, 470-477.
- [2] I. Meister, K. Ingram-Sieber, N. Cowan, M. Todd, M. N. Robertson, C. Meli, M. Patra, G. Gasser, J. Keiser, *Antimicrobial Agents and Chemotherapy* **2014**, *58*, 5466.
- [3] a) M. Woelfle, J.-P. Seerden, J. de Gooijer, K. Pouwer, P. Olliaro, M. H. Todd, *PLOS Neglected Tropical Diseases* **2011**, *5*, e1260; b) Maillard D., Waechtler A., Maurin J., Wakaresko E., Jasper C., *PCT Int. Appl.*, **2016**, WO2016078765
- [4] O. Sánchez-Guadarrama, F. Mendoza-Navarro, A. Cedillo-Cruz, H. Jung-Cook, J. I. Arenas-García, A. Delgado-Díaz, D. Herrera-Ruiz, H. Morales-Rojas, H. Höpfl, *Crystal Growth & Design* **2016**, *16*, 307-314.
- [5] F. C. Cunha, A. R. Secchi, M. B. de Souza Jr, A. G. Barreto Jr, *Chirality* **2019**, *31*, 583-591.
- [6] a) C. Viedma, *Physical Review Letters* **2005**, *94*, 065504; b) M. W. van der Meijden, M. Leeman, E. Gelens, W. L. Noorduin, H. Meekes, W. J. P. van Enckevort, B. Kaptein, E. Vlieg, R. M. Kellogg, *Organic Process Research & Development* **2009**, *13*, 1195-1198; c) W. L. Noorduin, B. Kaptein, H.

- Meekes, W. J. P. van Enckevort, R. M. Kellogg, E. Vlieg, *Angewandte Chemie International Edition* **2009**, *48*, 4581-4583; d) I. Baglai, M. Leeman, K. Wurst, B. Kaptein, R. M. Kellogg, W. L. Noorduin, *Chemical Communications* **2018**, *54*, 10832-10834; e) K. Suwannasang, A. E. Flood, C. Rougeot, G. Coquerel, *Crystal Growth & Design* **2013**, *13*, 3498-3504; f) K. Suwannasang, A. E. Flood, C. Rougeot, G. Coquerel, *Organic Process Research & Development* **2017**, *21*, 623-630; g) R. Oketani, M. Hoquante, C. Brandel, P. Cardinael, G. Coquerel, *Organic Process Research & Development* **2019**, *23*, 1197-1203.
- [7] a) G. Coquerel, in *Topics in Current Chemistry*, Vol. 269 (Ed.: H. N. Sakai K., Tamura R.), Springer, Berlin, Heidelberg, **2006**; b) E. J. Ebberts, G. J. Ariaans, J. P. Houbiers, A. Bruggink, B. Zwanenburg, *Tetrahedron* **1997**, *53*, 9417-9476.
- [8] Y. Liu, X. Wang, J.-K. Wang, C. B. Ching, *Chirality* **2006**, *18*, 259-264.
- [9] a) F. Zhang, Z. Yang, X. Guo, S. Xu, H. Jiao, Z. Tan, *HETEROCYCLES* **2017**, *94*, 122; b) Waechter A., Saleh-Kassim H., Jasper C., Kolb J., Maillard D., PCT Int. Appl., **2016**, WO 2016078758 A1; c) T. Jerphagnon, A. J. A. Gayet, F. Berthiol, V. Ritleng, N. Mršić, A. Meetsma, M. Pfeffer, A. J. Minnaard, B. L. Feringa, J. G. de Vries, *Chemistry – A European Journal* **2009**, *15*, 12780-12790; d) B. Kovács, R. Savelle, K. Honkala, D. Y. Murzin, E. Forró, F. Fülöp, R. Leino, *ChemCatChem* **2018**, *10*, 2893-2899; e) Y. Ahn, S.-B. Ko, M.-J. Kim, J. Park, *Coordination Chemistry Reviews* **2008**, *252*, 647-658; f) M. G. Schrems, U.S. Patent Application 13/922,619., **2013**, U.S. Patent Application 13/922,619.
- [10] F. Cameli, J. H. ter Horst, R. R. E. Steendam, C. Xiouras, G. D. Stefanidis, *Chemistry – A European Journal* **2020**, *26*, 1344-1354.
- [11] J. Jacques, A. Collet, S. H. Wilen, *Enantiomers, racemates, and resolutions*, Wiley, **1981**.
- [12] C. Rougeot, F. Guillen, J.-C. Plaquevent, G. Coquerel, *Crystal Growth & Design* **2015**, *15*, 2151-2155.
- [13] G. Belletti, C. Tortora, I. D. Mellema, P. Tinnemans, H. Meekes, F. P. J. T. Rutjes, S. B. Tsogoeva, E. Vlieg, *Chemistry – A European Journal* **2020**, *26*, 839-844.
- [14] A. H. J. Engwerda, H. Meekes, F. M. Bickelhaupt, F. P. J. T. Rutjes, E. Vlieg, *Chemistry – A European Journal* **2019**, *25*, 9639-9642.
- [15] L. Spix, A. Alfring, H. Meekes, W. J. P. van Enckevort, E. Vlieg, *Crystal Growth & Design* **2014**, *14*, 1744-1748.
- [16] R. R. E. Steendam, J. M. M. Verkade, T. J. B. van Benthem, H. Meekes, W. J. P. van Enckevort, J. Raap, F. P. J. T. Rutjes, E. Vlieg, *Nature Communications* **2014**, *5*, 5543.
- [17] F. Simon, S. Clevers, V. Dupray, G. Coquerel, *Chemical Engineering & Technology* **2015**, *38*, 971-983.
- [18] M. SAINT V8.38A. Bruker AXS Inc., Wisconsin, USA. .
- [19] SADABS-2016/2, Krause, L., Herbst-Irmer, R., Sheldrick, G. M. & Stalke, D. , *J. Appl. Crystallogr.* **2015**, *48*.
- [20] G. M. Sheldrick, *Acta Cryst.* **2015**, *A71*, 3-8.
- [21] G. M. Sheldrick, *Acta Cryst.* **2015**, *C71*, 3-8.
- [22] a) I. Baglai, M. Leeman, R. M. Kellogg, W. L. Noorduin, *Organic & Biomolecular Chemistry* **2019**, *17*, 35-38; b) P. Wilmink, C. Rougeot, K. Wurst, M. Sanselme, M. van der Meijden, W. Saletra, G. Coquerel, R. M. Kellogg, *Organic Process Research & Development* **2015**, *19*, 302-308; c) F.-X. Gendron, J. Mahieux, M. Sanselme, G. Coquerel, *Crystal Growth & Design* **2019**, *19*, 4793-4801.
- [23] V. Dupray, in *Recrystallization* (Ed.: K. Sztwiertnia), IntechOpen, **2012**.
- [24] a) A. Collet, L. Ziminski, C. Garcia, F. Vigné-Maeder, in *Supramolecular Stereochemistry* (Ed.: J. S. Siegel), Springer Netherlands, Dordrecht, **1995**, pp. 91-110; b) Z. J. Li, M. T. Zell, E. J. Munson, D. J. W. Grant, *Journal of Pharmaceutical Sciences* **1999**, *88*, 337-346.
- [25] The Synaptic Leap website. Available: <http://www.thesynapticleap.org/node/357>

- [26] A. Borrego-Sánchez, C. Viseras, C. Aguzzi, C. I. Sainz-Díaz, *European Journal of Pharmaceutical Sciences* **2016**, 92, 266-275.
- [27] K.-L. Loh, Y.-N. Tang, *Journal of the Chinese Chemical Society* **1987**, 34, 231-235.
- [28] C. Xiouras, J. H. Ter Horst, T. Van Gerven, G. D. Stefanidis, *Crystal Growth & Design* **2017**, 17, 4965-4976.

Chapter 4: Investigation of strategies for deracemization of Flurbiprofen

Abstract. The production of optically pure Flurbiprofen through resolution and deracemization of conglomerate salts of its racemic mixture has been investigated. While racemization under harsh basic conditions easily leads to decomposition, enzymatic catalysis is a clean reaction that can occur at room temperature in a narrow pH-frame. The conglomerate salts were characterized in terms of solubility, melting point, X-Ray Powder Diffraction and crystal structure, showing that no polymorphic transitions threaten the Viedma ripening deracemization process.

4.1. Introduction

4.1.1. Flurbiprofen as Active Pharmaceutical Ingredient

Flurbiprofen (**1**) is a Non-Steroidal Anti-Inflammatory Drug (NSAID) and is a member of a broad class of aryl propionic acid drugs. It was approved as a commercial preparation for the symptomatic treatment of rheumatoid arthritis and osteoarthritis. It is available as tablets and as ophthalmic solution used for intra-operative miosis. Flurbiprofen has a chiral center and therefore it exists as two enantiomers (Figure 50).

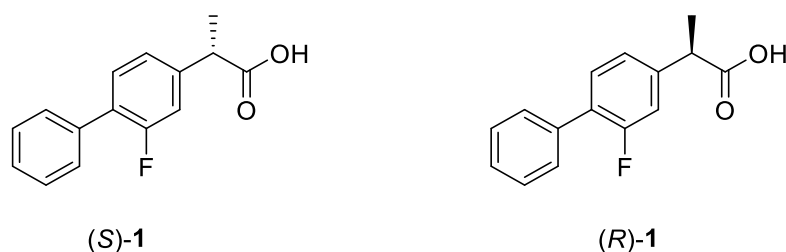


Figure 50: the two enantiomers of Flurbiprofen.

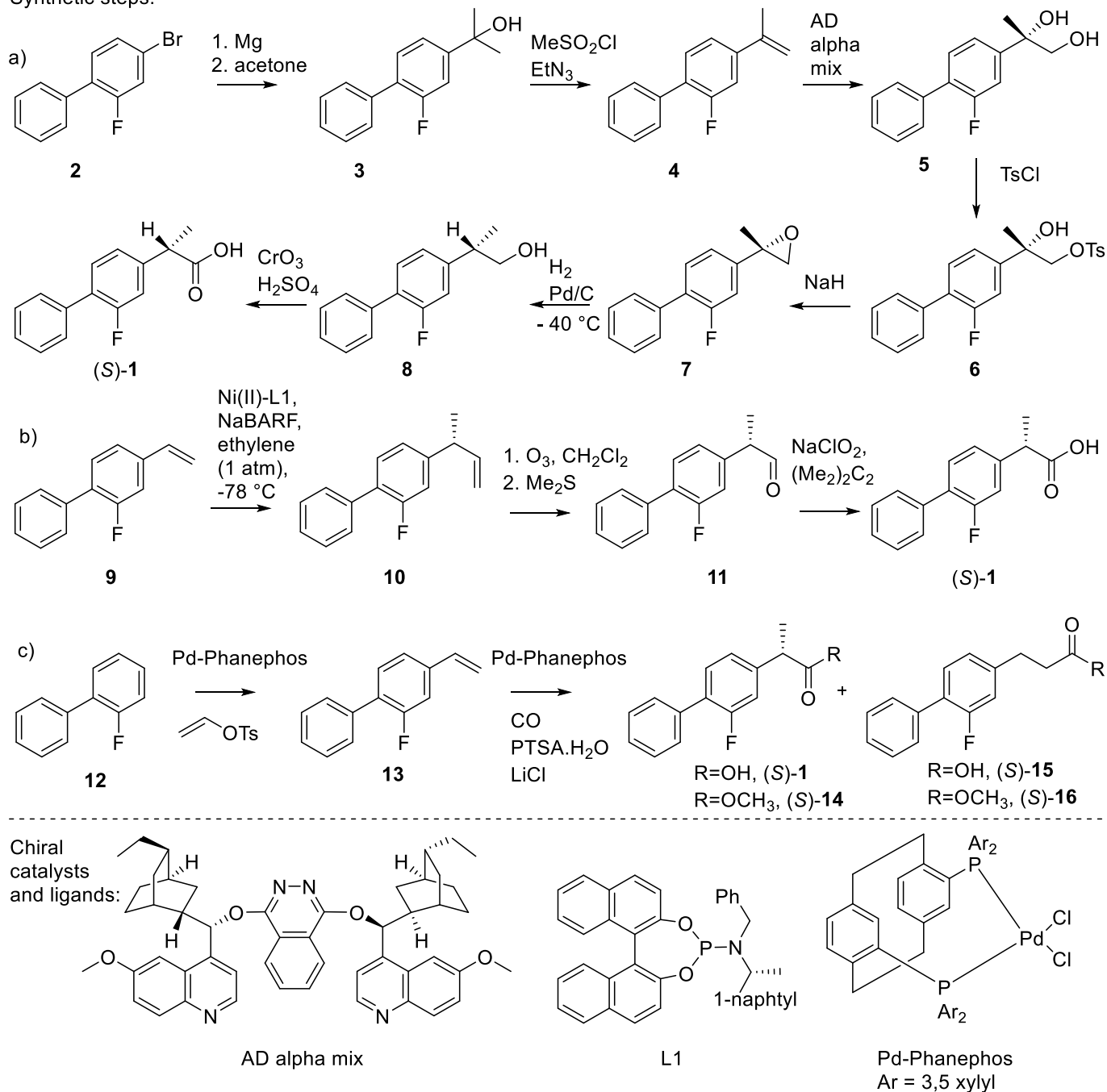
Pharmacological studies demonstrated that the anti-inflammatory activity comes chiefly from the (S)-enantiomer analogous to the other profens. Because the production of the single enantiomer is challenging, Flurbiprofen is marketed as a racemate. The (R)-enantiomer seemed to be promising for the treatment of Alzheimer disease but drug development was discontinued in phase 3 when lack of efficacy was evidenced in human patients.^[1] Unlike the other NSAIDs,^[2] Flurbiprofen does not undergo *in vivo* racemization in humans^[3] and therefore it would be highly desirable to administer only the active (S)-enantiomer.

4.1.2. Available strategies for the production of (S)-Flurbiprofen

The original syntheses of (S)-Flurbiprofen required a large number of steps, some of which at very low temperature, and explosive reagents like ozone which discouraged the scale up for the synthetic route of the single enantiomer (Scheme 4-1a and 1b)).^[4] A novel synthesis has been recently developed (Scheme

4-1c). Although intermolecular enantioselective alkene carbonylation using F₂₄-phanephos catalysts works well for the synthesis of the methyl ester pro-drug (*S*)-Flurbiprofen (yield = 69%, 40% after isolation, enantiomeric excess *E*(*S*) = 96%), so far poorer enantioselectivity has been found for the synthesis of enantiomerically pure Flurbiprofen free acid (yield = 69%, *E*(*R*) = 47%).^[5] (*S*)-**5** can be hydrolyzed to (*S*)-**1** without loss of optical purity, however, for both cases, purification by chromatography was necessary to remove **6** and **7** respectively, formed as byproduct.

Synthetic steps:



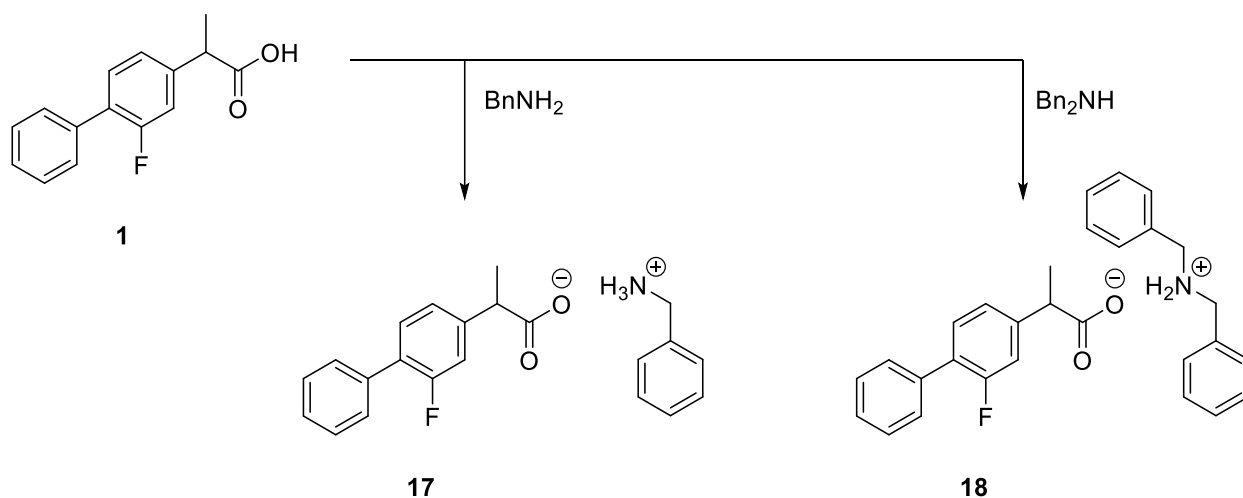
Scheme 4-1: a) Sharpless asymmetric dihydroxylation based strategy. Stereoselectivity is conferred to the chiral catalyst using AD alpha mix. b) Oxidative cleavage based asymmetric synthesis. Stereoselectivity is conferred using the chiral ligand L1. NaBARF = Tetrakis[3,5-bis(trifluoromethyl)phenyl]borate. c) Recent enantioselective synthesis of enantiopure Flurbiprofen. Stereoselectivity is conferred using the chiral catalyst Pd-Phanephos PTSA = para-toluene sulfonic acid, Ts = tosylate.

Enantiomerically pure Flurbiprofen can be obtained through resolution by enzymatic enantioselective esterification by lipase.^[6]

Crystallization enhanced technologies are attractive because of their robustness and for the high enantiomeric purity that is often achievable through their implementation. Racemic Flurbiprofen is crystalline but is a racemic compound, thus no chiral discrimination is possible in the solid state. Diastereomeric resolution is possible by using enantiomerically pure α -methylbenzylamine as a salt former.^[6-7] Combined heat/base catalyzed racemization applied to classical resolution with α -methylbenzylamine led to deracemization.^[8] This requires a chiral auxiliary, namely (*S*)-(-)- α -methylbenzylamine and a quick hot filtration in order not to hamper the enantiomeric excess of the solid phase which is described to reach 98%.

4.1.3. Conglomerate salts of Flurbiprofen

Conglomerate-based technology could provide an alternative and elegant method to obtain the desired pure enantiomer in the solid phase as a crystalline product. Four polymorphs of Flurbiprofen have been identified, but none of them is a conglomerate.^[9] However, the benzylammonium and dibenzylammonium salts (compounds **17** and **18** respectively, Scheme 4-2) of the racemate of Flurbiprofen are conglomerates and therefore suitable targets for Viedma ripening and other conglomerate-based techniques.^[10]



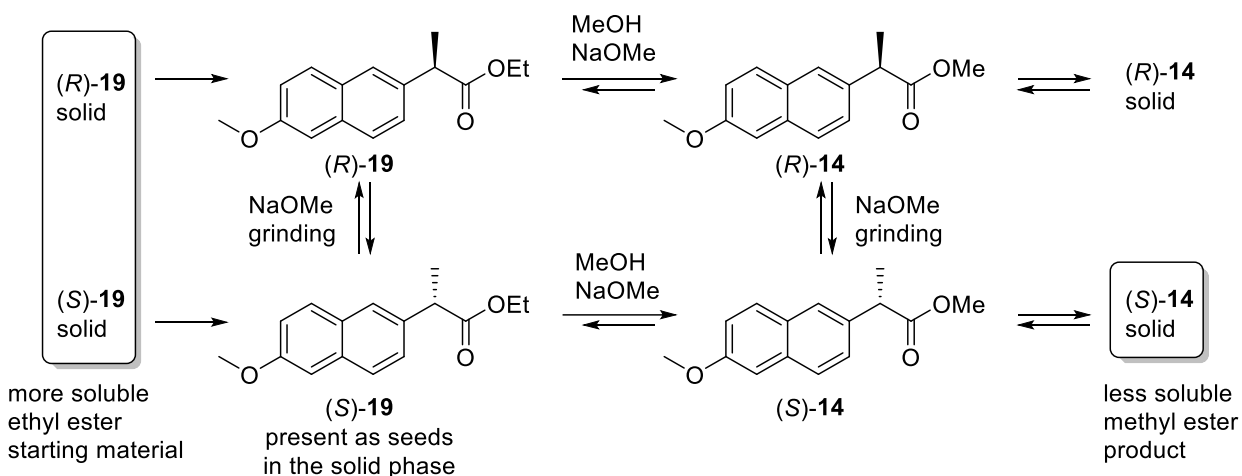
Scheme 4-2: two conglomerate salts known from patent literature^[10]

For a successful conglomerate-based deracemization, enantioselective crystal growth has to occur simultaneously with a racemization of the enantiomers in the surrounding solution.

4.1.4. Racemization of Flurbiprofen

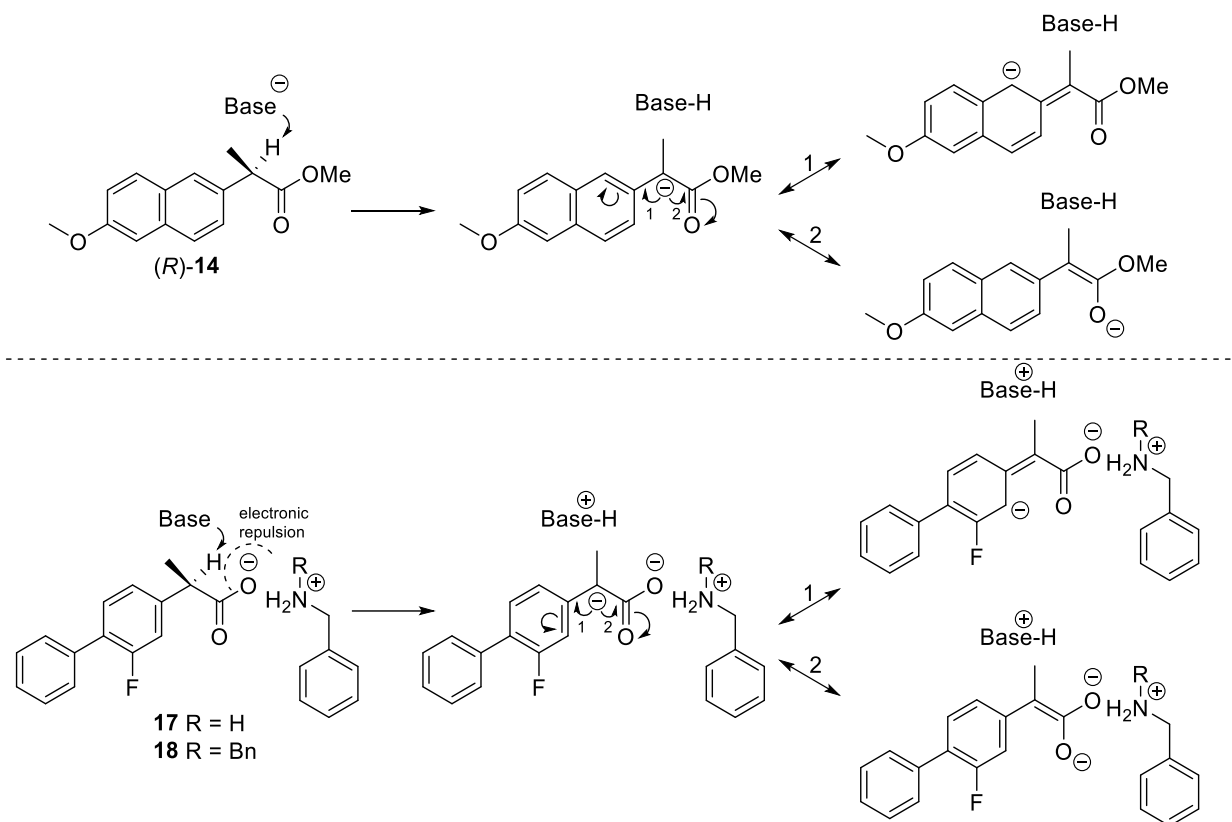
4.1.4.1. Base-catalyzed racemization of Flurbiprofen

It is known from the literature that profens can be racemized by base catalysis but this method requires relatively harsh conditions.^[11] On the other hand, esters of profens are more reactive towards base catalysed racemization. For instance, the methyl ester of Naproxen can be deracemized by using methoxide base as a racemizing agent at room temperature^[12].



Scheme 4-3: one-pot transesterification of Naproxen ethyl ester and deracemization of the corresponding methyl ester. The (S)-Naproxen methyl ester (conglomerate) racemizes with sodium methoxide at room temperature, while the (R)-Naproxen methyl ester crystallizes out upon addition of the more soluble racemic ethyl ester (conglomerate) which undergoes transesterification with the solvent methanol in solution.

Such difference in reactivity between the profen carboxylic acids and their relative esters is linked to the acidity of the proton bond to the chiral carbon, which is lower in free acids than in the corresponding esters. The profen free acids must be racemized by an external base most likely in their negatively charged carboxylate form ($\text{pK}_a \approx 3.5\text{--}4.5$ in water) which is obtained by hydrogen abstraction by means of solvent or base molecules. This negative charge close to the chiral carbon repulses the electron rich bases and it makes racemization more difficult (Scheme 4-4). Racemization of salts **17** and **18** follows the same principle. In profen esters this electronic repulsion is absent because there are no protons more acidic than the one attached to the chiral carbon which will be the first proton to be abstracted under basic conditions. In all the cases (profen free acids, salts and esters) the negative charge of the achiral intermediate can be stabilized by resonance both on the aryl moiety and on the carboxylate/ester functional group (Scheme 4-4). Exact measurements of the pK_a values of the proton bond to the chiral carbon are not available.



Scheme 4-4: delocalization of the negative charge during a base catalyzed racemization for Naproxen ester (top) and Flurbiprofenate (di)benzylammonium salt (bottom). Delocalization may occur 1) in the aromatic system or 2) on the carboxylate function. In path 1 only one resonance structure is represented but many others can be drawn. In case of Flurbiprofen salts an electronic repulsion is expected to prevent hydrogen abstraction by an electron rich base. This effect is expected to be more effective if the base bears a negative charge like in case of t-BuOK, KOH or alkoxydes.

Racemization by an added external base might hamper the conglomerate formation during a deracemization process also. A strong base could compete with the (di)benzylammonium ions for the proton needed for the conglomerate crystal structure, potentially leading to nucleation of the Flurbiprofen free acid or the flurbiprofenate salts with the protonated strong base used as racemization catalyst. This risk could potentially be overcome if the salt former is used both as a base and as (co)solvent, provided that **17** and **18** crystallize as a conglomerate from such solvent.

4.1.4.2. Biocatalyzed racemization of Flurbiprofen

Enzymatic catalysis can be considered for racemization of the conglomerate salts **17** and **18**. From a screening of soil microorganisms, Miyamoto *et al.*^[13] selected a strain of bacteria for their capability to decarboxylate α -aryl- α -methylmalonates (Scheme 4-1, Scheme 4-5). The enzyme responsible for decarboxylation, named by the authors “arylmalonate decarboxylase” (AMDase, EC. 4.1.1.76), was

isolated and characterized. The AMDase has cofactor free activity and does not contain metal ions in contrast to many other decarboxylases.



Scheme 4-5: AMDase catalyzed asymmetric decarboxylation. The wildtype AMDase has strict selectivity for the formation of the (R)-enantiomer.

The wild type enzyme has no racemization activity, but its structural similarity to glutamate racemase led the authors to induce a mutation in order to express two cysteines in the active site, in analogy to glutamate racemase. As a result, they obtained the first example of a racemase for unnatural compounds. This variant (G74C) was able to racemize profens, regardless of the configuration of the substrate. A second mutation (G74C/V43A) further led to enhanced racemization activity towards ketoprofen and naproxen.^[13]

Unfortunately, purified AMDase suffers from poor stability. This leads to a short lifetime, reported to be around 1.2 h. However, for the engineered AMDase variant G74C/M159L/C188G/V43I/A125P/V156L, this problem was circumvented by enzyme immobilization: significant improvements were achieved and the half-life was extended to 8.6 days for the enantioselective synthesis of α -arylpropionates by decarboxylation.^[14] The name of the variant tells how the mutation of the wildtype has been carried out: the first letter indicates the amino acid (according to the commonly used one-letter symbols) that has been replaced in the sequence, the number indicates the position of the amino acid replaced, while the last letter indicates the new expressed amino acid.^[15] This strategy could potentially be applied also to variants with racemizing activity to deracemize conglomerate salts of Flurbiprofen.

4.1.4.3. Photoracemization of Flurbiprofen

Recently theoretical calculations on the possibility of photoracemization of Flurbiprofen methyl esters have been carried out.^[16] (R)-Flurbiprofen methyl ester is claimed to be converted into the (S)-enantiomer by irradiating an aqueous solution of the (R)-enantiomer with a wavelength of 343.91 nm. Oddly, the authors report that the (S)-enantiomer is 1.5 kcal/mol more stable than the (R). Enantiomers must have the same physical properties and this claim casts doubt on the validity of the publication.

Another profen, namely Ketoprofen, was demonstrated to be photochemically reactive. Irradiation triggers a decarboxylation via a radical mechanism.^[17] Racemization of Flurbiprofen methyl ester is probably driven by the same mechanism, but the methyl substituent on the carboxylate moiety might

confer a certain stability towards decarboxylation. We have not attempted to reproduce any of these experiments.

4.1.5. Crystallization enhanced deracemization

Crystallization enhanced conglomerate deracemization technologies are useful strategies for the production of one single enantiomer with yields higher than 50%. They exploit enantioselective crystal growth from a liquid phase under racemization conditions and they rely on the often applied rule that racemic mixture is twice as soluble as the pure enantiomer, also known as Meyerhoffer “double solubility rule”.^[18] The most commonly used crystallization enhanced deracemization techniques are attrition enhanced deracemization (Viedma ripening), Temperature Cycling Induced Deracemization (TCID), and Crystallization Induced Asymmetric Transformation (CIAT, often referred to as Second Order Asymmetric Transformation, abbreviated SOAT).^[19]

In Viedma ripening, attrition enhanced deracemization, a suspension, usually with an initial bias in the solid in favor of the desired enantiomer, undergoes isothermal dissolution/crystal growth events induced by means of grinding induced by stirring glass beads or by applying ultrasound to the suspension.^[20]

In TCID, the dissolution crystal/growth events are not isothermal but rather induced by a controlled heating and cooling ramp. The dissolution/crystal growth sequence is repeated until achievement of the pure enantiomer.

In SOAT, unlike the previously described techniques, only one dissolution step is performed in order to dissolve all the unwanted enantiomer, while the desired enantiomer remains present as seeds in the solid phase. Similarly, to TCID supersaturation is induced by means of a temperature controlled cooling ramp. If the crystallization/solution racemization rates are well balanced, a simple filtration in the end of the process provides enantiopure product.

4.1.5.1. Decoupled deracemization with base catalysis

High temperature required for a fast base-catalyzed racemization leads to an increased solubility. In a crystallization enhanced deracemization this is undesirable because it leads to lower yields owing to the fact that most of the racemic mixture remains in solution. Such processes also require hot filtration in order to avoid the nucleation of the unwanted enantiomer during the isolation of the product. To overcome this issue, high temperature racemization can be conducted in an external plug flow reactor.

Through the use of a filter, the mother liquor can be selectively delivered to such a reactor, racemized and returned to the crystallization flask at low temperature (Figure 51).

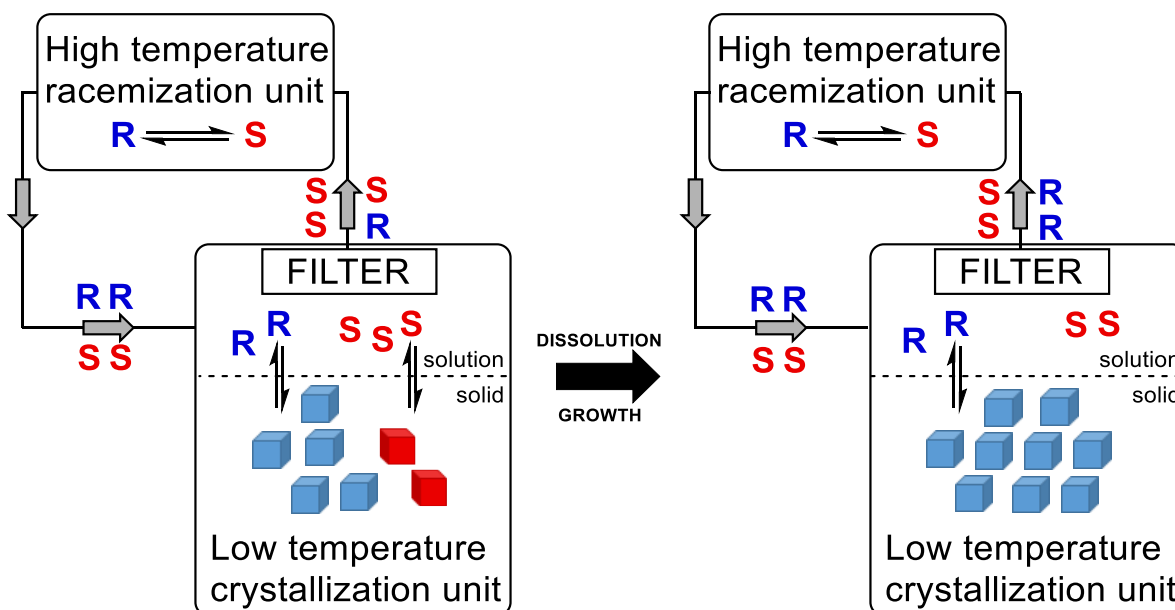


Figure 51: schematic representation of an external racemization reactor applied to a crystallization enhanced deracemization process.

4.1.5.2. Decoupled deracemization with enzyme catalysis

Because enzymes are often sensitive to grinding and temperature cycles often used in crystallization-enhanced deracemization,^[21] the racemase can be immobilized, packed into a column which is left at the optimal temperature for enzymatic activity. The slightly enantiomerically enriched mother liquor of a crystallization unit, in which a dissolution-crystal growth process takes place, can be continuously recycled through this column, leading to deracemization (Figure 52).

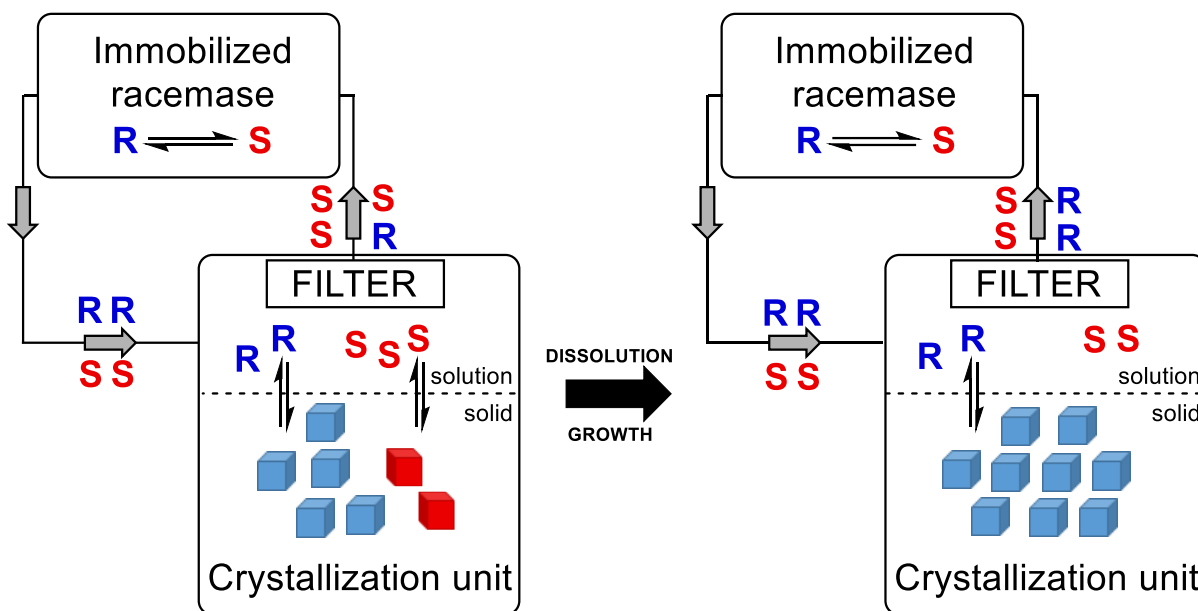


Figure 52: schematic setup for biocatalyzed crystallization-enhanced deracemization.

While decoupled deracemization with base catalysis is designed to isolate crystallization from harsh racemization conditions, decoupled deracemization with enzymatic catalysis is designed to preserve the biocatalyst (namely the enzyme) from the dissolution/crystallization process conditions that would dramatically reduce its lifetime.

4.1.5.3. Deracemization through melt crystallization

Another technique that could possibly be suitable for deracemization of conglomerates is “melt crystallization”. It is necessary that the conglomerate of interest racemizes in the melt. The racemization may continue in the metastable zone (MSZ). This latter is included in the temperature frame between the melting point of the racemate and the temperature at which the recrystallization of the racemate takes place.

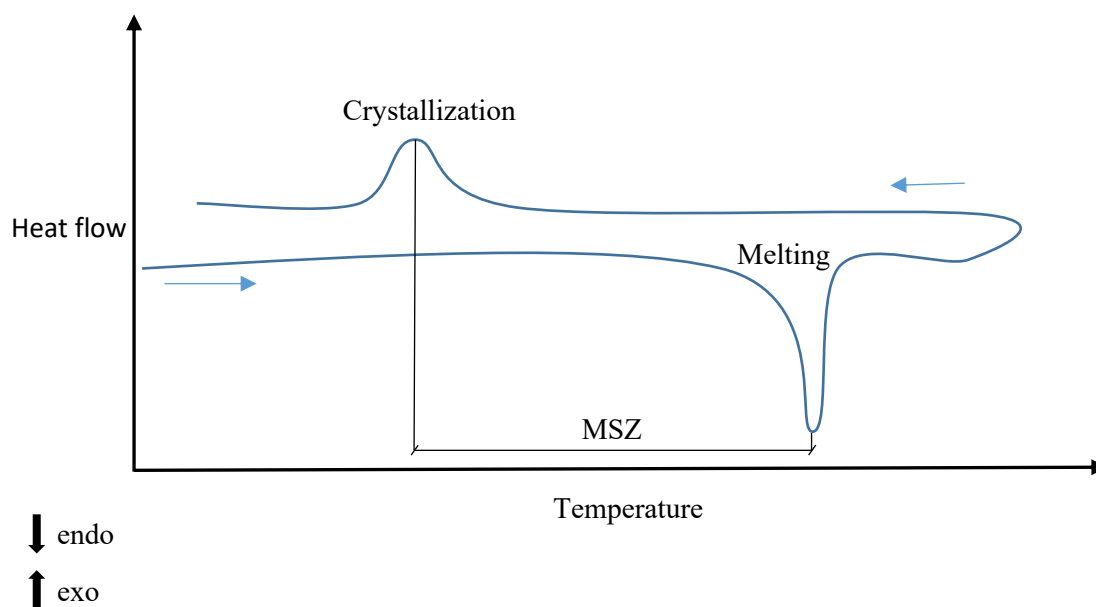


Figure 53: schematic representation of a DSC of a racemic conglomerate crystalline compound. Blue arrows represent the direction of the temperature ramp applied to the crystalline compound. Endo = endothermic event. Exo = exothermic event. Ideally the seeding of the melt with the desired enantiomer has to be carried out within the MSZ.

If the racemate is molten and if racemization occurs until the crystallization of the whole compound from the melt, the melt can be seeded with the desired enantiomer and mainly two events may take place:

- 1) All the desired enantiomer crystallizes on the surface of the existing pure enantiomer. If the cooling rate is slow enough, the counter enantiomer may be converted into the one in excess in up to 100% conversion.
- 2) The counter enantiomer may nucleate if its supersaturation is too high. In this case an exothermic peak linked to this event would become visible at DSC and it would correspond to the crystallization peak of the racemate.

In order to know how to perform a melt crystallization technique it is necessary to know the melting points (T^f) of racemic and enantiomerically pure compound, respectively. The difference between the melting point of enantiopure compound and racemic mixture in conglomerates is typically of 20 °C or higher. This allows the enantiopure crystals added as seeds to survive in the melt and to allow enantioselective crystal growth while racemization takes place in a supersaturated melt.

4.1.6. Preferential crystallization

Many conglomerates cannot be racemized. Sometimes solution racemization conditions hamper the enantioselective crystallization and carrying out racemization in an external reactor does not provide any benefit to the outcome of the process.^[22] Sometimes both enantiomers are economically valuable. In all these cases preferential crystallization represents a robust method to obtain both enantiomers that crystallize as conglomerates.^[23] For this kind of kinetically controlled resolution method only a few seeds of enantiopure material or an initial bias of one enantiomer are needed for a crystal growth that occurs through supersaturation obtained by means of cooling ramps or solvent evaporation. Also, a precise filtration timeframe is needed in order to collect enantiomerically pure material before nucleation of the counter enantiomer followed by its crystal growth. Preferential crystallization is represented in Figure 54 in an Auto-Seeded Polythermic Programmed Preferential Crystallization (AS3PC) mode. In step 1, a nearly saturated solution of racemate is seeded with typically 9 mol% of enantiopure seeds at T_B , which is the highest temperature achieved in the process: part of these seeds will be dissolved, while the remaining part will remain in suspension. In this way all the unwanted enantiomer will remain dissolved and its crystal growth during the following induced supersaturation will be averted. At the same time a relatively large surface area of crystals of the desired handedness is available for enantioselective crystal growth. In step 2, supersaturation is induced by means of a temperature-controlled cooling ramp and enantioselective crystal growth of the seeds takes place. In step 3 the suspension is filtered before a massive primary nucleation of the counter enantiomer occurs. The temperature of filtration (T_F) is previously determined by monitoring the mother liquor composition as function of time and thus as function of temperature during the same controlled cooling ramp. Step 3 represents the end of the first cycle and the step 1 of the second cycle is performed by increasing the temperature of the filtrate to T_B and by compensating the loss of material filtered in step 3 with a mass of racemate corresponding to the double of the mass of enantiomer that crystallized out from the solution. The second cycle will be in the opposite direction to the first cycle and will allow one to obtain the counter enantiomer theoretically in the same amount of the enantiomer obtained in the first cycle.

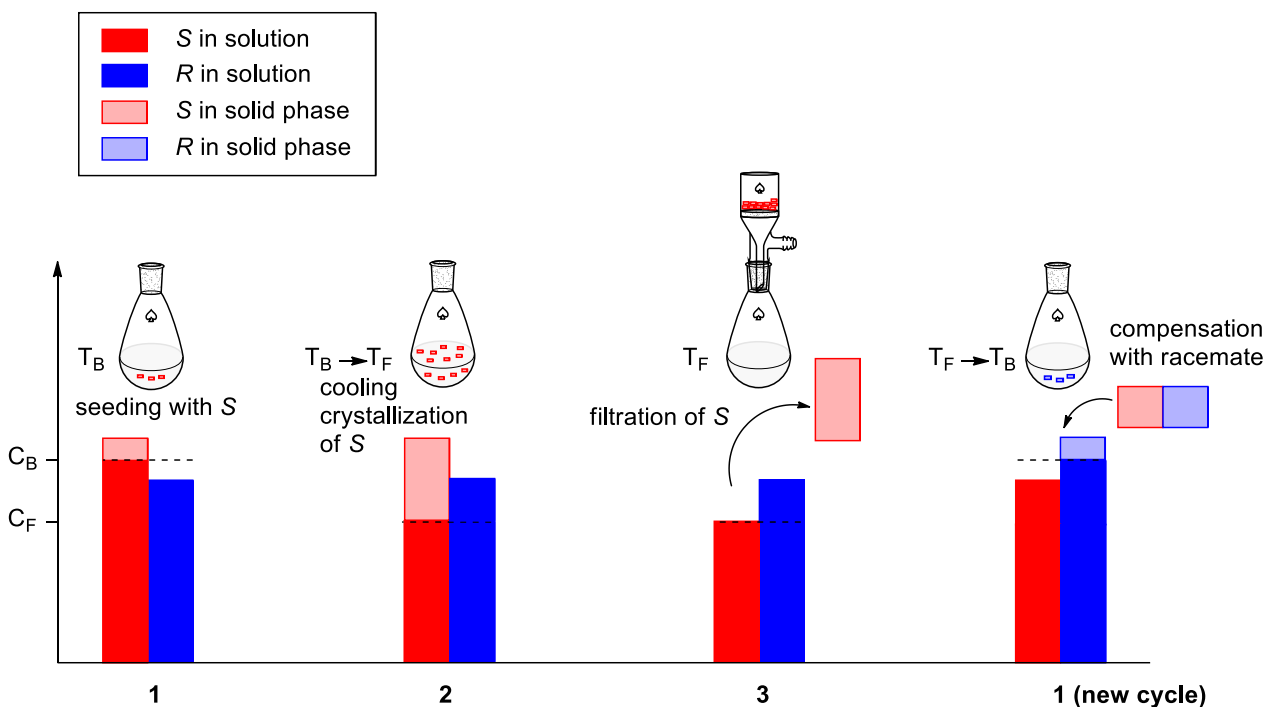


Figure 54: Preferential crystallization in an Auto-Seeded Polythermic Programmed Preferential Crystallization (AS3PC) mode. C_B = concentration of the enantiomers at the highest temperature achieved in the process (T_B). C_F = concentration of the enantiomers at the temperature of filtration (T_F).

The sequence can be repeated multiple times until the amount of impurities that accumulates after each cycle hampers the crystallization process. These impurities usually come from the racemate that is used as starting material.

Because enantioselective synthesis of racemic Flurbiprofen is much more challenging than the non-enantioselective one, efforts to deracemize the optically inactive Flurbiprofen are described in this chapter. Preliminary characterization of the solid state has been performed to confirm the appropriateness of the method used to obtain the single enantiomer and to identify and prevent possible threats to the conglomerate-based technology, namely polymorph or solvate formation. HPLC-MS and ^1H -NMR were used to detect chemical transformations in the liquid phase.

4.2. Methods

Racemic and (*R*)-Flurbiprofen were purchased from Sigma Aldrich. Benzylamine and dibenzylamine were purchased from Acros. Dibenzylamine was distilled prior to use. The enantiomerically pure material used in racemization experiments as well for seeds in deracemization experiments has always the (*R*) configuration, because the (*S*)-enantiomer is classified as highly toxic and no difference in reactivity is expected on using achiral bases in an achiral solvent.

NMR spectra of all compounds were obtained on a Varian Mercury 300 MHz machine. All solvents were spectral grade. Chemical shifts δ of NMR spectra are reported in ppm relative to $(\text{CH}_3)_4\text{Si}$ at $\delta = 0$.

4.2.1. Racemization of Flurbiprofen

Chiral HPLC analyses were carried out on a Phenomenex Lux Amylose-1 (3.0 x 150 mm; 3 μm) column with a carrier solution of CO_2 mixed with a solution of ethanol/acetonitrile (50/50) with 0.2% trifluoroacetic acid (TFA) in a gradient mode for separation of Flurbiprofen enantiomers.

4.2.1.1. Base-catalyzed racemization of Flurbiprofen

DBU was purchased from Sigma Aldrich, and TMG, KOH and t-BuOK were purchased from Acros.

4.2.1.2. Biocatalyzed racemization of Flurbiprofen

The pH of the aqueous solution of **17** and **18** was monitored by using a pH meter InoLab pH 7170. The enzyme arylmalonate decarboxylase (AMD) was available from University of Graz with the following variants: AMD V43A G74C and AMD V43A G74C L77M V156L both in purified form and Cell Free Extract (CFE). The enzyme was immobilized at the University of Graz on EziG supporting material. The EziG material has a core of controlled pore glass coated with organic polymer, designed for selective binding of His-tagged enzymes.^[24] EziG 1 = EziG Opal, hydrophilic surface. Silica surface, no polymer coating. EziG 2 = EziG Coral, hydrophobic surface Poly(vinylbenzylchloride) coating. EziG 3 = EziG Amber, semi-hydrophilic surface, co-polymer (polystyrene derivative).

4.2.1.2.5 Racemization in the melt

DSC measurements were carried out at a ramp rate of 10 $^\circ\text{C}$ per minute on a DSC Q20 V24.11 Build 124.

4.2.2. X-Ray Powder Diffraction (XRPD)

X-Ray Powder Diffraction (XRPD) analyses were performed at room temperature using a D8 Discover diffractometer (Bruker Analytic X-Ray Systems, Germany) with Bragg-Brentano geometry in θ/θ reflection mode. The instrument was equipped with a copper anticathode (40kV, 40 mA, $\text{K}\alpha$ radiation 1.5418 \AA) and a lynx eye linear detector. The diffraction patterns were collected by steps of 0.04 $^\circ$ (in 2-theta) over the angular range 3–30 $^\circ$.

4.2.3. Single Crystal X-ray Diffraction (SC-XRD)

The crystal structure of salt **17** $[\text{C}_{15}\text{H}_{12}\text{FO}_2][\text{C}_7\text{H}_{10}\text{N}]$ has been determined from single crystal X-Ray diffraction. The chosen crystal was glued on a glass fiber and mounted on the full three-circle goniometer

of a Bruker SMART APEX diffractometer with a CCD area detector. Three sets of exposures (a total of 1800 frames) were recorded, corresponding to three ω scans (steps of 0.3°), for three different values of ϕ . The cell parameters and the orientation matrix of the crystal were preliminarily determined by using SMART Software^[25]. Data integration and global cell refinement were performed with SAINT Software^[26]. Intensities were corrected for Lorentz, polarization, decay and absorption effects (SAINT and SADABS Software) and reduced to FO^[26]. The program package WinGX^[27] was used for space group determination, structure solution and refinement.

4.2.4. Preferential crystallization (PC)

All PC experiments were performed in a 30 mL glass tube crystallizer. Magnetic stirring was set at 700 rpm and the amount of seeds was adjusted to 9 % of the total mass of the racemic mixture.

Chiral analyses were performed by High Performance Liquid Chromatography (HPLC) equipped with a Chiralpak AD-H column. The mobile phase was a hexane/methanol mixture (90/10 v/v) with TFA (0.05% v/v) delivered with a flow rate of 0.7 mL/min. The UV detection was carried out at 254 nm at 20 °C. Under these conditions, retention times of 9 and 13 minutes were observed for *R* and *S* enantiomers of Flurbiprofen respectively. Prior to the entrainment, the prepared racemic solutions were heated above their saturation temperatures to make sure that all the solid had dissolved (T_{HOMO}). The clear solutions were then cooled down to the final temperature (T_F).

DSC analyses were performed on a DSC 204F1 Netzsch operating under a constant flow of helium. For these analyses ca 5 mg of salts **17** and **18**, respectively were heated in sealed aluminum pans using a heating rate of 10 °C/min.

4.2.5. Solubility measurements

The solubility of salts **17** and **18** was measured by means of the gravimetric method. A supersaturated solution was stirred in sealed vials at 700 rpm in a thermostatted double jacketed vessel. After at least 12 hours of stirring, the suspension was filtered, weighed and the resulting solution was evaporated in a ventilated oven at 50 °C for 24 hours giving the amount of solvent and dissolved material.

4.3. Results

4.3.1. Benzylammonium Flurbiprofen salt

4.3.1.1. Single Crystal X-ray Diffraction (SC-XRD)

Crystals were obtained from a saturated solutions of a racemic mixture of benzylammonium Flurbiprofen salt in methanol and water respectively. These solutions were allowed to evaporate slowly until single crystals of sufficient dimension were obtained. The crystals obtained from water solution have the same cell parameters as those formed from methanol solution, indicating that the same crystal structure is obtained in both solvents.

4.3.1.1.1 Crystallographic data

The crystal data are collected in Table 9.

Table 9: Crystal data

Chemical Formula	[C ₁₅ H ₁₂ FO ₂][C ₇ H ₁₀ N]
Molecular Weight / $g.mol^{-1}$	351.4
Crystal System	Monoclinic
Space Group	$P2_1$ (n4)
Z , Z' (asymmetric units per unit cell)	2,1
a / Å	10.8958(14)
b / Å	6.6009(8)
c / Å	13.2564(17)
α / °	90
β / °	91.712(2)
γ / °	90
V / Å ³	953.0(2)
d _{calc} / $g.cm^{-3}$	1.225
F(000) / e ⁻	372
Absorption coefficient μ (MoK α_1) / mm^{-1}	0.085
Absolute structure parameter	undetermined

4.3.1.1.2 Structural description

The asymmetric unit is composed of [C₁₅H₁₂FO₂][C₇H₁₀N] (Figure 55). The anions establish strong ionic hydrogen bonds^[28] (table 2, figures 2, 3) that give rise to ribbons spreading around the 2₁ screw axis. Along axis a, the ribbons are close enough to generate π stacking in T-shape (Figure 58 and Figure 59). Therefore, the molecules are organized in layers of about d001 thickness. The cohesion between the layers is ensured

by van der Waals interactions (Figures 6, 7, 8). The comparison of the calculated and experimental powder pattern shows that the crystal is perfectly representative of the sample.

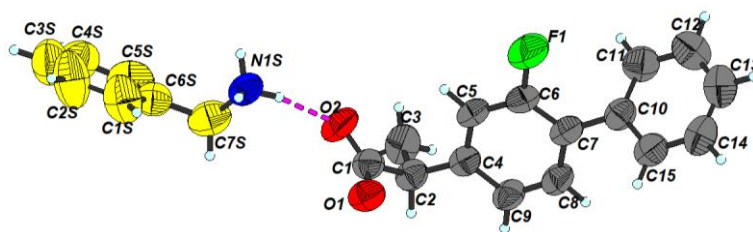


Figure 55: asymmetric unit with atoms labelled in thermal ellipsoidal representation

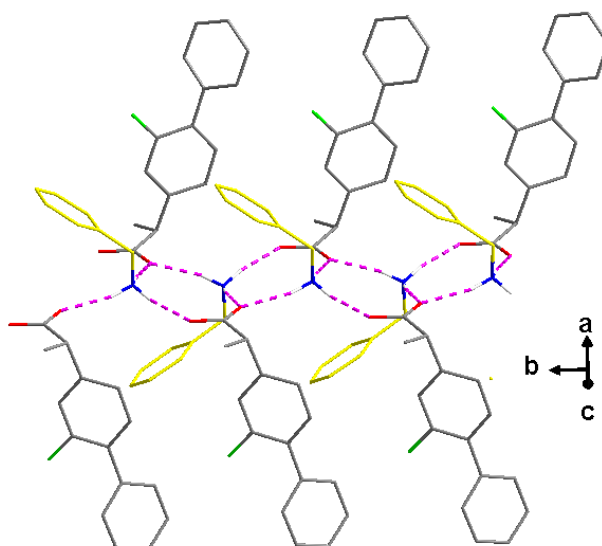


Figure 56: Molecular ribbon built through the ionic hydrogen bonds (dashed pink lines)

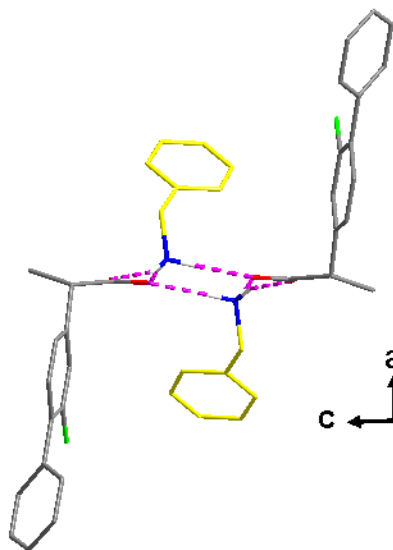


Figure S7: Molecular ribbon along b

Table 10: ionic hydrogen bonds

D-H...A	d(D-H)	d(H...A)	d(D...A)	<(DHA)
N(1S)-H(1S1)...O(1)#1	0.89	1.93	2.796(4)	165.6
N(1S)-H(1S2)...O(2)	0.89	1.91	2.769(4)	160.9
N(1S)-H(1S3)...O(1)#2	0.89	1.86	2.737(4)	169.2

Symmetry transformations used to generate equivalent atoms :

#1 $x, y+1, z$; #2 $-x+1, y+1/2, -z+1$

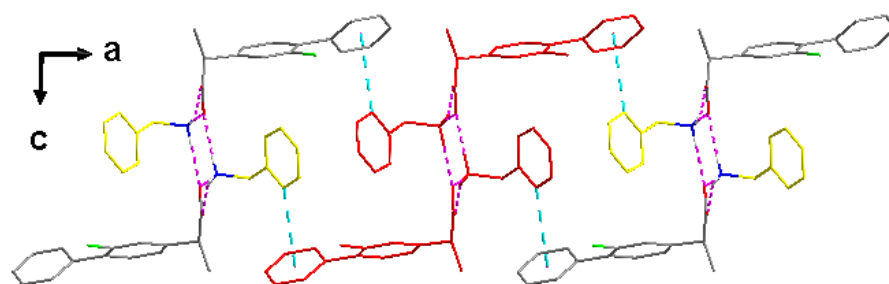


Figure 58: Adjacent ribbons interacting through T shaped π interactions, leading to layers in ab

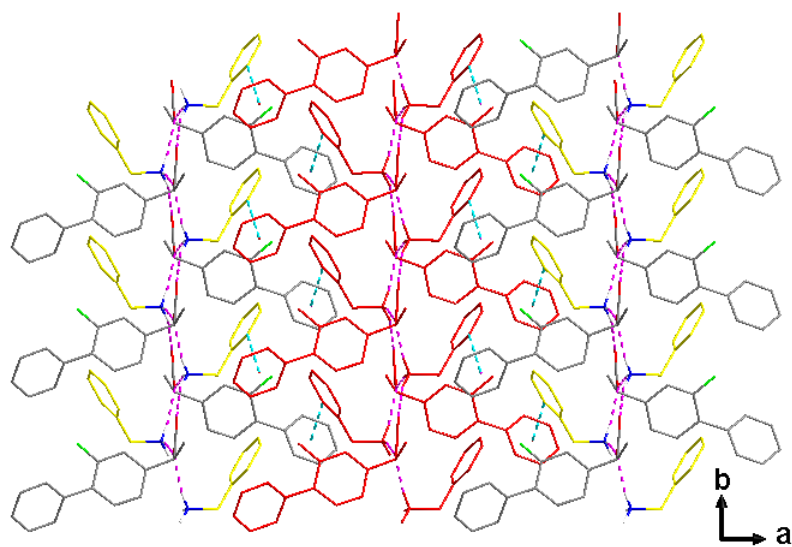


Figure 59: Projection along c, of one layer built from molecular ribbons

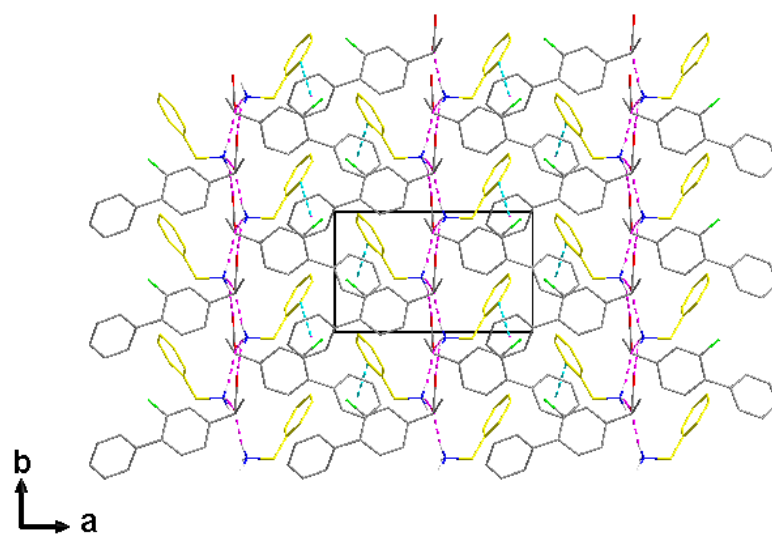


Figure 60: Projection of the whole packing along c

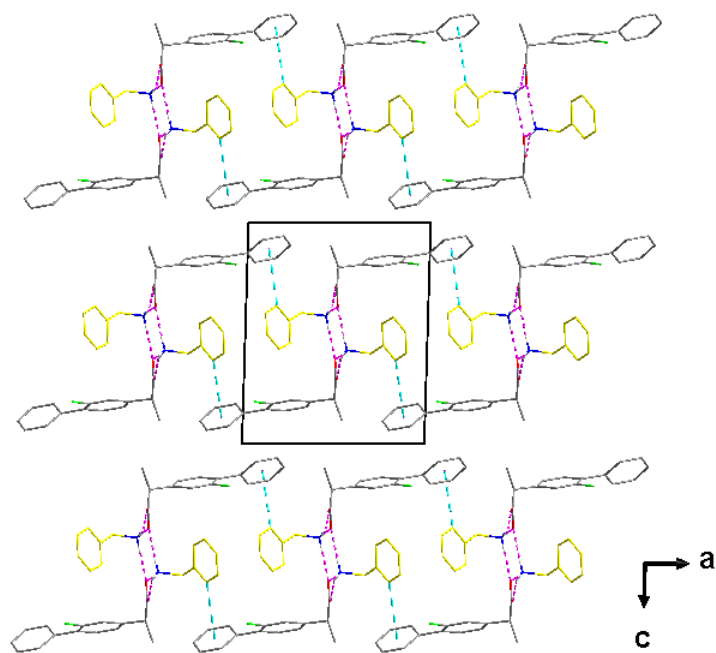


Figure 61: Projection of the whole packing along b

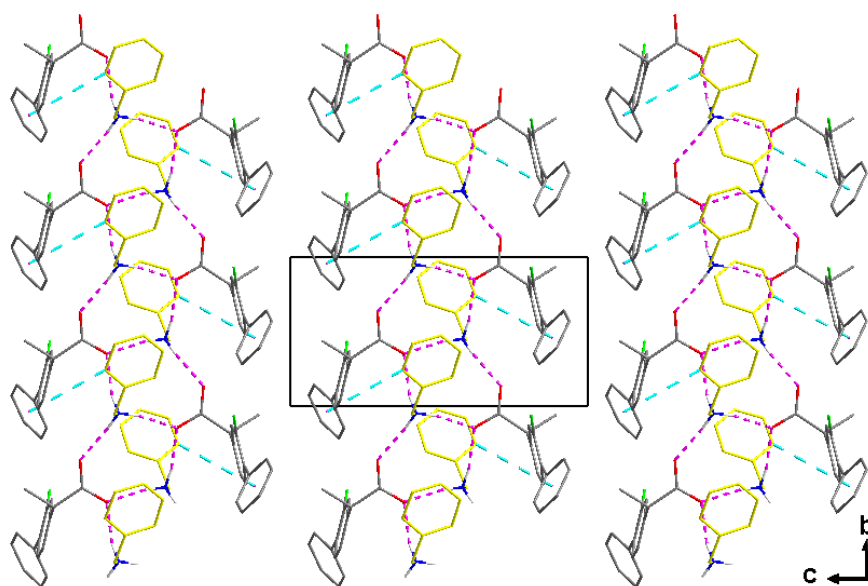


Figure 62: Projection of the whole packing along a

4.3.1.2. Solubility measurements

Solubility measurements of racemic salt **17** at 20 °C were carried out in different solvents in order to determine the highest concentration that can be used in the deracemization and resolution processes. This is very important for crystallization enhanced deracemization exploiting enzymatic catalysis. Indeed, in such cases, racemization rates rely on the mass/molar ratio between substrate in solution and the enzyme. In Viedma ripening this would be an underestimated indication since solubility is somewhat enhanced by grinding: the higher the grinding rate, the higher will be the solubility. Measurements will still be accurate enough owing to the fact that Viedma ripening is less sensitive to primary nucleation than other crystallization induced deracemization techniques like TCID or CIAT, thus a slower racemization rate does not hamper the successful outcome of the process.

The first measurements were conducted in water in order to have an estimation of the highest concentration achievable during decoupled crystallization enhanced deracemization using biocatalysis. Other solvents like ethanol (EtOH), methanol (MeOH), ethyl acetate (EtOAc), and isopropanol (IPA) were tested for preferential crystallization purposes. Results are reported in Table 11.

Table 11: solubility measurements of racemic salt **17** in different solvent at 20 °C.

	H ₂ O	IPA	EtOH	MeOH	EtOAc
Solubility [mg/mL]	3.5	14.9	63.8	281.2	6.7
Solubility [wt%]	0.35	1.85	7.84	26.20	0.74

The solubility in water is poor, due to the high lipophilicity of the salt. Much higher solubility was found in ethanol and methanol. XRPD analyses of the filtered solids suspended in the slurry at the end of the solubility measurements confirmed that neither polymorphic transition nor hydrate/solvate formation occurred in the used solvents.

4.3.1.3. X-Ray Powder Diffraction (XRPD)

The predicted XRPD obtained from SC-XRD overlaps with the experimental XRPD measurement of crystals obtained by slow addition of benzylamine to an ethanolic solution of racemic Flurbiprofen free acid. This means that the single crystal is of the same material and polymorph as the bulk of the material.

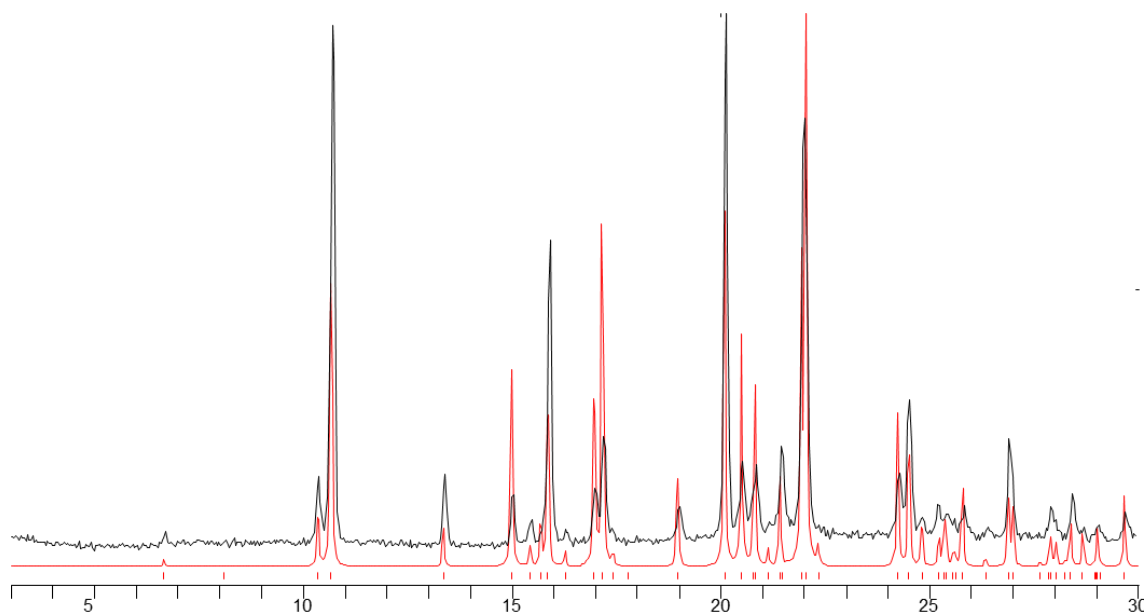


Figure 63: superimposition of calculated (red) and experimental (black) powder pattern of racemic Flurbiprofen benzylammonium salt.

4.3.1.3.1 XRPD from solubility measurements

All the experimental XRPDs of crystals of a racemic mixture filtered from the slurries stirred at isothermal conditions for solubility measurement purposes overlap, indicating that the same conglomerate form is maintained in all the solvents shown (Figure 64).

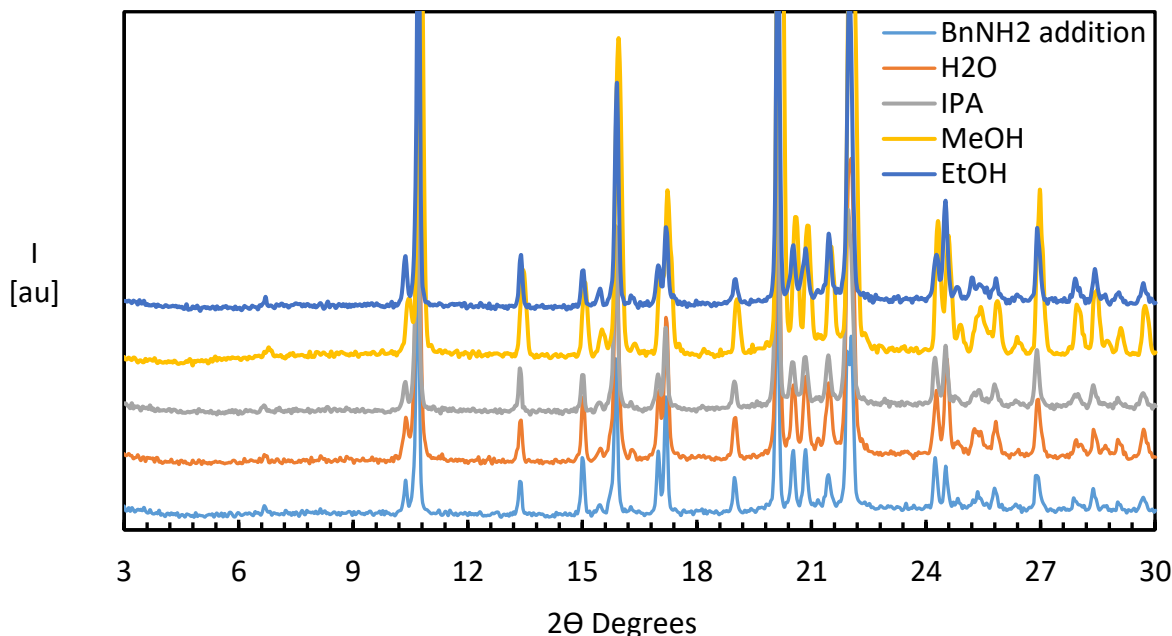


Figure 64: stacked XRPD of the solid filtered after isothermal recrystallization under stirring conditions in different solvent. The turquoise line labeled as “BnNH₂ addition” refers to crystals obtained by slow addition of benzylamine to an ethanolic solution of racemic Flurbiprofen free acid.

4.3.1.3.2 XRPD of ground material

In order to establish if Viedma ripening could be used with simultaneous *ex-situ* racemization in a flow reactor with immobilized racemase, the evolution of the solid state upon grinding over time was monitored. Salt **17** suspended in mixtures water (80% w/w) / co-solvent (20% w/w) was allowed to grind at 700 rpm for seven days at room temperature in different 10 mL vials. The resulting suspensions were filtered under vacuum and the resulting dry solids were analyzed by XRPD (Figure 65).

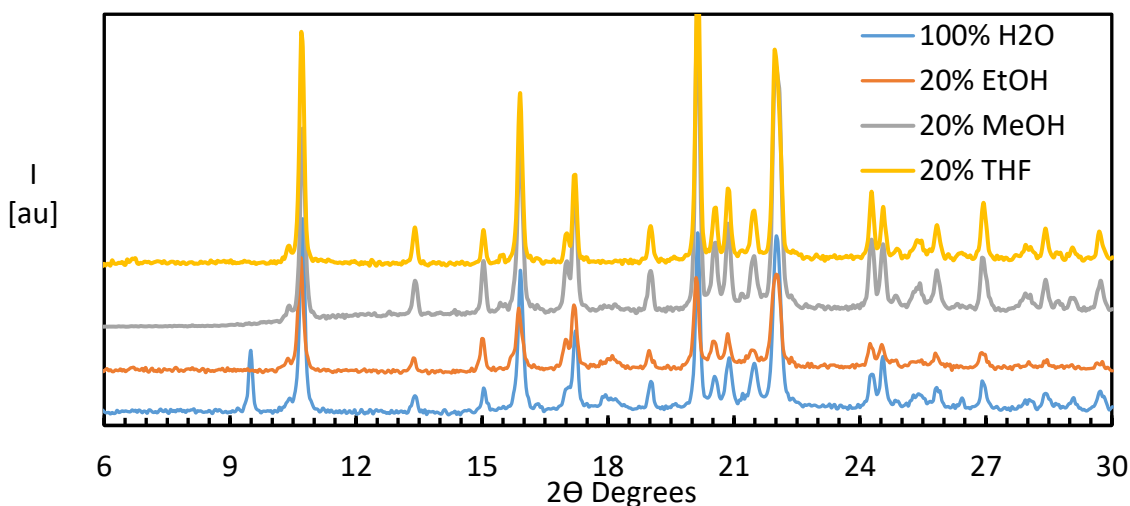


Figure 65: stacked XRPD of the solid filtered after isothermal recrystallization in water and with 20% of co-solvent under grinding conditions.

The patterns of all the ground material with exception of the one suspended in THF exhibit a peak at 18° , which is compatible with some polytetrafluoroethylene (PTFE) coating that could have been lost from the magnetic stirrer during the grinding.^[29] Results suggest that grinding in presence of 20% of the co-solvent used does not affect the crystallization of salt **17** in the previously identified conglomerate form. When only water is used, the crystals float, thus grinding was probably not as efficient as grinding in the presence of co-solvents. The intense peak at 9.5° , which does not belong to the previously identified conglomerate, might indicate a change of the crystal structure into a polymorph, perhaps a hydrate. In principle the peak at 9.5° could also belong to the Flurbiprofen free acid, however it does not belong to any XRPD pattern of Flurbiprofen free acid present in the CSD database. Interestingly this transition was not observed after 24 hours of stirring with a magnetic bar. According to these data, in presence of a clean and fast racemization in solution, grinding could be safely performed at the aforementioned conditions maintaining the conglomerate system necessary for deracemization by means of Viedma ripening.

4.3.1.4. Racemization

4.3.1.4.1 Base-catalyzed racemization

Some preliminary racemization tests were performed at high temperatures with different bases in different solvents to check the reactivity of the salt (Table 12).

Table 12: initial screening of racemization conditions of the enantiopure (*R*)-17 salt.

Entry	Solvent	Base	pKaH in water	pKaH in DMSO	Equivalents of base	T [°C]	Reaction time [h]	Final <i>E</i> %
1	Water	KOH	15.7 ^[30]	32 ^[30]	0.1	80	5	100
2	Water	KOH	15.7 ^[30]	32 ^[30]	0.5	100	5	95
3	Octane	DBU	13.5 ^[31]	13.9 ^[32]	0.3	80	64	55
4	Toluene	t-BuOK	17.0 ^[30]	29.4 ^[30]	0.5	110	5	88
5	Toluene	a) BnNH ₂ + b) DBU	a) 9.3 ^[32] b) 13.5 ^[31]	a) 10.2 ^[32] b) 13.9 ^[32]	a) 483 + b) 0.3	110	5	15
6	Toluene	a) BnNH ₂ + b) TMG	a) 9.3 ^[32] b) 13.0 ^[32]	a) 10.2 ^[32] b) 13.2 ^[32]	a) 483 + b) 0.3	110	5	40

Methoxide catalyzed racemization of the structurally related analogues Naproxen methyl and ethyl esters is achievable at room temperature.^[12] In the case of profen salts, racemization would most likely pass through an intermediate that has a double negative charge. This intermediate is higher in energy than the one required for the racemization of a neutral molecule like the Naproxen esters. As a consequence, the racemization of Flurbiprofen salts is energetically less favorable and requires a higher temperature. Also, the base used for racemization can compete with the base used as salt former (benzylamine or dibenzylamine) for the hydrogen ion. This makes the racemization more difficult, and the protonated strong base could co-crystallize together with the negatively charged Flurbiprofenate hampering conglomerate formation. Strongly negatively charged bases like KOH and t-BuOK do not seem to be effective racemization catalysts with the Flurbiprofen salts. Their basicity would lead to the deprotonation of the benzylammonium ion, which would lead to their conversion to H₂O and t-BuOH respectively. Thus, more than one equivalent of such bases is needed for an efficient racemization, but this would lead to the neutralization of the positive charge, which is necessary for benzylamine and dibenzylamine to co-crystallize with Flurbiprofen as a conglomerate salt and possibly allowing Flurbiprofen to crystallize as a potassium salt.

Racemization of Flurbiprofenate was then tested with the salt former of **17**, namely benzylamine, at different temperatures. The reaction is expected to follow (pseudo) first order kinetics because benzylamine is present in large excess. Results are shown in Figure 66.

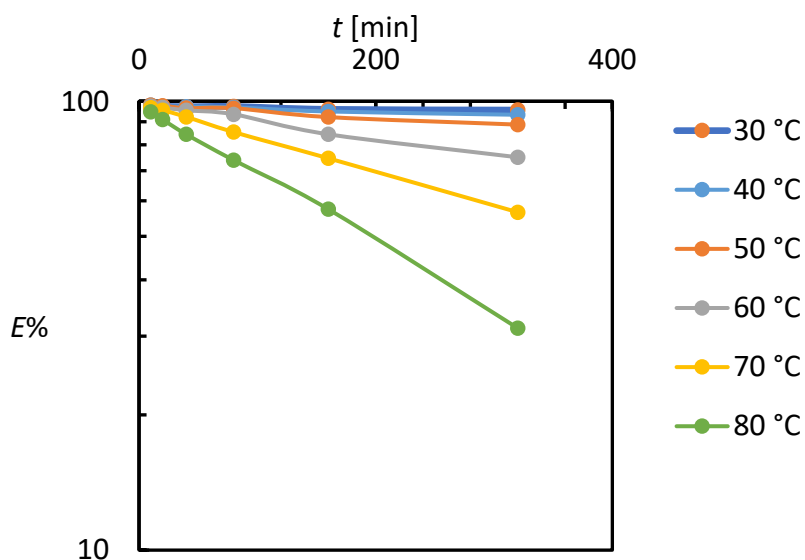


Figure 66: racemization kinetics of (R)-**17** in BnNH₂. For clarity the numbers given on the y axis are actual enantiomeric excess *E* values although the scale is logarithmic.

The linearity of the curve obtained from the plot of the logarithm of the enantiomeric excess as function of time confirms that the reaction follows a (pseudo) first order reaction. Racemization seems to occur quite quickly at high temperatures. The faster racemization shown in Figure 66 obtained at 80 °C exhibits a half-life of 191 min.

With the aim of conducting racemization externally in a flow reactor, the racemization of a solution of salt **17** in benzylamine through a plug flow reactor was tested.

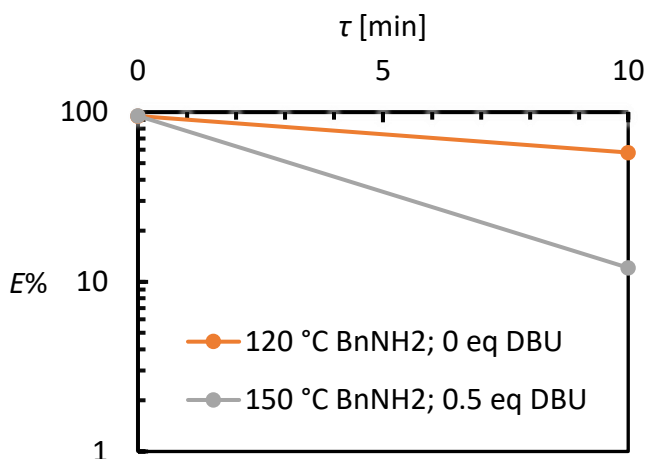


Figure 67: racemization in flow in a 2 mL PFA coil with 10 minute of residence time at 120 °C and 150 °C.

Racemization occurred within the flow reactor ($\tau = 10$ min) in benzylamine with a half-life of approximately 14 min at 120 °C without DBU and with a half-life of 3 min at 150 °C with 0.5 equivalents of DBU.

4.3.1.4.2 Biocatalyzed racemization

Biocatalyzed racemization is known to work with Flurbiprofen as a free acid using the racemizing variant of the arylmalonate decarboxylase (AMDase). However, in order to carry out a crystallization enhanced deracemization, the activity of the enzyme has to be tested with the salt. The optimal solvent for the enzyme is the one that emulates its natural environment, namely water. The solubilities of both salt **17** and **19** at room temperature in water are low, but highest for salt **17** (3.5 mg/mL). Therefore **17** is chosen as preferred target for deracemization. The pH of a saturated aqueous solution of racemic salt **17** was measured and found to be 8.1 which is an optimal pH range for the AMDase.

4.1.4.2.1. Purified racemases

A 5 mM solution of salt (*R*)-**17** was allowed to react at 28 °C with purified AMD V43A G74C 1 mg/mL containing residual Tris buffer. Almost total racemization took place in 400 min and the half-life is about 75 min (Figure 68).

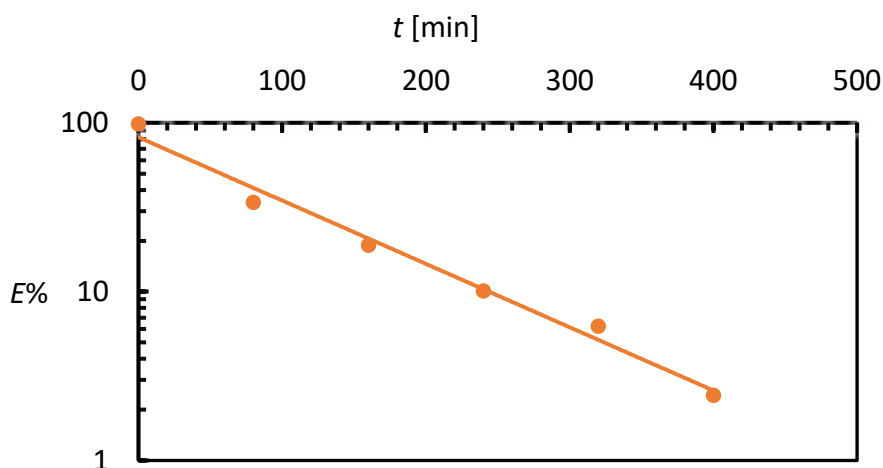


Figure 68: racemization of a 5 mM aqueous solution of salt (*R*)-**17** is with purified AMD V43A G74C at 28 °C.

Next, an experiment is carried out to observe if racemization occurs also in absence of the buffer. It is indeed desirable to carry out a crystallization enhanced deracemization in the absence of external salts that could co-crystallize with the benzylammonium ion, thus affecting the crystallization of salt **17** as a conglomerate. A 4 mM solution of salt (*R*)-**17** was combined with purified enzyme 1.6 mg/mL. After 40 minutes at 28 °C the racemization was already complete.

Because of the short lifetime of the enzyme, especially under grinding conditions used in Viedma ripening experiment, the AMDase can be immobilized on solid supporting material and placed into a packed bed reactor where racemization can occur in the flow analogously to the strategy previously adopted for the base catalyzed racemization. The AMDase AMD V43A G74C L77M V156L immobilized on 3 different solid supporting materials (35 mg) was tested in Eppendorf tubes with 0.5 mL of 4 mM solution of **17** (Figure 69). Racemization with AMDase AMD V43A G74C L77M V156L immobilized on Ezig3 is faster than racemization immobilized on EziG1 and EziG2 supporting material. This might mean that the loading of the enzyme on Ezig3 is higher than on EziG1 and EziG2.

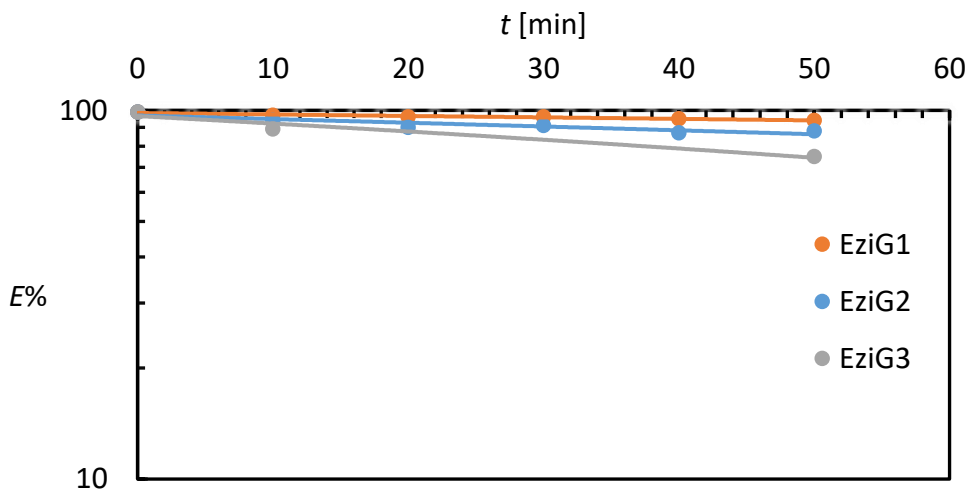


Figure 69: racemization by means of immobilized AMDase (AMD V43A G74C L77M V156L) with mass ratio enzyme/substrate = 4.98 at 28 °C.

After the activity had been determined in batch, racemization was tested in flow. Each supporting material loading the immobilized enzymes (100 mg) are packed in cartridges (Catcart) warmed up to 28 °C and a 4 mM aqueous solution of Flurbiprofen benzylammonium salt was pumped through at a set flow rate. The outcoming solution was collected and analyzed by chiral HPLC. Unfortunately, no substantial racemization was observed at the flow rates used (see Table 5). The residence time τ , that is the time spent by a single molecule in the flow reactor, was not calculated because of the challenging measurement of the dead volume. This latter, in the case of packed-bed reactors, is the space within the column left empty after the addition of catalyst particles. No organic solvents immiscible with water, like toluene or heptane, were used to measure the dead volume in order to avoid the risk of denaturing the enzyme and therefore of inhibiting its catalytic activity.

Table 13: biocatalyzed racemization in flow performed with a continuous syringe pump. The E% of the isolated product refers to the output.

Purified AMDase variant	Supporting material	Flow rate [μL/min]	E% isolated product	T [°C]
V43A G74C L77M V156L	EziG1	1.0	98	r.t
V43A G74C L77M V156L	EziG1	1.0	98	r.t
V43A G74C L77M V156L	EziG1	1.0	98	r.t
V43A G74C L77M V156L	EziG1	0.5	98	r.t
V43A G74C L77M V156L	EziG1	0.5	98	r.t
V43A G74C L77M V156L	EziG1	0.5	98	r.t
V43A G74C L77M V156L	EziG2	500	98	28
V43A G74C L77M V156L	EziG2	250	97	28
V43A G74C L77M V156L	EziG2	10	98	28
V43A G74C L77M V156L	EziG2	500	98	35
V43A G74C L77M V156L	EziG2	250	98	35
V43A G74C L77M V156L	EziG2	125	98	35
V43A G74C L77M V156L	EziG2	500	98	40
V43A G74C L77M V156L	EziG2	250	98	40
V43A G74C L77M V156L	EziG2	125	97	40
V43A G74C	EziG 3	500	98	30
V43A G74C	EziG 3	250	98	30
V43A G74C	EziG 3	125	98	30
V43A G74C	EziG 3	500	98	35
V43A G74C	EziG 3	250	98	35
V43A G74C	EziG 3	125	98	35
V43A G74C	EziG 3	500	98	40
V43A G74C	EziG 3	250	98	40
V43A G74C	EziG 3	125	98	40

4.1.4.2.2. Cell free extract (CFE)

Racemization with buffered CFEs of Aryl Malonate Decarboxylase (AMDase), with enhanced racemization activity, is very fast already at 28 °C, in particular when the variant AMD V43A G74C L77M V156L is used. (Figure 70)

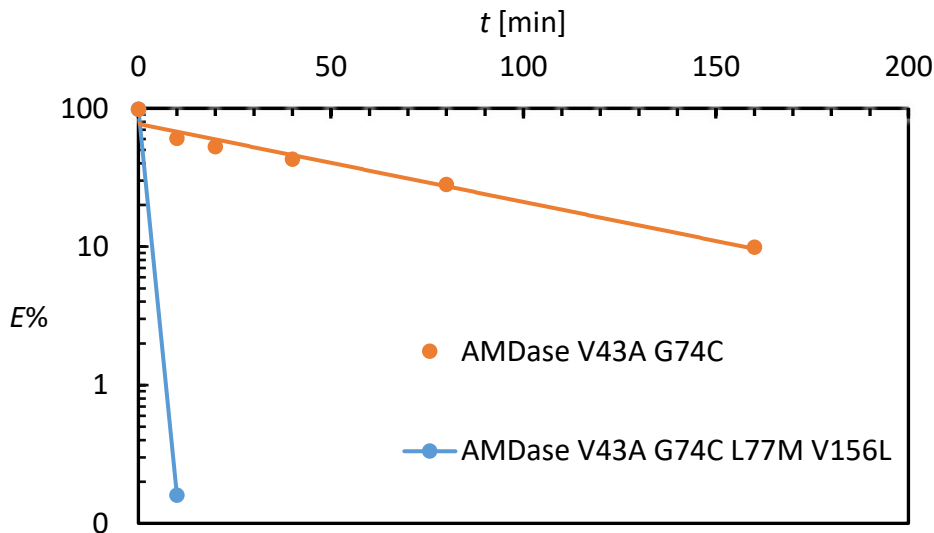


Figure 70: racemization of salt **17** at 28 °C in presence of two variants of AMDase with CFE/substrate ratio = 3.8.

Both the CFE containing the two variants of the AMDase respectively, are able to racemize salt **17**, but the double mutant variant does it much faster.

4.3.1.5. Crystallization enhanced deracemization

Deracemization of salt **17** is initially attempted by a one-pot Viedma ripening strategy on 2 gram scale with 9 mol% of (*R*) seeds and with benzylamine as a base (7.5 mol% on total amount of salt) in 20 mL of octane at 100 °C. The suspension is ground with 10 g of glass beads at 1000 rpm, but no enhancement in optical purity is observed over four days.

with a crystallization unit thermostatted at 20 °C and a racemization unit of 2 mL heated at 120 °C. Racemic salt **17** (3.00 g) is suspended in benzylamine (39 mL) and enantiopure (*R*)-**17** (200 mg) is introduced to generate an initial bias which should make the deracemization autocatalytic. Initially, the ratio between the total volume of the solution and the volume of the reactor is set at 19.5 mL. After 15 hours of grinding by stirring glass beads (15 g) at 500 rpm, no increase in optical purity is detected. Another 2 mL plug flow reactor unit was connected to the one already in use, allowing a faster recirculation of the mother liquor with the same residence time (τ). The ratio between the total volume of the solution and the volume of the reactor was now 9.7 mL. This, together with changes in residence time (τ), as shown in Table 14, does not lead to any improvement in terms of optical purity of the suspended solid (Table 14, Figure 71).

Table 14: τ = residence time. Refreshing time = ratio between the volume of the mother liquor in the crystallization unit and the flow rate. $V_{TOT}/V_{REACTOR}$ = ratio between the total volume of the solution and the volume of the reactor.

Time [h]	<i>E</i> % solid	<i>E</i> % mother liquor	$V_{REACTOR}$ [mL]	Flow rate [mL/min]	τ [min]	$V_{TOT}/V_{REACTOR}$	Refreshing time [min]
6	27	1 (R)	2	0.2	10.0	19.5	152.4
11	26	1 (R)	2	0.2	10.0	19.5	152.4
15	26	0	2	0.2	10.0	19.5	152.4
17.5	27	1 (R)	4	0.4	10.0	9.7	71.2
22.5	26	0	4	0.4	10.0	9.7	71.2
35	28	0	4	0.03	133.3	9.7	949.1
41	20	0.3 (S)	4	0.09	44.4	9.7	316.4
82	18	0.5 (R)	4	0.09	44.4	9.7	316.4

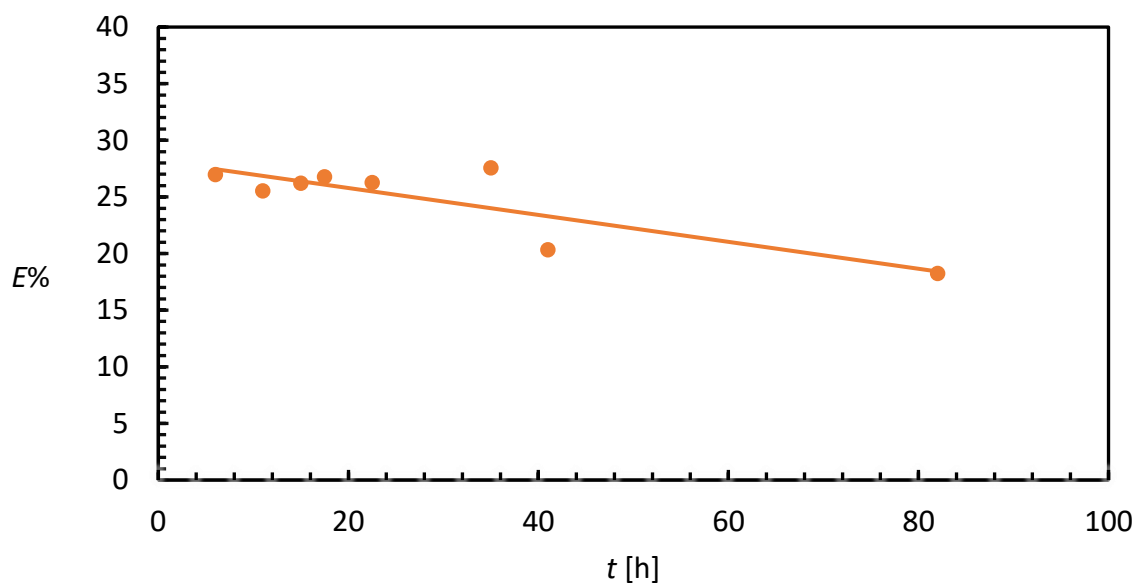


Figure 71: evolution of enantiomeric excess of the solid phase over time.

The mother liquor remains nearly racemic in all the analyses indicating that salt **17** crystallizes as a conglomerate. This conclusion was confirmed by XRPD analysis that, with the exception of two peaks (evidenced by rectangular frames, Figure 72), shows the same pattern.

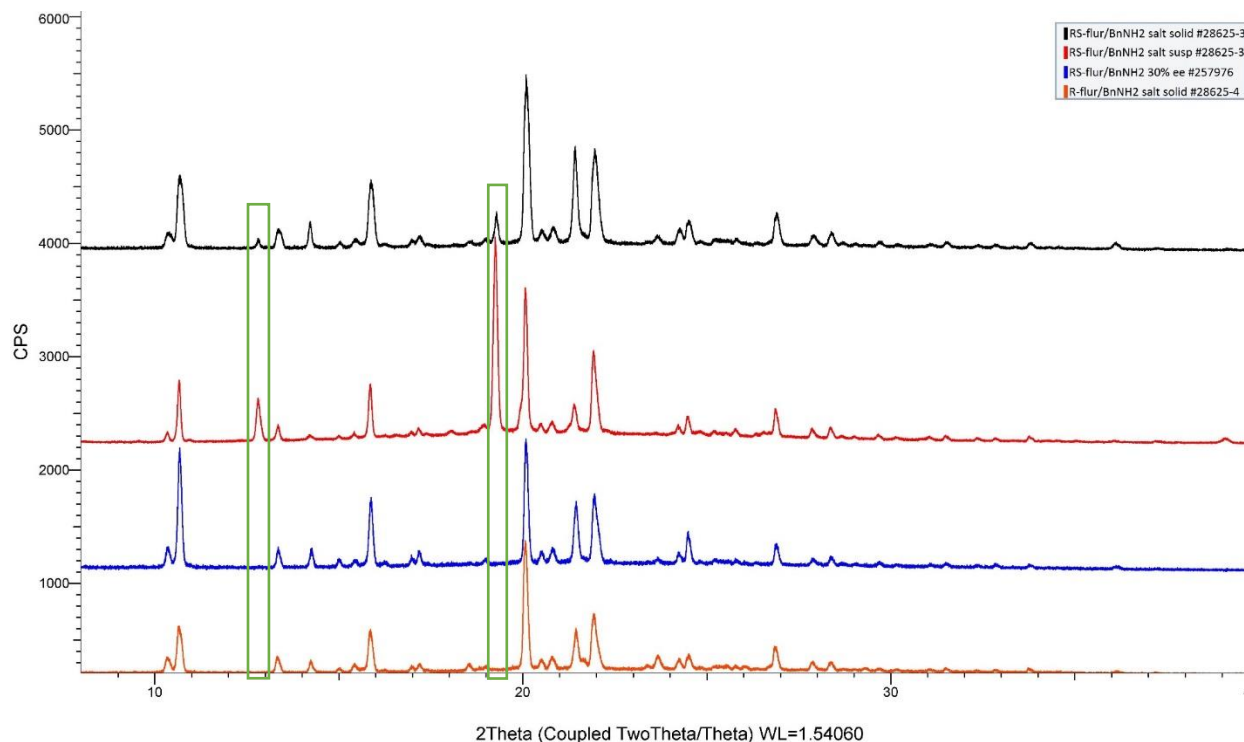
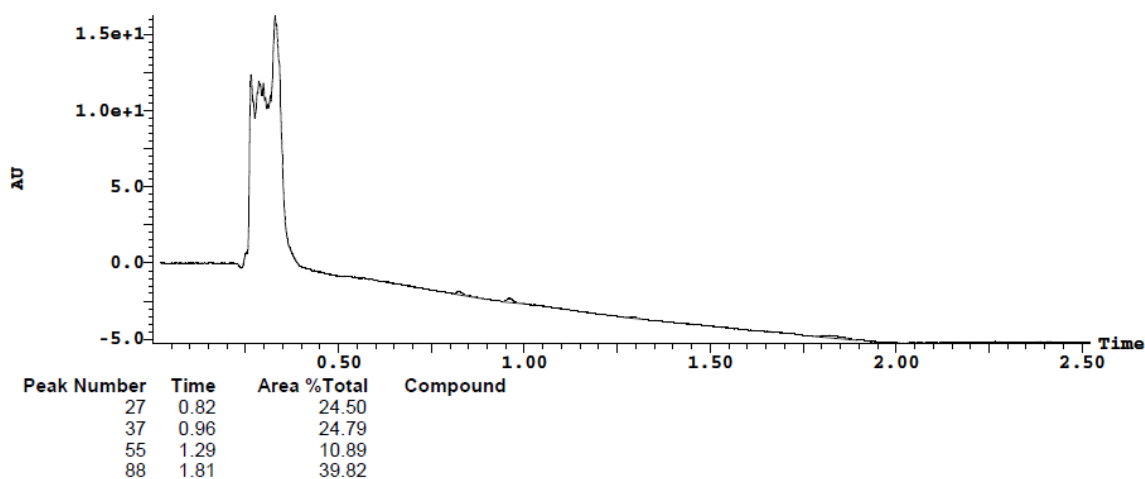


Figure 72: stacked XRPD measurements from the top to the bottom of 1) (in black) racemic salt **17** crystallized from ethanol 2) (in red) racemic salt **17** suspended in benzylamine 3) (in blue) sample with optical purity equal to 30% withdrawn and washed with toluene after 35 hours or mother liquor recirculation through the flow reactor at 120 °C with $\tau = 10$ min. 4) (in orange) enantiopure salt **17**. Green rectangular frames evidence the differences in the pattern.

After one hour, a peak with retention time of 1.30 min is detected by HPLC-MS and the m/z in the positive mode is $[M+1]^+ 196$. This peak is also found in commercially available undistilled dibenzylamine and the mass is compatible with the oxidative loss of hydrogen from dibenzylamine.

3: UV Detector: TIC

1.621e+1
Range: 2.148e+1



3: UV Detector: TIC

7.335e+1
Range: 7.881e+1

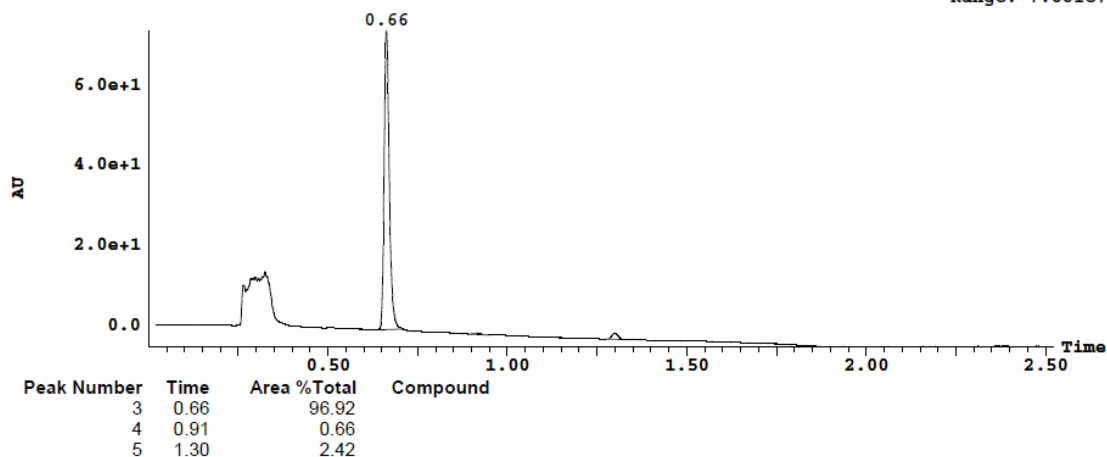


Figure 73: HPLC-MS analysis of distilled benzylamine (top) and the mother liquor after 1 hour of recirculation in the flow reactor at 120 °C with $\tau = 10$ min (bottom).

The PFA coil used in previous experiments was no longer transparent even after washing with toluene, acetone and methanol. The next experiment was conducted with a new PFA 1 mL racemization coil heated to 150 °C. Once again, benzylamine is used both as solvent and as racemization catalyst, this time with addition of DBU (0.53 mL) to speed up the racemization rate. Racemic salt **17** (4.108 mg) was suspended in the mother liquor (15 mL) that was recirculated at a flow rate of 1 mL/min, thus with $\tau = 1$ min. Enantiomerically pure seeds of salt **17** (96 mg) produced an initial enantiomeric enrichment 30% in the *R* enantiomer. An increase in enantiomeric excess was detected (Figure 74), but after 47 hours the crystals

completely dissolved into the reaction mixture, most likely because of decomposition in solution which led to dissolution of the suspended crystals.

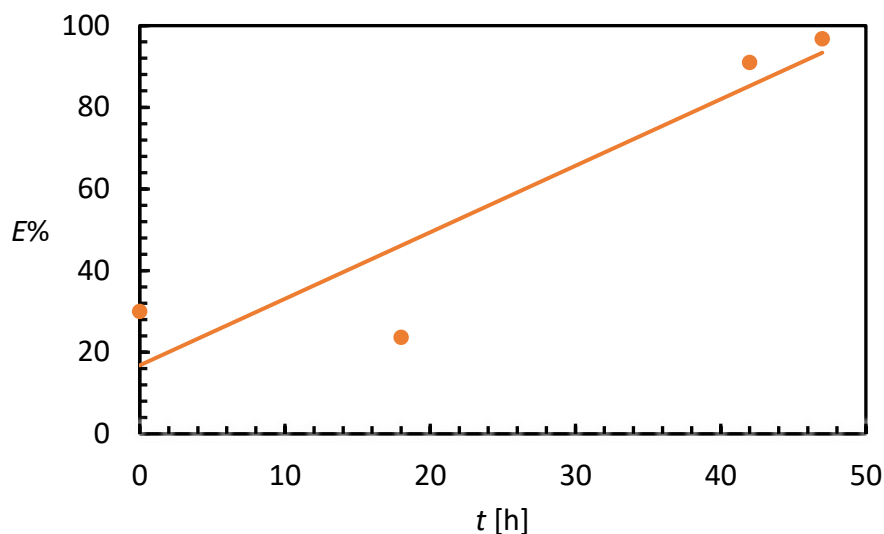


Figure 74: evolution of enantiomeric excess of the solid phase over time.

HPLC-MS of the mother liquor showed a major peak with m/z equal to 333 corresponding to the amide, formed by condensation, thus with liberation of water, and a minor peak with m/z equal to 334 corresponding to the ester formed by liberation of ammonia.

4.3.1.6. Preferential crystallization

In order to perform a preferential crystallization in Auto-Seeded Polythermic Programmed Preferential Crystallization (AS3PC) mode, preparatory studies are necessary. Solubility measurements in different solvents carried out at 20 °C suggest that fairly good starting concentrations of racemic salt **17** in an AS3PC are achievable in ethanol. Solvents like methanol where solubility at 20 °C of salt **17** was close to 280 mg/mL were discarded since unwanted primary nucleation events of the unwanted enantiomer were likely to occur. Solvents like IPA where solubility of salt **17** was close to 15 mg/mL were discarded because of the resulting process was expected to be too little productive. XRPD analyses of the solid resulting from solubility measurements confirm that no polymorphic transition occurred in this solvent. A precise measurement of the temperature of dissolution (clear point temperature) of the racemic fraction of a mixture is conducted with 1595 mg racemic salt **17** in 25 mL of ethanol to get a more accurate value of solubility previously estimated on 1 mL scale. The crystals of racemic salt **17** dissolve completely at 30 °C and, on crash-cooling in a water bath thermostatted at 5 °C, the solution produced very fine crystals with homogeneous size distribution (Figure 75).

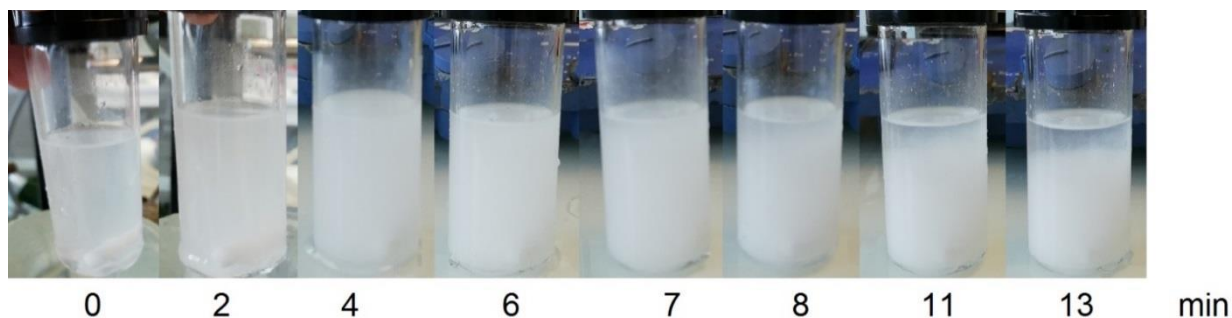


Figure 75: qualitative detection of sedimentation over time of fine particles obtained after crash cooling of racemic salt **17**. The crystallization tube was moved out from the thermostatted water bath at 5 °C for picture purposes. Soon after the test tube was re-submerged into the thermostatted water bath.

The suspension dissolved only at 22 °C. The same procedure was repeated three times after consecutive additions of 3% of the total mass of enantiomerically pure seeds, obtaining a final enantiomeric excess of 9%. Every time the time needed to reach the cloud point, was measured. Results are reported in Table 15.

Table 15: determination of the starting temperature (T_B) of the AS3PC. Clear point is the temperature at which the suspension turns into a clear solution.

Overall $E\%$	Clear point [°C]	Symbol	Time to reach the cloud point upon crash cooling from the corresponding T_{Homo}
0	22.0	T_L	13' 40"
3	24.0	$T_{Homo\ 3\%}$	8' 10"
6	25.5	$T_{Homo\ 6\%}$	6' 38"
9	27.0	$T_{Homo\ 9\%}$	3' 20"

The difference in the clear point of mixtures with a difference in enantiomeric excess of 3% is about 1.5-2.0 °C, which is consistent with a ternary phase diagram of a conglomerate system. Such difference in clear point is generally favorable for preferential crystallization processes.^[23] The induction time shows that primary nucleation of a saturated solution after crash cooling occurs every time faster after every addition of seeds, as expected, because supersaturation is higher at every addition. With these data in hand, the highest temperature (T_B) chosen for the cooling ramp of the AS3PC is 24.5 °C starting from an initial overall composition of $E = 9\%$. At this temperature, at the thermodynamic equilibrium all the

racemate is in solution, while a large surface of enantiomerically pure crystals is suspended and available for crystal growth during supersaturation events like a cooling ramp. The cooling ramp was set starting from 24.5 °C to 4.5 °C in 20 minutes, thus with a cooling rate of 1 °C/min. The enantiomeric excess profile in the mother liquor during this cooling ramp is depicted in Figure 76.

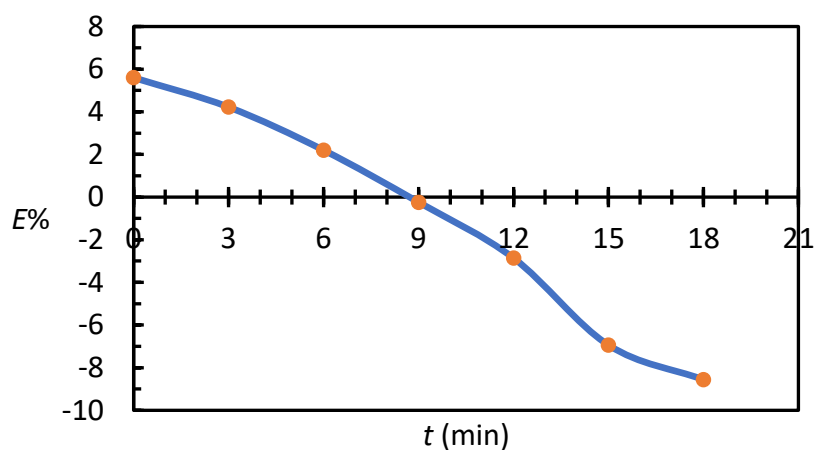


Figure 76: mother liquor composition profile during a cooling ramp of a mixture of 1595 mg of racemic **17** in presence of 9% of seeds from 24.5 °C to 4.5 °C in 20 minutes. Positive values of the enantiomeric excess correspond to an excess of R enantiomer, while negative values correspond to an excess of (S)-enantiomer. Due to limitations in the cooling system, reproducibility could not be assessed. Future experiments with improved thermal control are recommended to validate these findings.

According to the enantiomeric excess measured before the beginning of the cooling ramp (time = 0, Figure 76), at 24.5 °C about one third of the enantiopure seeds were still suspended and available from crystal growth. Unfortunately, the heat transfer capacity of the thermostat was not high enough to perform the programmed cooling ramp. A longer cooling ramp gave lower yield and poor optical purity (Table 16).

Table 16: each experiment: 1594 mg of *RS* + 150 mg of *R* in 25 mL. Pure enantiomer in excess in the harvest. ^aYields are corrected subtracting the amount of seeds from the "Pure enantiomer in excess in the harvest". To the mixture obtained from Entry 1, 96 mg of racemic **17** were added and the experiment described in Entry 2 was started.

Entry	Temperature ramp	Harvest [mg]	Optical purity	Pure enantiomer in excess in the harvest [mg]	Yield ^a %
1	24.5 °C → 8.5 °C (80 min)	243	90%	219.3 (<i>R</i>)	5
2	24.5 °C → 8.5 °C (80 min)	180	90%	240.3 (<i>S</i>)	5

Salt **17** at the concentration used has quite good chance to crystallize in good enantiomeric excess and yield when a cooling ramp of roughly 1 °C/min can be achieved from 24.5 °C to 4.5 °C. A thermostat with more powerful cooling capacity is needed for this purpose.

4.3.2. Dibenzylammonium Flurbiprofen salt

4.3.2.1. X-Ray Powder Diffraction (XRPD)

Racemic and enantiopure salt **18** are prepared using different crystallization conditions and the filtered crystals are measured by XRPD. The same pattern is observed in all the cases, although broader peaks are detected for salts crystallized from dibenzylamine. The larger size of the peaks could be attributed to the use of a different diffractometer.

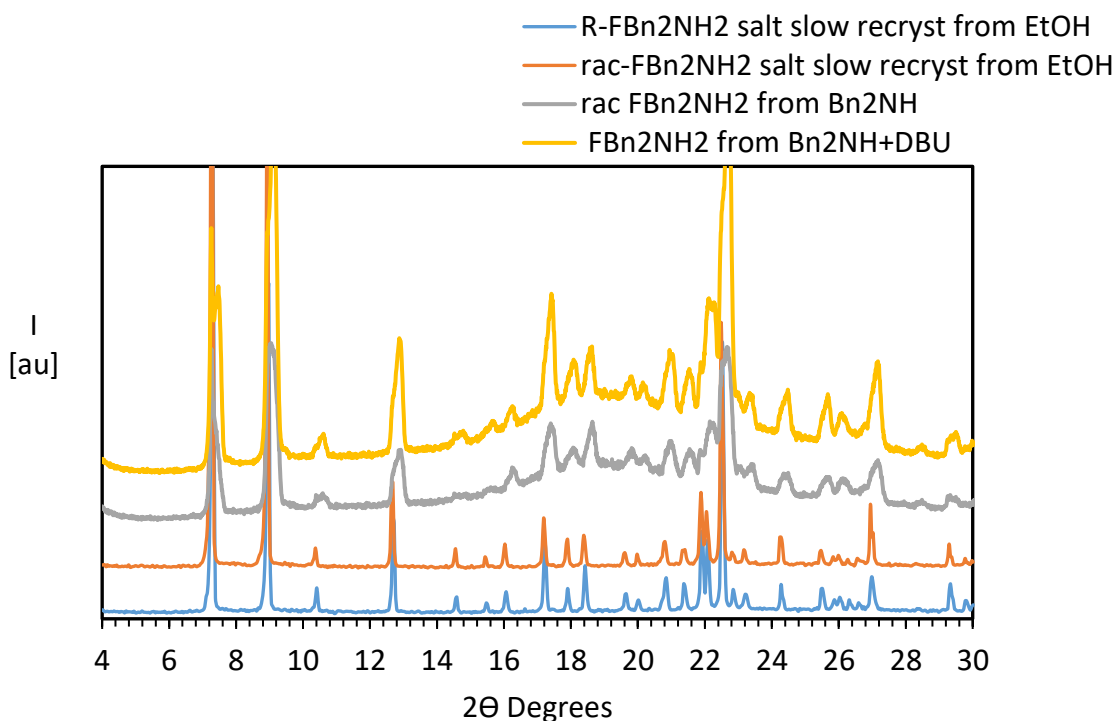


Figure 77: From the bottom to the top: enantiopure (in blue) and racemic (in orange) salt **18** crystallized by slow evaporation of ethanol at room temperature (in blue); racemic salt **18** crystallized by slow cooling (0.3 °C/min) of dibenzylamine without (in gray) and with DBU (0.1 eq, in yellow) from 80 °C to 0 °C and then left at room temperature for 1 hour.

4.3.2.2. Racemization

4.3.2.2.1 Base-catalyzed racemization

Preliminary studies carried out with salt **17**, evidenced that satisfactory racemization rates of Flurbiprofenate anion for a crystallization enhanced deracemization process are achievable at high temperatures. Because the anion that has to undergo hydrogen abstraction by a base is the same both for **17** and **18**, racemization of Flurbiprofenate salt **18** was conducted directly in dibenzylamine at 120 °C. Because the racemization rate seems rather slow, the addition of DBU was necessary to speed up the stereoinversion in solution. Results are shown in Figure 78.

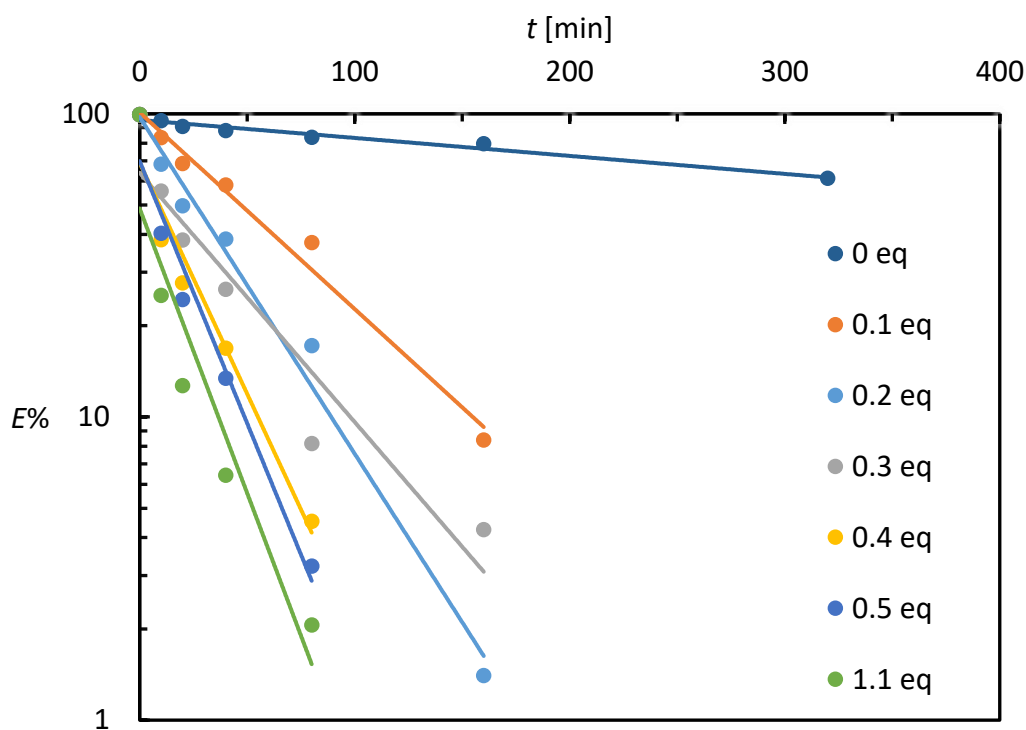


Figure 78: Racemization in Bn_2NH with different DBU equivalents at 120 °C

DBU clearly influences the racemization rate also in this media. The racemization rate at 120 °C increases with the amount of DBU, from a half-life of 464 min (no DBU added) to a half-life of 16 min (0.5 equiv DBU). Although the experimental results are not perfect and results with 0.2 and 0.3 equivalents of DBU

are not consistent, the racemization seems to follow (semi) first order kinetics. As for the salt **17**, racemization in flow of Flurbiprofenate was tested in dibenzylamine at 120 °C with a residence time of 10 minutes (Figure 79). DBU (0.5 equivalents) was added to speed up the racemization.

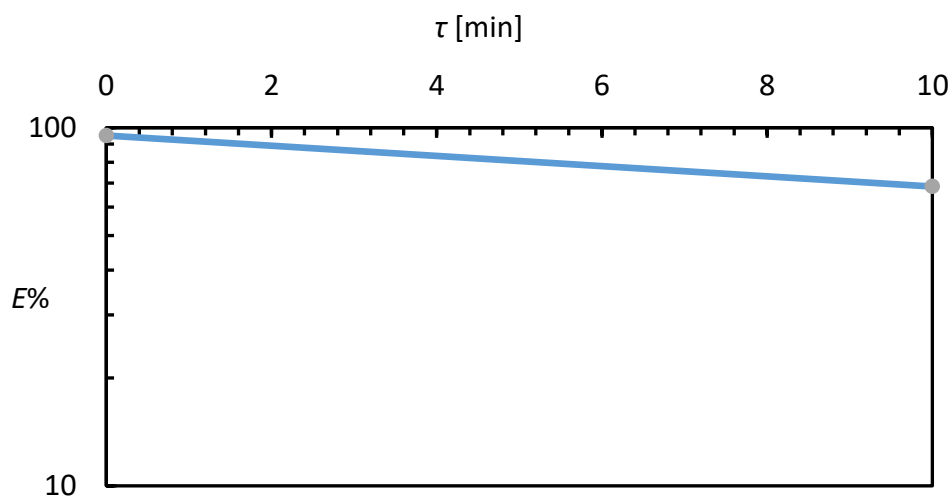


Figure 79: racemization of **18** dibenzylamine in presence of 0.5 eq of DBU in a flow reactor at 120 °C with a residence time (τ) of 10 minutes.

The solution flowing out of the reactor, heated up to 120 °C with a residence time of 10 minutes, had a substantially decreased enantiomeric excess of $E = 68.5\%$. Although this is not racemic, even partial racemization could lead to deracemization during an actual Viedma ripening experiment. These racemization conditions are then adapted to carry out deracemization of salt **18** by means of Viedma ripening.

4.3.2.2 Racemization in the melt

The melting points (T^f) of racemic and enantiomerically pure salts **17** and **18** were determined by DSC (Table 17). The difference between the melting point of enantiopure and racemic salt **17** is slightly lower than the average among conglomerates. The enthalpy of fusion (ΔH) is oddly low for the enantiopure (*R*)-**17**.

Table 17: melting point (onset) of racemic (rac) and enantiopure dibenzylammonium flurbiprofen salt (*R*)-**9** with their relative heat fusion (ΔH).

Compound	T_{rac}^f [°C]	ΔH [kJ/mol]	T_R^f [°C]	ΔH [kJ/mol]	ΔT_{R-rac}^f [°C]
1	115 ^[9]	29.1 ^[9]	104-106 ^[33]	n.a.	-11.0
17	139.0	41.1	156.2	0.5	17.2
18	121.8	58.2	136.8	56.5	15.0

Dibenzylammonium salt seems to be more suitable for these kinds of experiments because its melting point is lower than the melting point of the benzylammonium flurbiprofen salt, thus less decomposition is expected. Moreover, even if the nucleophilicity of a secondary amine is generally higher than the nucleophilicity of primary amines,^[34] nucleophilicity of dibenzylamine is expected to be somewhat reduced by steric hindrance of the benzyl groups, thus amide formation in the melt for salt **18** is expected to be slower when compared to salt **17**.

Racemization was checked by melting enantiopure salt **18** at different conditions. In the first temperature cycles performed by DSC (Figure 80), the enantiomer is completely molten by increasing the temperature from 25 °C to 200 °C. No crystallization was observed during the subsequent cooling ramp, but in the following rise in temperature, an exothermic event, compatible to a glass transition, took place at 50 °C. The following endothermic peak at 114 °C is compatible with the melting point of the form I of racemic Flurbiprofen free acid.^[9]

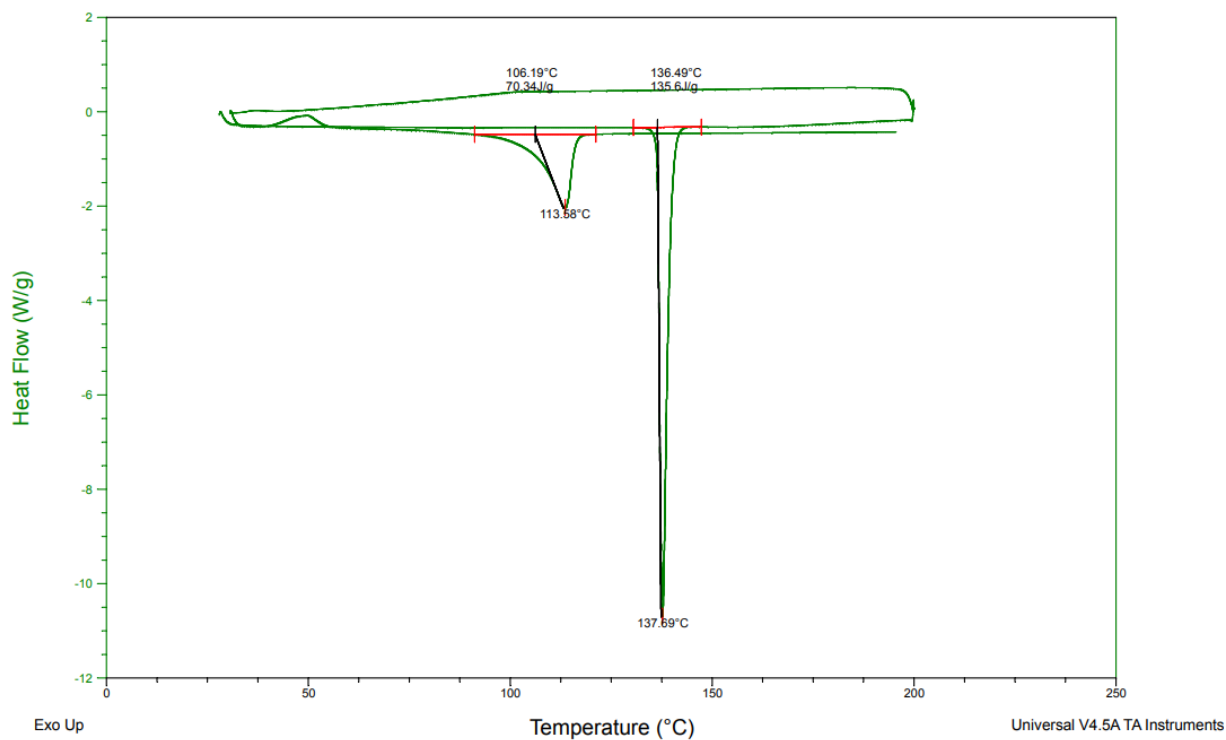


Figure 80: heating and cooling cycles with the highest temperature of the ramp set at 200 °C

In the second ramp the sample is heated up to 145 °C at 10 °C/min and immediately cooled down to 28 °C at 10 °C/min (Figure 81). The sequence was repeated twice. A sharp exothermic peak at 70 °C indicates a crystallization event. The endothermic event detected in the following heating ramp (onset = 133.83 °C) indicates that the previous exothermic peak most likely corresponds to the crystallization of the salt **18**. Some impurities may have lowered the melting point of the enantiopure material. No melting peak of the racemate (eutectic) is detected at 122 °C indicating that no racemization took place.

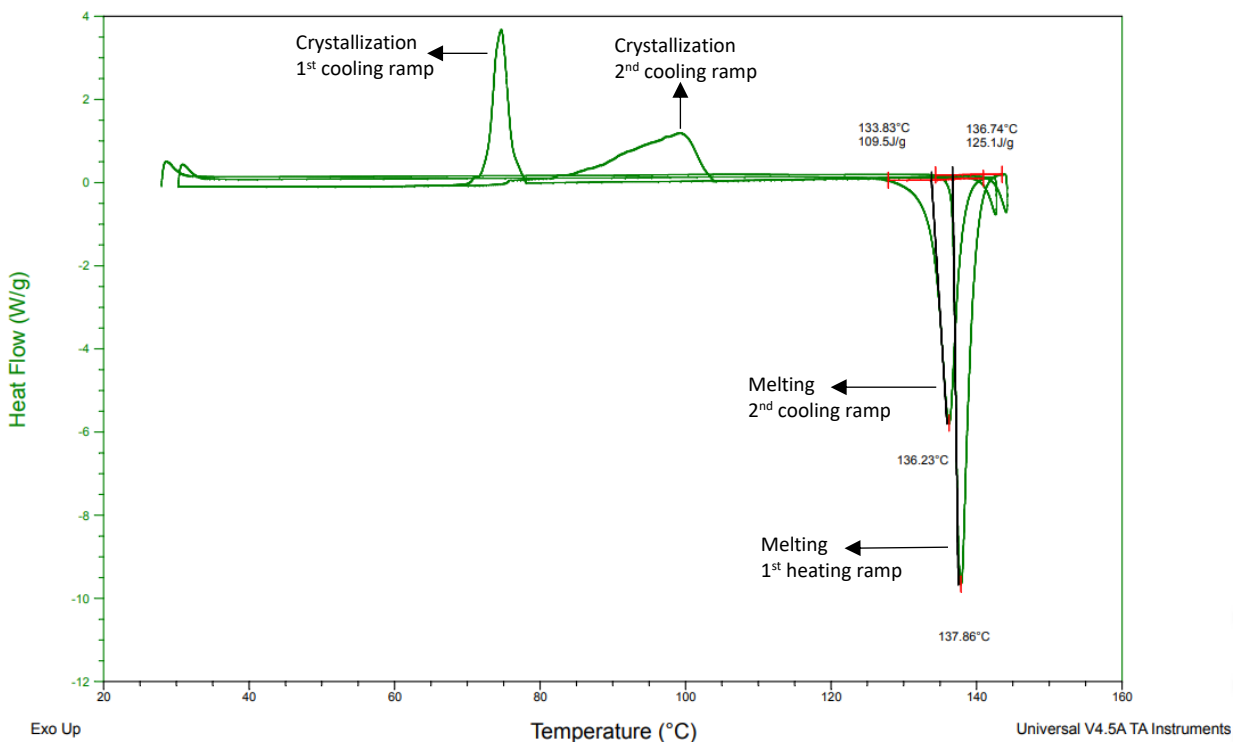


Figure 81: heating and cooling cycles with the highest temperature of the ramp set just over the melting point of enantiopure salt **18**.

4.3.2.3. Deracemization

After it was ensured that racemization takes place in a flow reactor with a relatively short residence time, deracemization was attempted. The flow reactor was connected to an HPLC filter to ensure a selective transport of the mother liquor to the racemization reactor. The mother liquor (32 mL of dibenzylamine + 0.94 mL of DBU) was recirculated with a residence time of 10 minutes, thus with a refreshing time of 145 min and volume/reactor volume ratio equal to 16. According to the amount of racemic salt **18** (3.4 g) introduced into the mixture dibenzylamine/DBU, the solubility was estimated to be 107 g/L, thus the amount of DBU corresponds to 0.4 equivalents. No deracemization was observed over 126 hours.

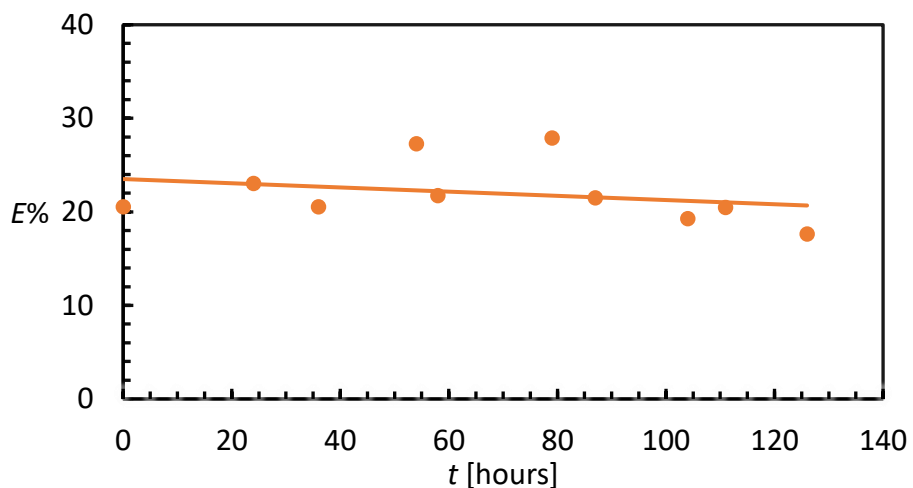


Figure 82: Viedma ripening in Bn_2NH with 0.8 eq of DBU

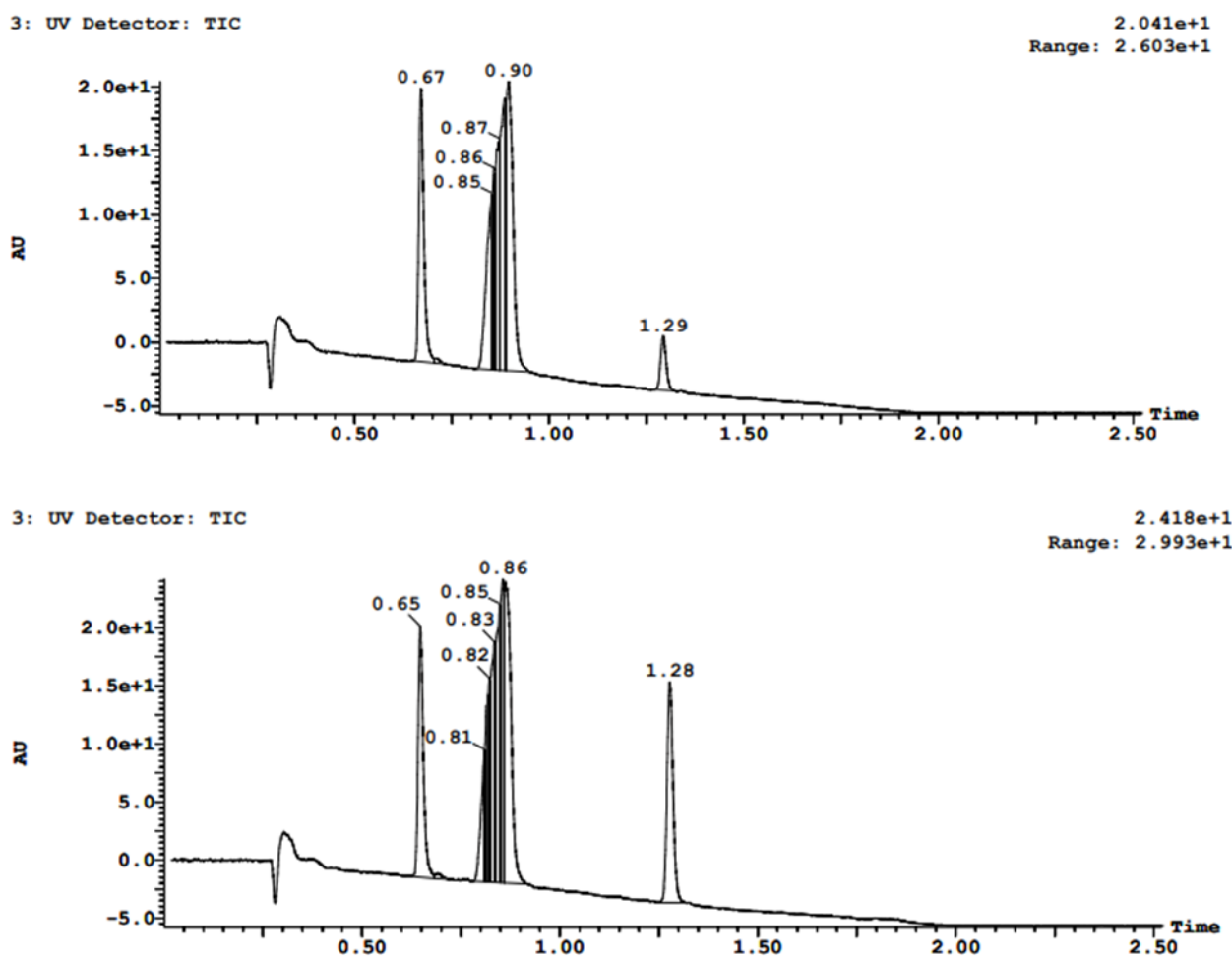
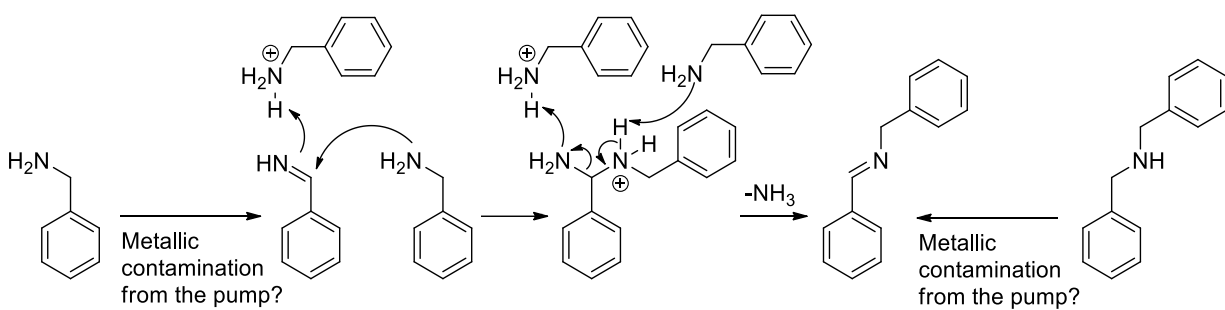


Figure 83: HPLC-MS measurements of the mother liquor after 24 hours (top) and 126 hours (bottom).

^1H -NMR spectrum of the mother liquor after liquid/liquid extractions first with HCl 1N and later with NaOH 1M suggests that the byproduct formed, detected at 1.28 min at HPLC-MS with $m/z = 196$ in the positive

mode, is the product of condensation of benzylamine and the imine formed by oxidation of benzylamine (Scheme 4-6).



Scheme 4-6: proposed mechanism for the formation of amine byproduct detected both in benzylamine and in dibenzylamine.

4.3.2.3.3 Deracemization in the melt

An attempt at deracemization of a mixture with an optical purity of 74% was carried out with a DSC apparatus (Figure 84). The temperature was held at 130 °C (8 °C above the melting point of the racemate, 7 °C below the melting point of the pure enantiomer) for 3 min to make sure that all the (*S*)-enantiomer was in the molten state rather than in the solid state. The endothermic peak of the racemate was indeed detected. Then the temperature was decreased to 120 °C (just below the onset of the racemate) and an exothermic peak consistent with the crystallization of the (*R*)-enantiomer was visible. The temperature was then held at 120 °C for 30 minutes in order to allow the crystal growth of the *R* enantiomer. The sample was cooled down to room temperature and another exothermic event was detectable, suggesting the crystallization of the racemate.

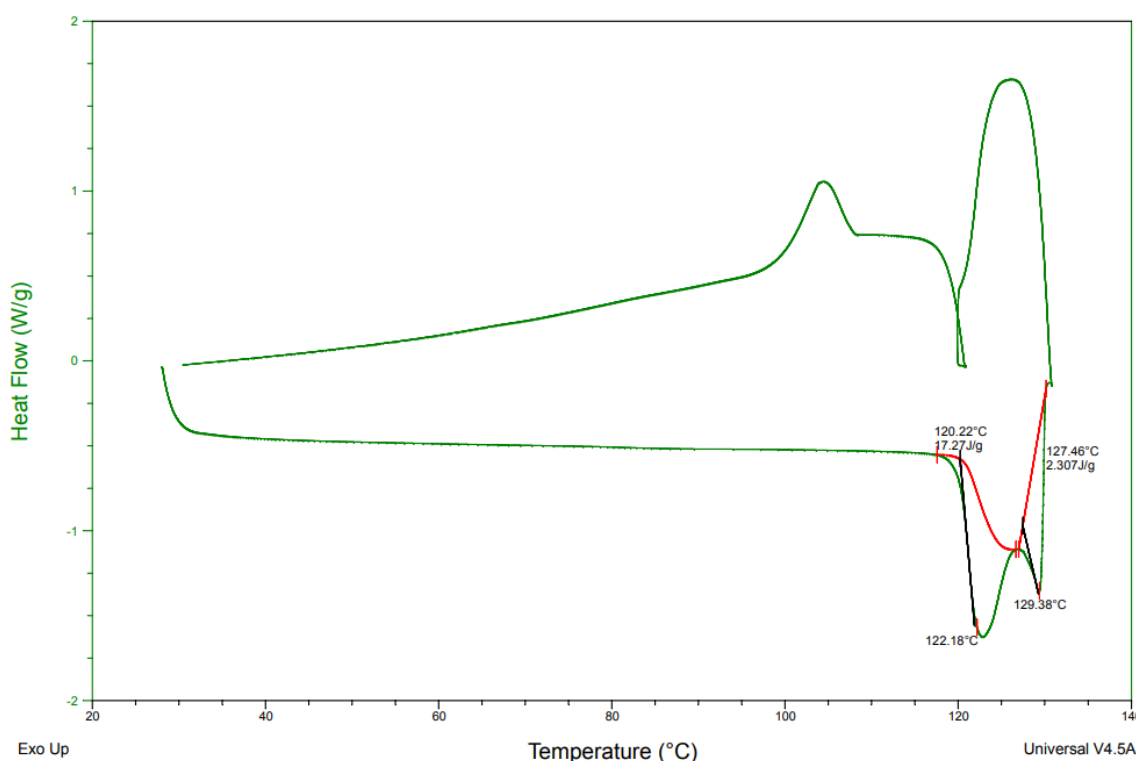


Figure 84: attempted deracemization of a mixture of **18** with initial E of 74% (*R*).

The optical purity of the processed sample is the same as the one of the starting material by chiral HPLC, therefore no deracemization occurred. HPLC-MS of the processed sample (Figure 85: HPLC-MS of the processed sample. Figure 85) shows the peak of Flurbiprofenate at 0.65 min and a second peak of the

dibenzylammonium ion salified with TFA (present in the eluent) at 0.83 min evidencing no decomposition of salts **18**.

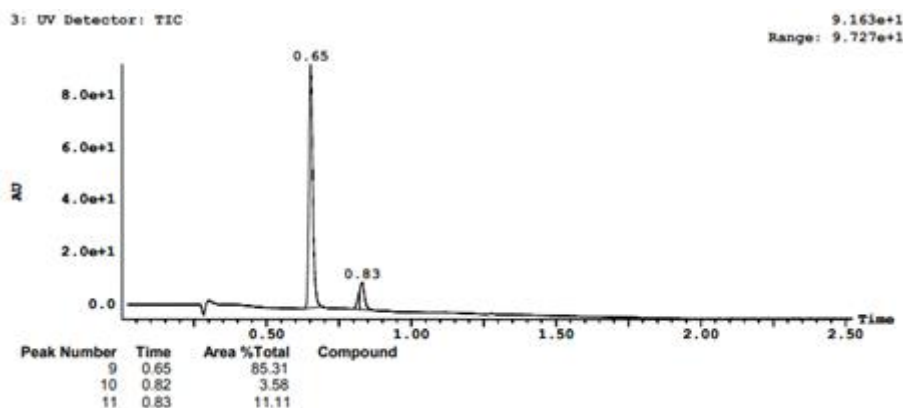


Figure 85: HPLC-MS of the processed sample.

4.4. Discussion

4.4.1. Single Crystal X-Ray Diffraction (SC-XRD)

The crystals of Flurbiprofen benzylammonium salt **17** obtained from a water solution have the same cell parameters as those formed from methanol solution, indicating that the same crystal structure is obtained in both solvents. As a consequence, water, which is the solvent necessary for the biocatalyzed racemization can be used as a crystallization solvent, eventually with a small addition of methanol as a co-solvent to increase the solubility of the media. Crystal structure of salt **18** still has to be determined.

4.4.2. X-Ray Powder Diffraction (XRPD)

The predicted XRPD diffractogram from crystals of Flurbiprofen benzylammonium salt **17** have the same pattern as the experimental pattern. No polymorphic transitions have been observed for either salt **17** and **18**, for which experimental patterns of racemic mixture and enantiopure perfectly overlap. An exception has been observed for a sample of ground salt **17** in benzylamine, where among the typical peaks of salt **17** only two peaks not belonging to such pattern were detected. Such peaks could potentially indicate a competition with another crystal form, but so far there are no further data that can validate this hypothesis. All things considered, it seems that the two salts are suitable for resolution/deracemization processes since polymorphism does not seem to represent a threat.

4.4.3. Base-catalyzed racemization

Experiments in flow reactors at 150 °C demonstrated that DBU played an essential role in aiding racemization: the optical purity dropped from 95% to 12% both in benzylamine and dibenzylamine. After prolonged times, decomposition of Flurbiprofen in benzylamine was observed. At 120 °C, even if some racemization has been shown to occur, no enhancements in optical purity were detected. As a consequence, base catalyzed racemization seems to be inconvenient for the deracemization of Flurbiprofen salts, or at least a fine tuning of reaction conditions to find a trade off between fast racemization and decomposition would be needed. Greener approaches like enzymatic catalysis might allow racemization of Flurbiprofenate salt in less toxic solvents, at near room temperature.

4.4.4. Biocatalyzed racemization

Racemization, previously demonstrated for Flurbiprofen free acid, occurs also with salt **17** in water at 38 °C, which in water forms a solution at pH 8, optimal for the activity of the enzyme. The solubility of **17** can be enhanced by using co-solvent like MeOH, EtOH, THF or DMSO. For optimization of crystallization enhanced deracemization exploiting enzyme catalysis a co-solvent will help to enhance the solubility and thus the productivity of a single process. The enzyme bearing a double mutation is more active than the single mutant.

Unfortunately, most of the batches of the immobilized form of both mutant of the racemase were found to be inactive. Immobilized CFE can be an efficient and cost-effective alternative to immobilized purified enzyme, because of enzyme purification steps, but so far it was not available. Once immobilization of AMDase can produce a long-lived active biocatalyst, this kind of racemization can be embedded into a crystallization-enhanced deracemization process.

4.4.5. Photoisomerization of Flurbiprofen

If photoisomerization of Flurbiprofen free acid would occur without being accompanied by the decarboxylation side reaction, then deracemization could be achieved simply through irradiation of a solution of Flurbiprofen with simultaneous slow addition of the salt former (benzylamine or dibenzylamine). The conglomerate salts are less soluble than the free acid racemic compound, therefore supersaturation of the salt can be achieved by addition of the amine salt formers. The induction time should be determined as a function of flow rate of amine salt former added to the solution of racemic Flurbiprofen at isothermal conditions. Seeds of the desired (*S*)-enantiomer can be introduced into the racemic supersaturated solution before primary nucleation of the salt occurs, allowing enantioselective

crystal growth of salts (*S*)-**17** and (*S*)-**18**, after addition of respectively benzylamine and dibenzylamine to a racemic solution of Flurbiprofen. Enantioselective crystal growth combined with photoracemization would allow an easy and cost-effective deracemization process. Nevertheless, the decarboxylation represents a threat and its occurrence upon irradiation, together with racemization of the Flurbiprofenate ion must be demonstrated. In case decarboxylation occurs at the wavelength of absorption of Flurbiprofenate, ruthenium^[35] or iridium^[36] based photosensitizer might catalyze a reversible hydrogen abstraction necessary to racemization at wavelengths where decarboxylation does not take place.

4.4.6. Preferential crystallization (PC)

Preferential crystallization of salt **17** in ethanol shows potential if a reproducible cooling ramp close to 1 °C/min can be performed from 24.5 °C to 4.5 °C, reaching at least 9% of enrichment of the counter enantiomer in solution. With such enrichment in the liquid phase a productive and strong entrainment can be expected, but to confirm this claim optical purity of the filtered crystals must be checked and it should be over 90% without any further purification.^[37] The thermostat used was not powerful enough to reproduce such cooling rate. Further experiments should be carried out by using thermostats with higher heat capacity. This implies that such process, once optimized, will not be suitable for kilogram scale production, since such performance is very difficult to achieve on that scale.

4.5. Conclusion

So far, the deracemization of Flurbiprofen conglomerate salts remains a challenge because of a lack of fast and clean racemization methods. The base catalyzed racemization in amine conglomerate salt-former solutions does not represent a promising approach because enhancement of optical purity in the solid phase has been linked to decomposition in the liquid phase.

Biocatalyzed racemization seems a much more elegant and greener process where no workup is needed other than the filtration of the deracemized product, because the biocatalyst would remain confined into a packed bed reactor. In order to exploit such racemization, a long-lived immobilized catalyst needs to be obtained through a suitable immobilization procedure. Unfortunately, the immobilized enzyme used in this research seems to be often inactive. Deracemization in the melt would also represent an elegant alternative because of its simple operating procedure, but racemization within the metastable zone does not seem to occur quickly. Finally, preferential crystallization of salt **17** with fast cooling ramps seems to produce a productive process, which could possibly be coupled to the biocatalyzed racemization in the eventuality that the immobilized enzyme shows tolerance with high concentration of organic solvents.

Transition metal catalyzed racemization applied to a decoupled deracemization^[38] would be in principle possible because the chiral center is placed in the alpha position in respect to an aryl group which enhances its acidity, however side reactions are expected. One is that fluorine attached to the aryl moiety of Flurbiprofen is a relatively good leaving group and can be easily displaced by a hydride adsorbed on the pre-hydrogenated catalyst. Moreover, the nitrogen of the salt former both in **17** and **18** might poison the catalyst.

4.6. References

- [1] R. C. Green, L. S. Schneider, D. A. Amato, A. P. Beelen, G. Wilcock, E. A. Swabb, K. H. Zavitz, f. t. Tarenflurbil Phase 3 Study Group, *JAMA* **2009**, *302*, 2557-2564.
- [2] J. V. Andersen, S. H. Hansen, *Journal of Chromatography B: Biomedical Sciences and Applications* **1992**, *577*, 362-365.
- [3] F. Jamali, B. W. Berry, M. R. Tehrani, A. S. Russell, *Journal of Pharmaceutical Sciences* **1988**, *77*, 666-669.
- [4] a) C. R. Smith, T. V. RajanBabu, *The Journal of Organic Chemistry* **2009**, *74*, 3066-3072; b) R. C. Griesbach, D. P. G. Hamon, R. J. Kennedy, *Tetrahedron: Asymmetry* **1997**, *8*, 507-510.
- [5] G. J. Harkness, M. L. Clarke, *European Journal of Organic Chemistry* **2017**, *2017*, 4859-4863.
- [6] H. Y. Zhang, X. Wang, C. B. Ching, J. C. Wu, *Biotechnology and Applied Biochemistry* **2005**, *42*, 67-71.
- [7] R. Hardy, P. F. Coe, A. Hirst, H. O. O'Donnell, PCT Int. Appl., **1997**, WO1994012460A1
- [8] J. S. Nicholson, J. G. Tantom, **1978**, DK154418B
- [9] A. L. Grzesiak, A. J. Matzger, *Journal of Pharmaceutical Sciences* **2007**, *96*, 2978-2986.
- [10] B. Kaptein, E. Vlieg, W. L. Noorduin, PCT Int. Appl., **2012**, WO2010089343 (A1)
- [11] a) A. A. Choudhury, A. Kadkhodayan, D. R. Patil, Ethyl Corp., **1993**, US5221765; b) R. D. Larsen, P. Reider, Merck and Co., Inc., **1990**, US 4946997, 900807 (890607)
- [12] W. L. Noorduin, B. Kaptein, H. Meekes, W. J. P. van Enckevort, R. M. Kellogg, E. Vlieg, *Angewandte Chemie International Edition* **2009**, *48*, 4581-4583.
- [13] Miyamoto, in *Green Biocatalysis*, **2016**.
- [14] M. Aßmann, C. Mügge, S. K. Gaßmeyer, J. Enoki, L. Hilterhaus, R. Kourist, A. Liese, S. Kara, *Frontiers in Microbiology* **2017**, *8*.
- [15] S. Ogino, M. L. Gulley, J. T. den Dunnen, R. B. Wilson, *The Journal of Molecular Diagnostics* **2007**, *9*, 1-6.
- [16] S. Hadidi, Norouzibazaz, M & Shiri, F., *Current Chemistry Letters* **2020**, *9*, 161-170.
- [17] a) F. Boscá, M. A. Miranda, G. Carganico, D. Mauleon, *Photochemistry and Photobiology* **1994**, *60*, 96-101; b) M. Liu, M.-D. Li, J. Huang, T. Li, H. Liu, X. Li, D. L. Phillips, *Scientific Reports* **2016**, *6*, 21606.
- [18] A. Collet, L. Ziminski, C. Garcia, F. Vigné-Maeder, in *Supramolecular Stereochemistry* (Ed.: J. S. Siegel), Springer Netherlands, Dordrecht, **1995**, pp. 91-110.
- [19] R. Oketani, M. Hoquante, C. Brandel, P. Cardinael, G. Coquerel, *Organic Process Research & Development* **2019**, *23*, 1197-1203.

- [20] a) C. Viedma, *Physical Review Letters* **2005**, *94*, 065504; b) C. Rougeot, F. Guillen, J.-C. Plaquevent, G. Coquerel, *Crystal Growth & Design* **2015**, *15*, 2151-2155.
- [21] C. Xiouras, J. H. Ter Horst, T. Van Gerven, G. D. Stefanidis, *Crystal Growth & Design* **2017**, *17*, 4965-4976.
- [22] Waechtler A., Saleh-Kassim H., Jasper C., Kolb J., Maillard D., PCT Int. Appl., **2016**, WO 2016078758 A1
- [23] G. Coquerel, in *Topics in Current Chemistry*, Vol. 269 (Ed.: H. N. Sakai K., Tamura R.), Springer, Berlin, Heidelberg, **2006**.
- [24] Karim Engelmark Cassimjee, Hans-Jürgen Federsel, in *Biocatalysis: An Industrial Perspective* (Eds.: Gonzalo de Gonzalo, Pablo Domínguez de María), Royal Society of Chemistry, **2017**, pp. 345-361.
- [25] SMART for WNT/2000 V5.622 (2001), Smart software reference manual, Bruker Advanced X Ray Solutions, Inc., Madison, Wisconsin, USA.
- [26] SAINT+ V6.02 (1999), Saint software reference manual, Bruker Advanced X Ray Solutions, Inc., Madison, Wisconsin, USA.
- [27] WinGX: Version 1.70.01: An integrated system of Windows Programs for the solution, refinement and analysis of Single Crystal X-Ray Diffraction Data, By LouisJ. Farrugia, Dept. of chemistry, University of Glasgow. L. J. Farrugia (1999) *J. Appl. Cryst.* **32**, 837-838.
- [28] M. Meot-Ner, *Chemical Reviews* **2005**, *105*, 213-284.
- [29] B. Feng, X. Fang, H.-X. Wang, W. Dong, Y.-C. Li, *Polymers* **2016**, *8*, 356.
- [30] W. N. Olmstead, Z. Margolin, F. G. Bordwell, *The Journal of Organic Chemistry* **1980**, *45*, 3295-3299.
- [31] K. Kaupmees, A. Trummal, I. Leito, *Croatica Chemica Acta* **2014**, *87*, 385-395.
- [32] S. Tshepelevitsh, A. Kütt, M. Lõkov, I. Kaljurand, J. Saame, A. Heering, P. G. Plieger, R. Vianello, I. Leito, *European Journal of Organic Chemistry* **2019**, *2019*, 6735-6748.
- [33] S.-F. Zhu, Y.-B. Yu, S. Li, L.-X. Wang, Q.-L. Zhou, *Angewandte Chemie International Edition* **2012**, *51*, 8872-8875.
- [34] T. Kanzian, T. A. Nigst, A. Maier, S. Pichl, H. Mayr, *European Journal of Organic Chemistry* **2009**, *2009*, 6379-6385.
- [35] M. Rueping, R. M. Koenigs, K. Poscharny, D. C. Fabry, D. Leonori, C. Vila, *Chemistry – A European Journal* **2012**, *18*, 5170-5174.
- [36] N. Y. Shin, J. M. Ryss, X. Zhang, S. J. Miller, R. R. Knowles, *Science* **2019**, *366*, 364.
- [37] L. Pasteur, *C.R.T.* **1853**, *37*, 162– 166.
- [38] G. Valenti, P. Tinnemans, I. Baglai, W. L. Noorduin, B. Kaptein, M. Leeman, J. H. ter Horst, R. M. Kellogg, *Angewandte Chemie International Edition* **2021**, *60*, 5279-5282.

Chapter 5: Conclusions and future works

5.1. Conclusions

The overall aim of this thesis was to develop new methods to overcome limitations of crystallization enhanced deracemization techniques, and to demonstrate that even harsh racemization conditions, when needed, can be applied to enantioselective crystallization processes. Enabling technologies like flow chemistry were used as a tool to conduct solution racemization in a safe and reproducible fashion. Plug flow coil reactors and packed bed reactors were selected for investigation because of their suitability for the racemization of the compounds of interest. Alternative crystallization methods like crystallization from the melt were attempted to exploit a racemization occurring in the melt without the use of an external base.

In Chapter 2 the 2-chlorophenylglycinamide, a valuable intermediate of the platelet aggregation inhibitor Clopidogrel, during its characterization was found to racemize in the melt without addition of an external base. Despite promising results potentially exploitable in a melt crystallization, the process was hampered by lack of recrystallization after melting and by irreversible cyclization as a side reaction. Deracemization was then performed in presence of DBU as a base by using a flow reactor to enhance the racemization rate.

In Chapter 3 a conglomerate of Praziquantel was identified as possible intermediate among a library of 30 derivatives. The method of the determination of the eutectic composition together with XRPD showed to be a reliable, fast and robust method to distinguish a SHG signal of a conglomerate sample from false positive signals. Such techniques, which do not necessarily require very expensive instrumentation or analysis and particular precaution in the preparation of the sample, contrary to SC-XRD, are methods of choice whenever small amounts of both enantiomerically pure and racemic crystals are available. Racemization of Praziquantel was demonstrated to occur in flow in a packed bed column packed with Pd/C partially preactivated with hydrogen and the same reaction conditions were suitable for the racemization of the conglomerate **3u**. Finally, by adjusting the total volume/dead volume ratio, given a certain flow rate used for recirculating the mother liquor, it was possible to deracemize the Praziquantel conglomerate precursor by means of CIAT and TCID. The lack of racemization and near quantitative yields in the hydrolysis of the conglomerate and subsequent acylation of enantiomerically pure praziquanamine make this process suitable for the production of enantiomerically pure Praziquantel.

In Chapter 4 the base and bio catalyzed racemization of Flurbiprofen were studied in presence of the salt former benzylamine and dibenzylamine. A thorough characterization of the two salts was carried out. Base catalyzed racemization seems difficult to exploit in a CED technique due to the high amount of decomposition. However, biocatalyzed racemization clearly appears to be a valid alternative since it requires a clean reaction at mild conditions. However, in order to be exploited in a CED technique, immobilization of such biocatalysts needs to take place with a guarantee of retention of the enzyme activity.

The research presented in this thesis has led to advancement in conglomerate technology, extending the use of CED techniques also to less reactive compounds through the use of enabling technologies like flow chemistry. All the obtained results will facilitate the extension of the application of flow technology to other less reactive compounds.

5.2. Future work

5.2.1. Preferential crystallization of Flurbiprofen benzylammonium salt

Preliminary studies on preferential crystallization of Flurbiprofen benzylammonium salt showed an enrichment of the mother liquor in the counter enantiomer of about 9%. Such a percentage can be considered a promising result for a good yielding process. However, the heating capacity of the used thermostat did not allow to reproduce the results, because the heat from the surrounding environment (the experiments described in the section 4.3.1.6 were carried out in summer) significantly interfered with the process.

The most obvious strategy to optimize the process with such an encouraging result would be to perform a set of different well-controlled cooling ramps. Amount of solvent, seed crystal enantiopurity, size and mass, temperature frame and stirring rate should be maintained constant in all the experiments, in order to make sure that the cooling ramp would be the only variable in the screening. The enantiomeric excess of the dry solid obtained by filtration should be then determined by polarimeter or by chiral chromatography techniques.

5.2.2. Biocatalytic racemization of Flurbiprofen benzylammonium salt

The biocatalytic racemization of the Flurbiprofen benzylammonium salt still remains the most promising approach for multiple reasons (section 4.1.4.2). Among them there are:

- 1) a clean racemization with no side product

- 2) the possibility to use high percentage of co-solvent with the EziG supporting material with only a little risk to inactivate the enzyme
- 3) compatible pH working region of the solution of Flurbiprofen benzylammonium salt and the enzyme activity
- 4) no need of enzyme co-factors.

Thus, activity of the immobilized enzymes with one single and double variant should be tested by using higher flow rate by recycling a little volume of Flurbiprofen benzylammonium salt to define the optimal flowrate/residence time ratio in order to avoid mass-transfer limitations. In other words, at lower flow rates, mixing might not be intense enough to facilitate diffusion of the reactants from the bulk to the active sites of the enzyme. At higher flow rates, the reaction time might be too short to allow racemization to occur.

5.3. General conclusion

In summary, this thesis has demonstrated that the integration of enabling technologies, particularly flow chemistry, can significantly expand the applicability of CED methodologies. By addressing both fundamental and practical challenges in racemization and crystallization, this work has established that even substrates requiring harsh racemization conditions can be effectively managed and incorporated into enantioselective processes. The exploration of alternative crystallization methods and in situ racemization, including biocatalytic approaches, further illustrates the diverse strategies available for overcoming longstanding limitations in the field.

Collectively, the approaches and findings elaborated in this thesis contribute to a more versatile and robust toolkit for the resolution of chiral compounds, serving valuable roles in both pharmaceutical production and broader synthetic applications. The successful application of flow reactors for precise control and safety, as well as the demonstration of reliable methods for characterizing conglomerate systems, set the stage for future expansion of these technologies to a wider range of compounds, including those previously considered unsuitable for CED processes.

Moreover, the insights gained regarding the compatibility of racemization methods, the challenges in salt and melt systems, and the potential of biocatalysis signal promising directions for future research and practical development. These advancements not only enhance our fundamental understanding of chiral

resolution technologies but also offer tangible pathways to greener, safer, and more efficient synthesis strategies.

Ultimately, the work presented here lays important groundwork for the next generation of enantioselective manufacturing, with the potential to influence both academic research and industrial practice. By enabling more sustainable and broadly applicable approaches to chiral resolution, this thesis contributes to shaping the evolving landscape of stereoselective chemistry.